Progress in Materials Science 129 (2022) 100967

Contents lists available at ScienceDirect

Progress in Materials Science

journal homepage: www.elsevier.com/locate/pmatsci

MXene-based aptasensors: Advances, challenges, and prospects

Qurat ul Ain Zahra [a,b,1], Salim Ullah [c,d,1], Faisal Shahzad [e,*], Bensheng Qiu [a], Xiaona Fang [b,c,d], Ayesha Ammar [f], Zhaofeng Luo [b,*], Shabi Abbas Zaidi [g,*]

[a] Biomedical Imaging Center, University of Science and Technology of China, Hefei, Anhui 230026, China
[b] The Key Laboratory of Zhejiang Province for Aptamers and Theranostics, Institute of Basic Medicine and Cancer (IBMC), Chinese Academy of Sciences, Hangzhou 310022, China
[c] CAS Key Laboratory of Nano-Bio Interface, Suzhou Institute of Nano-Tech and Nano-Bionics, Chinese Academy of Sciences, Suzhou 215123, China
[d] School of Nano-Tech and Nano-Bionics, University of Science and Technology of China, Hefei 230026, China
[e] National Center for Nanotechnology, Department of Metallurgy and Materials Engineering, Pakistan Institute of Engineering and Applied Sciences (PIEAS), Islamabad, Pakistan
[f] Nuclear Medicine, Oncology & Radiotherapy Institute (NORI), Islamabad, Pakistan
[g] Analytical Chemistry Program, Department of Chemistry and Earth Sciences, College of Arts and Sciences, Qatar University, Doha 2713, Qatar

ARTICLE INFO

Keywords:
MXenes
Aptamer
Aptasensors
Cancer diagnosis
Mycotoxins detection
MXenes surface functionalization
Optical aptasensors

ABSTRACT

The combination of 2D MXenes with high affinity aptamers has resulted in the development of innovative aptasensing approaches for food/water safety and clinical diagnosis. Aptamers have quite a number of benefits over conventional methods as unique molecular recognition components for versatile bio-sensing devices. Recent breakthroughs in the concept, development, and bio-sensing applications of various MXene-based aptasensors have been discussed in this study. The authors address sensing platforms for the identification of several types of cancers, mycotoxins, and other analytes. More emphasis has been placed on aptamer conjugation with various MXenes, sensor fabrication methodologies, and biosensing mechanisms. We observed that optical aptasensing applications are in their infancy when compared to electrochemical MXene based aptasensors. As a result, we attempted to forecast revolutionary developments in MXenes that may contribute to their integration into emerging optical aptasensors such as fluorescence, photoluminescence, surface-enhanced Raman Scattering, colorimetric, and Surface Plasmon Resonance. Finally, potential constraints and future prospects have been highlighted. This study is expected to help readers understand the fabrication of MXene-based aptasensors and their concomitant sensing mechanisms, hence encouraging the development of flexible MXene-based aptasensors.

1. Introduction

Early disease detection lowers fatality rates and speeds up recovery for patients when combined with a personalized treatment program [1]. In the past, conventional diagnostic systems, including protein chip related protocols [2], electrochemiluminescence immunoassays (ECLIs) [2], electrochemical immunoassays [3], chemiluminescence immunoassays [4], and enzyme-linked immunosorbent assays [5] exhibited high specificity and sensitivity. But such diagnostic procedures involve the use of highly skilled

* Corresponding authors.
E-mail addresses: faisal@pieas.edu.pk (F. Shahzad), lzf@ustc.edu.cn (Z. Luo), shabizaidi@qu.edu.qa (S. Abbas Zaidi).
[1] Equal Contribution.

https://doi.org/10.1016/j.pmatsci.2022.100967
Received 7 November 2021; Received in revised form 8 April 2022; Accepted 16 May 2022
Available online 21 May 2022

personnel in addition to the expensive and bulky analytical equipment. As a result, there is a necessity for low-cost, accurate, and portable diagnostic equipment. [5]. Biosensors have a number of advantages including portability, easy detection, cost effectiveness, accuracy, user friendliness, and rapid detection [6,7]. A biosensor, in general, is composed of two critical functional parts: target recognition and signal transduction. In principle, the target recognition feature is fundamental to the sensor's efficiency. Aptasensors are biosensors relying on aptamers to exhibit exceptional sensing capabilities for a broad range of biomolecules [8]. Aptamers comprise single-stranded RNAs or DNAs with a high affinity for their targets (ligand), for example small molecules, drugs, peptides, proteins, organic or inorganic compounds, and even whole cells, etc. [9–11]. Aptamers are widely employed in a number of applications as molecular recognition components, such as specific-target capture assays [12] and biosensors [13].

Aptasensor performance has been enhanced by integrating them with different nanomaterials (NMs) that are helpful for immobilizing aptamers. The NMs improve the electrochemical behavior and conductivity of the transducers and can alter the interface's attributes, resulting in improved aptamer-ligand interactions [14]. The coupling of NMs with aptamers is a rapidly developing field wherein a variety of aptamer-nanomaterial conjugates with exceptional biosensing efficiencies have been established [15–17]. NMs have been utilized to build sensing devices because of their unique structural, mechanical, optical, and electrical properties [18,19]. In addition to the aforementioned features, NMs might be employed as aptamer carriers in biosensing devices [20]. A reliable nanoplatform exhibiting a sheet-like architecture with a huge surface area, a thickness normally below 5 nm, excellent physicochemical properties, and transverse dimensions greater than 100 nm might be more demanding among the numerous nanomaterials for this purpose [21–24]. Due to their unique electrical, chemical, and physical properties, 2D-NMs-based electrochemical signal amplification has the potential to significantly improve the selectivity and sensitivity of biosensors [19,25–27]. In particular, the large specific surface area with a sheet like structure increases surface immobilization and biomolecule loading efficiency [28,29]. More precisely, the rich surface properties of certain 2D-NMs provide abundant active functional groups suitable for conjugation with antibodies or aptamers in order to bind their target molecules [30]. Thus, integrating aptamers with 2D-NMs may open up a plethora of exciting possibilities for the production of new aptasensors with improved performance [31].

MXenes are considered relatively new additions to the 2D-NMs family [32,33]. Their unique surface chemistry and intriguing electrochemical behavior, combined with their high biocompatibility, make them ideal as a support matrix for the development of cutting-edge electrochemical sensing and biosensing devices [34–36]. Despite the fact that several reviews [36–40] have recently been published on the role of MXene in biosensors, none of the existing reviews summarize the potential of MXene-based aptasensors. Interestingly, several reviews have been published on graphene and other nanomaterial-based aptasensors for analytical applications [31,41,41–43]. In our opinion, there is a need for a comprehensive review, therefore, we reviewed the current research advances, challenges, and the future prospects of MXene-based aptasensors. This study is aimed at equipping and updating the readers with preliminary but valuable instructions on how to fabricate new MXene-based aptasensors and the accompanying sensing mechanisms, the advances in this field, and challenges that will contribute towards the development of novel and high-performance MXene-based aptasensors. To enhance the reader's awareness, Fig. 1 sketches a historical perspective of MXene-based aptasensor development. It is

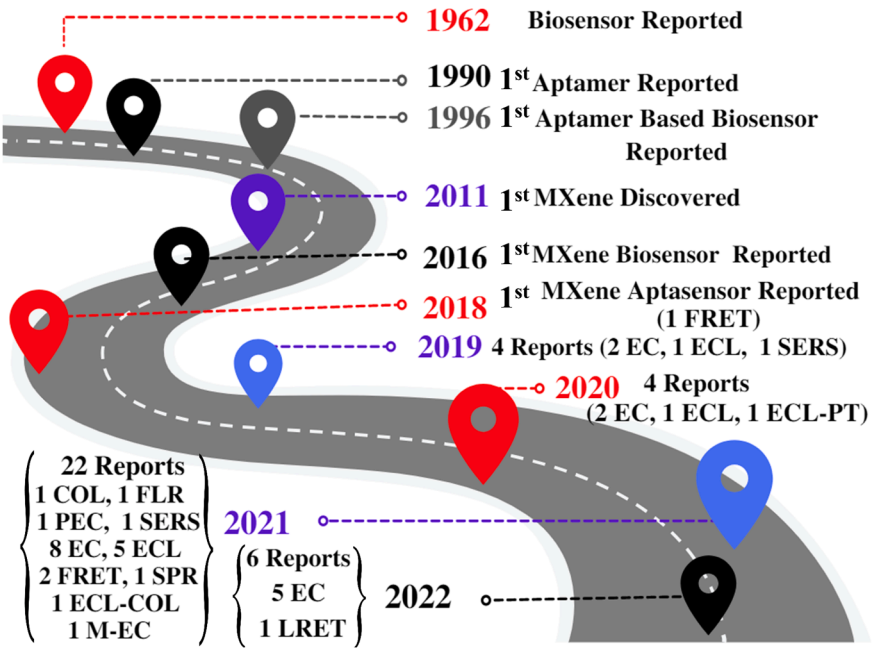

Fig. 1. Story of the MXene based aptasensors. A short journey from October 2018 to March 2022. (COL = Colorimetric, FLR = Fluorescence, PEC = Photo-electrochemical, ECL = Electrogenerated chemiluminescence, SERS = Surface-enhanced Raman spectroscopy, EC = Electrochemical, PT = Photo thermal, FRET = Fluorescence resonance energy transfer, SPR = Surface plasmon resonance, LRET = Luminescence resonance energy transfer, M-EC = Microfluidic electrochemical).

obvious that majority of the research works appeared recently. This is also worth noticing that most of the published aptasensing research works are related to the electrochemical aptasensors, whereas few are related to different types of optical aptasensors.

2. General aspects of MXenes

2.1. Structure

MXenes have a similar hexagonal crystal structure like their parent MAX phase [44]. MAX phases have a general formula of $M_{n+1}AX_n$, where n typically varies from 1 to 4, such that, resulting MAX phases are M_2AX (211), M_3AX_2 (312) & M_4AX_3 (413), as shown in Fig. 2**A**. The MXene possesses a layered structure of stacked nanosheets (NSs) with abundant surface functional groups and a certain amount of point defects. These MXenes are mono transition metal MXenes, however with the discovery of in-plane ordered MAX phases in 2014 [45], and out of plane ordered MAX phases in 2017 [46], the ordered double transition metal MXenes and ordered

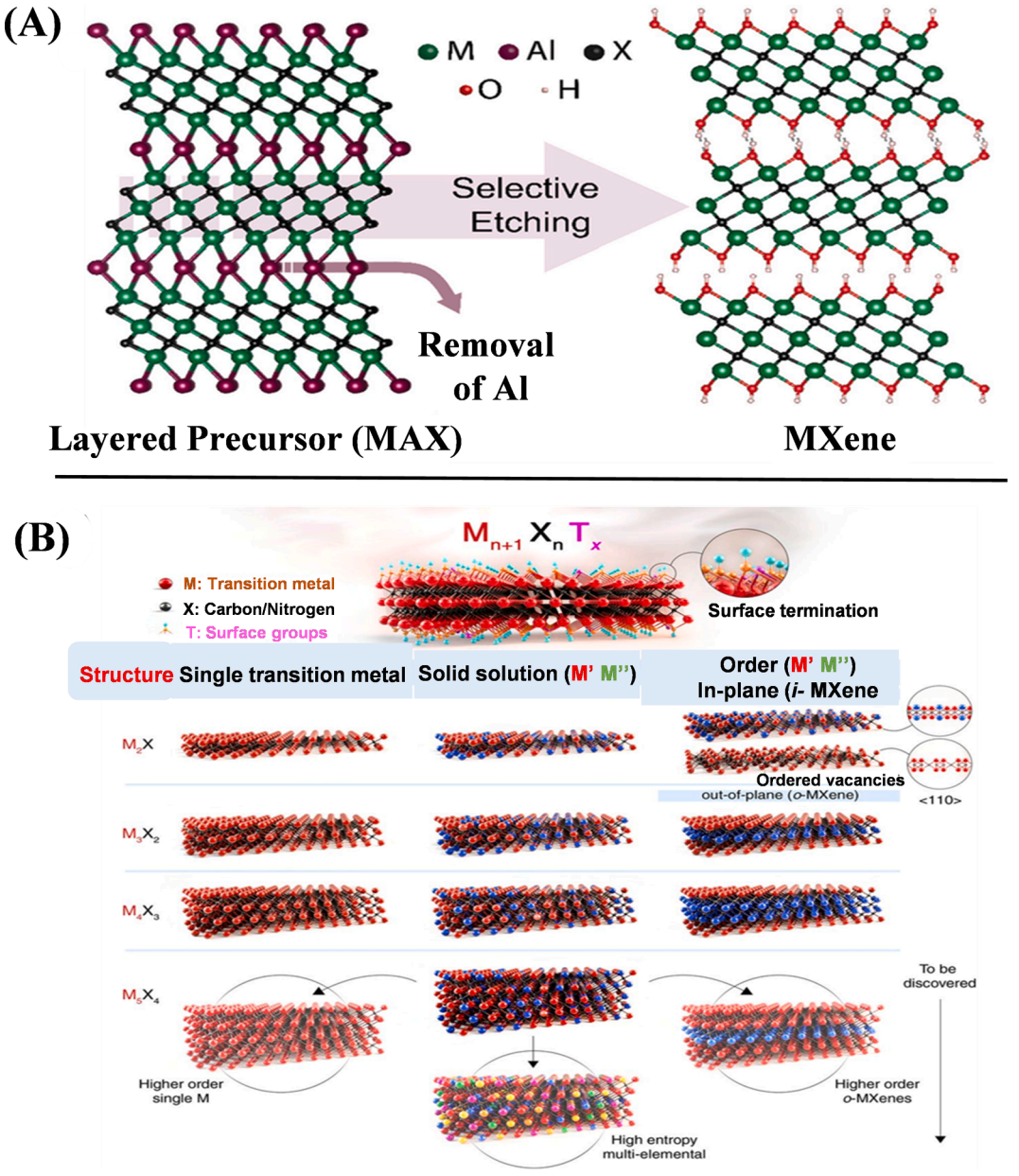

Fig. 2. **(A)** MAX phase and layered MXene crystal structure. Reproduced with permission from [48]; **(B)** Numerous forms of MXenes and their representative structures. Reproduced with permission from [47] @ springer 2019.

divacancy MXenes have also emerged as shown in Fig. 2**B** [47].

The in-plane order MXenes (i-MXenes) refer to the group of MXenes where "M" transition metals are arranged in order in the in-plane direction, whereas in the out of plane order MXenes (o-MXenes), the "M" transition metals are arranged in regular symmetry in the out of plane direction [49]. There exists unlimited possibilities of solid solution MXenes and with the discovery of high entropy MXenes, the number of possible MXene compositions have become limitless [50]. Interestingly, in the MXene aptasensors domain, only few research papers exist based on conventional titanium based MXenes, and there exists a considerable potential in exploring different MXenes structure and composition for aptasensing applications.

2.2. Synthesis

Till date, more than 30 different MXenes have been produced [51] by using different approaches, the details of which can be found in recent review articles [52–54]. The ability to organize metal atoms in-plane and out-of-plane extends the number of potential MXene structures to well over 100 [55]. Surface terminations increase the range of possible MXene compositions by another order of magnitude, while the possibility of forming solid solutions on M and X sites, as well as mixed terminations, leads to a potentially unlimited number of 2D MXenes with distinct properties.

MXenes are typically produced from the selective etching of "A" group metal layer from the parent MAX phase structure where, M represent a metal from early transition metals, A represent the group IIIA or IVA elements and X is either carbon, nitrogen or both. The M—A bonds in MAX are metallic in nature [56], whereas the M—X bonds have a mixed covalent/ionic/metallic character. MXenes are synthesized via top-down synthesis approach by using different methods such as Hydrofluoric (HF) etching, fluoride salt-derived in-situ HF etching, fluoride-free etching, molten salt etching, and electrochemical derived etching of MAX phase. For example, $Ti_3C_2T_x$ is a commonly used MXene, where T_x denotes the functional groups e.g., fluorine (—F), oxygen (—O), and hydroxyl (—OH) groups [57,58]. This section briefly discusses all the synthesis method of MXenes.

i) Hydrofluoric acid etching

MXene were first produced as a result of "A" metal layer etching by using concentrated hydrofluoric (HF) acid (50 wt%) at room temperature [56]. The resultant product was an accordion like structure consisting of bunch of 2D sheets weakly stacked together. The 2D sheets were delaminated by using dimethyl sulfoxide (DMSO) that separated the MXene nanocrystals into single-to-few layer sheet structures. The exposed outer surface of 2D MXene sheets quickly reacts with the species present in the solution (F, OH, O) and make stable bonds resulting in different surface terminations which were denoted with T_x. Soon after, different intercalants, including isopropyl amine, tetra propyl ammonium hydroxide, or tetra-butyl-ammonium hydroxide (TPAOH) followed by sonication, were used to not only assist in the delamination process, but also to increase the d-spacing which would eventually favor the metal ion intercalation for charge storage applications [59]. The HF based etching method has remained a popular method due to its simple one-step process, however, the toxic effects of using concentrated HF could not be overlooked and a continuous effort to develop milder and cheap methods has remained the researchers focus.

ii) Fluoride salt etching

Instead of using the concentrated HF acid, a mild etching condition could be developed by treating the fluoride-based salts (LiF, CaF, NaF, KF, etc.) with dilute hydrochloric (HCl) acid. The concentration of HF as a result is generally between 5 and 10 %, unlike commercially available 50 wt% HF [60]. This method has an obvious advantage that, not only mild conditions are used but delamination step also occurs simultaneously due to the presence of metal ions such as Li^+ [61,62]. Due to small ionic radii, these ions could intercalate the MXene sheets and assist in delamination. Interestingly, such reactions do not require the sonication step, which led to the development of minimally intensive delamination (MILD) procedure [63]. The omission of sonication step resulted in high quality large size MXene sheets which has the ability to be processed into thin films with superior properties such as electrical conductivity. However, the control of different physicochemical properties greatly lies in the optimized experimental conditions which include etching time, etchant strength, reaction temperature, MAX phase stoichiometry, and post etching protocols [64,65,60].

iii) Fluoride-free etching

To avoid the fluoride based etching methods due to toxicity issues and the negative influence that fluorine atoms can bring in decreasing the electrical properties of MXene, recently, efforts are diverted to search for etchants other than fluorine. In this direction, Li et al. [66] reported a hydrothermal alkali-assisted etching process to fabricate fluorine-free $Ti_3C_2T_x$. The entire process was free of fluorine and the resultant product was 92 % pure. Although the reaction conditions of the alkali-assisted method were harsh, the research was instrumental in broadening the scope of using different etching strategies to fabricate MXenes. Interestingly, the fluoride free MXenes were shown to possess better charge storage properties as compared to HF-derived fluorine terminated MXenes [66].

iv) Molten salt etching

In addition to fluoride-/fluoride-free etching, MXene can also be synthesized by treating MAX phases in a mixture of molten salts such as $CuCl_2$, $ZnCl_2$, etc. at high temperatures under argon protection [67,68]. In this direction, Li et al. [69] presented redox-controlled A-site etching of MAX phases in Lewis acidic melts and established the synthesis of different MXenes produced from a large variety of MAX phases containing "A" elements such as Si, Zn and Ga. This approach could etch the otherwise difficult to manage MAX phases, for example, Ti_3SiC_2. This discovery has led to unlimited possibilities and opens up a huge avenue where not only the etching of different MAX phases could be realized, but also the surface chemistry can be tuned with different surface terminations [70].

v) Electrochemical etching method

In continuation to the efforts for finding fluoride free etching methods, electrochemical synthesis of MXene from MAX phase present an interesting alternative. Sun et al. reported the electrochemical etching of Al from porous Ti_2AlC electrodes in dilute hydrochloric acid to form Ti_2CT_x MXene layer [71]. The etching mechanism is similar to the one proposed for fluoride salt based etching

methods with chlorine terminations on the surface of MXene. Li et al. also synthesized electrochemical generated MXene, but by using F-rich electrolyte in a direct application of battery electrode [72]. The as-prepared battery delivers outstanding cyclic stability and rate performance. In contrast to the aqueous based solution processing methods, the electrochemical methods are safer, environmently friendly, and conditions are not harsh. However, the reaction kinetics are generally slow and further efforts are needed to understand this emerging synthesis technique.

vi) Chemical vapor deposition (CVD)

MXenes can also be produced by using bottom-up synthesis methods, such as CVD [73,74]. CVD has been widely employed for producing high-quality and large-area 2D materials which is an effective tool in applications such as integrated electronic devices and flexible optoelectronics [75]. In a typical procedure, the substrate and raw materials are placed in a reaction chamber, and large-scale ultrathin 2D materials are obtained under appropriate conditions. Importantly, the CVD derived MXene crystals have a large lateral size with few defects and they are very stable under ambient conditions, which facilitates the study of their fundamental intrinsic properties [49]. In 2015, Xu et al. synthesized few nanometers thick and over 100 μm in size ultrathin Mo_2C crystals by CVD [74]. The authors used methane as the carbon source and a Cu foil placed on a Mo foil at a temperature of ~1100 °C. The most important advantage of this method is that it circumvents the need for transfer processes, which are usually required for vertically stacked 2D heterostructures [76]. Although this is a truly exciting method, the synthesis process is slow with low yields and required high temperatures [76].

2.3. Properties

Ultrathin 2D MXene materials exhibit versatile chemical, physical, mechanical, and optical features. They have a wide spectrum of electronic characteristics including metallic, semimetal, semiconducting, and insulating properties [57]. The atomic thickness offers superb mechanical flexibility and optical transparency. MXene exhibit exceptional electrical conductivity of ~20,000 S/cm, which is the highest reported so far for any synthesized nanomaterials [77]. Due to their unique layered structure, MXene offers an invaluable opportunity to intercalate metal ions such as Li, Na, and K, which could help fabricate high energy storage devices [52]. The M—X bonds are very strong, and as a result the produced MXenes could exhibit outstanding mechanical properties as evident with a very high value of Young's Modulus > 330 GPa [78]. The UV and visible light absorption are important properties for photocatalytic, optoelectronic, photovoltaic, and transparent conductive electrode applications. The MXene films could absorb the light in UV–Visible range from 300 to 800 nm, at nanometer thickness with over 91 % transmission. MXene exhibit a strong absorption band in ~700–800 nm range, which is important for photo-thermal therapy (PTT) applications. The rich surface chemistry of MXenes provides numerous catalytically active sites which are crucial in chemical reaction such as water splitting, CO_2 reduction, nitrogen reduction, and others. The ability of variation in the surface terminal groups over MXene sheets expands the chemical properties to accommodate a wide range of applications [79,80].

MXene also possesses a reasonable thermal conductivity and could deliver the thermal heating potential arising from the Joules heating phenomenon [77]. MXene's inherent ability to tune properties through the use of different transition metal(s), carbon/nitrogen, and surface functionalities is unique to the field of 2D-NMs [81]. Based on the type of application, different properties of

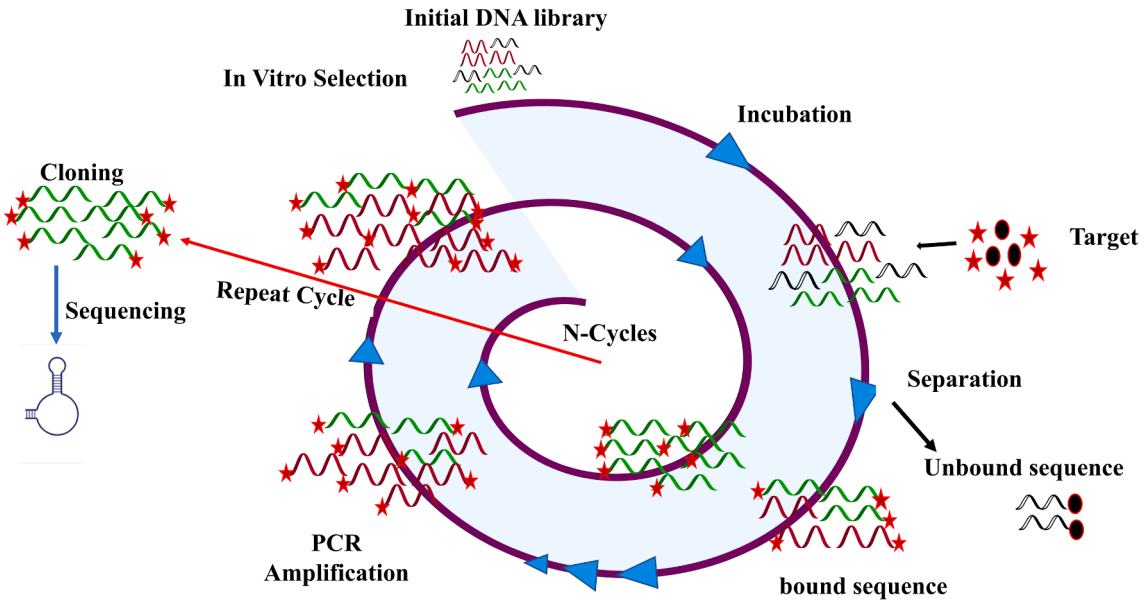

Fig. 3. Schematic diagram to show the basic steps such as incubation, separation and PCR amplification involved in a generalized conventional SELEX for DNA aptamer selection.

MXenes can be achieved by tweaking the chemical composition and manipulating the surface functionalities [82].

3. The aptamers, their selection, and the role of MXenes in biosensors and aptamer based biosensors

Biosensors have emerged as an essential component of laboratory medicine's state-of-the-art device, notably in point of care testing [83]. Biosensing platforms are frequently used for the quantification, detection, and analysis of biomolecules with substantial health implications [84,85]. Analytical devices like biosensors have two key components: a bio-recognition component like enzymes, antibodies or nucleic acids, and a transduction part for transmitting signals via electrochemical or optical means to display quantitative analytical data and measurable signals [86,87]. Signal transduction and bio-recognition element loading are critical in biosensor configuration. Integrating bio-recognition features into biosensors increases their specificity and sensitivity. Interfaces with maximum loading capacities of recognition components and strong biocompatibility are therefore essential [88]. When transforming from biosignals to optical or electrical signals, a transducing element with superior electrical conductivity and surface area is recommended since it yields higher output signals while producing less noise. 2D materials are frequently used as photon-electron or electrode interface materials in optical and electrochemical (EC) biosensors.

Aptasensors recognize biomolecules using single-stranded DNA (ssDNA) or RNA aptamers [86,89,90]. These oligonucleotide sequences exhibit high specificity and affinity against various biomolecules and are selected *in-vitro* using Systematic Evolution of Ligands by Exponential Enrichment (SELEX) from randomized nucleic acid libraries [9,10,91]. Tuerk et al. were the first to select an RNA based oligonucleotide against bacteriophage T4 DNA polymerase [10], followed by Ellington et al. who selected an RNA oligonucleotide the same year against an organic dye [9]. They were subsequently termed as "aptamers", the name derived from the Latin word "aptus", which means "to fit" [92]. Conventional SELEX, based on the preferred aptamer requirements, involves several steps. To screen DNA aptamers, target molecules are incubated with a specially designed DNA library. After incubation, the DNA-target complexes or the bound sequences are retained while removing the unbound sequences. A Polymerase Chain Reaction (PCR) is used to amplify the bound sequences (Fig. 3). This process is repeated for several selection cycles to get enriched sequences, which are then sequenced and characterized to analyze their binding kinetics in various ways [93], for example, surface plasmon resonance (SPR), circular dichroism (CD), and isothermal titration calorimetry (ITC) [94], etc. Several other techniques can also be used to precisely investigate the binding kinetics between a target and their aptamer [95]. Even though the traditional SELEX method was not meant to be used for aptamer selection, it was changed repeatedly to meet the needs of the desired aptamers and eventually became the main way to screen aptamers. The SELEX technique has been continuously modified and improved over the last three decades to fulfill a variety of requirements [96]. Recently, aptamers can be selected using various techniques in just a few hours, rather than the weeks or months as compared to traditional SELEX. Modern strategies assisted by computer software systems enable the prediction of binding affinity of an aptamer and structure prior to its selection, significantly reducing the cost of the selection process [93]. Structure-switching particle display, molecular dynamics simulation, and a few other methods have also been used for aptamer selection [95].

To date, the literature has documented over 1000 well-characterized high affinity oligonucleotide aptamers to detect or quantify a variety of analytes (from small molecules to whole cells or tissues). In the last few years, the number of papers on aptamer technologies has undergone exponential growth. Biosensors are the primary focus of most aptamer technology investigations [96]. Drolet et al. and Davis et al. published the first biosensor based on aptamer in 1996 [97,98]. Following that, aptamers were coupled to a variety of sensing platforms (electrochemical, surface-enhanced Raman scattering, fluorescent, and colorimetric) for the purpose of analyzing the target molecules in the sample [99]. In a recent review on aptasensors, Zahra et al. have discussed the fundamentals and the design strategies used to develop the most common types of aptamer-based biosensors [100]. These include pre-programmed techniques to convert aptamer identification actions into readable signals [101].

Aptamers act as molecular bio-recognition element when they fold into distinct tertiary or secondary structures, allowing them to detect and bind target with greater affinity (the dissociation constant K_d values range from micro-molar to pico-molar concentrations) [102]. Proteins, metal ions, small organic molecules, cells, tissues, bacteria and viruses, etc. are among some of the possible targets [31]. To put it another way, because of the peculiar features of aptamers e.g., high chemical stability, cost-effectiveness, and in vitro synthesis [103], they can be used as beneficial molecular recognition markers in the development of high-efficiency biosensors [104,105], and have garnered a huge interest in the last 30 years from a range of research disciplines, including disease diagnostics [106–109] and food safety [110], etc. The fundamental step in developing an aptasensor is immobilizing the aptamer on a substrate. A variety of aptamer immobilization techniques have been documented in the literature. Controlling the immobilization process is critical for ensuring the high stability, accessibility, orientation, enhanced target binding, and reactivity of the aptamer as well as avoiding non-specific adsorption processes. To prevent non-specific binding of interfering molecules, an affinity reaction must be conducted with the target. The immobilization method chosen is determined by the detection principle and assay format, and it is believed to have a direct effect on the capability of aptamer to bind the target. The size of the target molecules determines the format of the assay and the mechanism for aptasensing. Once the target is captured on the sensor surface, multiple approaches for transducing the bio- recognition event can be employed [111]. Since the aptamer immobilization and binding occur at the surface of transducer, effective transducer utilization is vital for developing promising aptasensors [112]. As previously stated, MXene has shown to be an excellent substrate for transducer surface applications.

Aptamers are compatible with a wide range of diagnostic and biosensor platforms, allowing them to contribute significantly to the global diagnostic sector [113]. Even though aptamer-based sensors are still in their early phase of development in comparison to enzyme-based biosensors and immunoassays, nevertheless when combined with NMs, they have the potential to become powerful biosensing tools in the future [114]. To facilitate bio-functionalization, 2D-NMs that combine the advantages of an abundance of active sites, stable dispersity, and superior biocompatibility are extremely competitive. While aptamers, enzymes, and antibodies are

frequently exploited as recognition components in the construction of biosensors, MXenes typically provide an excellent transducing platform and circumvent some of the constraints associated with graphene or other related materials [88,115]. MXenes' fundamental features make them an excellent candidate for use as a biosensor material. Biosensing technology based on MXene has advanced at a breakneck pace over the last several years. Because of their exceptional combination of properties, MXene materials together with an effective bio-recognition platform have been demonstrated to be a highly selective and sensitive detection system for biosensor applications despite their extremely short journey [38]. Nanotechnology has enabled the coupling of various nanomaterials with aptamers, resulting in extremely selective and sensitive aptasensors that have added great value to the diagnostics and analytical fields. The unique features of NMs, including shape-and size-dependent optical properties, catalytic activity, and flexible tuning of surface chemistry, make them extremely valuable for signal induction and amplification [116–119]. The combination of NMs and aptamers has been extensively investigated in order to build sensitive and unique sensing devices [17]. It is essential to synthesize reliable, stable, and reproducible nanostructures that could offer an appropriate environment for the immobilization of recognition components (i.e. aptamer or other probes), before moving on to building biosensor techniques for use in complicated bio-environments [120]. Composite NMs have now been widely used in EC biosensors for labelling and signal amplification [121–124]. Even though MXene was originated in late 2011 and possessed excellent intrinsic physicochemical features, the very first MXene based biosensing device was introduced in 2015. MXenes were introduced by Xu and colleagues for probing neural function [125]. They developed a very sensitive field-effect transistor (FET) biosensor based on extremely thin MXene micro-patterns for label-free probing of small molecules under ordinary biological settings and rapid identification of action potential in primary neurons. This discovery provided a new pathway for biosensing applications based on MXene, allowing more scientists to discover the significance of this broad family of 2D NMs known for their superior electrical behavior [126].

MXenes have the ability to interact with various biomolecules via coordination bonds, electrostatic interactions, van der Waals forces, and hydrogen bonds [127], making them an ideal interface for biosensor development [128]. The long-term durability of the constructed MXene biosensors ensures great reproducibility of data over time, which might be immensely beneficial when using these biosensors for a variety of diagnostic applications. MXenes' high biocompatibility and increased surface area provide an impetus for incorporating innovative nano(bio)hybrid frameworks with bio-receptors such as antigen-antibody (Ag-Ab), enzymes, protein, whole cells, and aptamers (DNA/miRNA) that enable suitable integration of biomolecules onto their surface to behave as a sensitive recognition interface. It is anticipated that these advances in the construction of MXene based biosensors will further contribute to the emergence of modern detection methodologies utilizing techniques such as EC, colorimetric, and fluorescent luminescence for the highly selective identification of multiple biomarkers for use in point-of care diagnostics and early detection of diseases [38]. Recently, the development of 2D NMs-based biosensors for ultrasensitive disease diagnostic testing applications, such as the identification of tumor biomarkers existing in ultra-low amounts in various clinical samples (e.g., urine, serum, blood, and tissues), has been driven by emerging concepts in bio-sensing systems and their translation into clinical trial [129,130]. Thus, in the sensing arena, combining various functionalized nanomaterials (including MXenes) with aptamers is expected to open new opportunities in next-generation biosensors. Numerous advanced aptasensors have been employed exclusively to fabricate field-deployable and clinical analytical devices in view of their excellent optical, thermal, mechanical, and electronic features [20].

4. Advances in MXene-based aptasensors

To construct MXene aptasensors, it is crucial to immobilize aptamer on the surface of MXene that acts as a transducer [31]. Therefore, covalent, and non-covalent functionalization techniques for the aptamer immobilization over MXene are being studied actively. The functionalization of MXene is promoted by the abundant hydroxyl groups on the surface of MXene. For example, a facile reaction with triethoxysilane derivatives was designed to functionalize MXene via silanization [131–133]. This modification resulted in the formation of Ti_3C_2-MXene NSs evenly patterned with amino silane groups, enabling covalent immobilization of bioreceptors including aptamers [134] antibodies, and anti-carcinoembryonic antigen via EDC/NHS -based amine coupling [39]. Another possible method of MXene surface modification involves coupling with zwitterions. It was demonstrated that sulfobetaine (SB) and carboxybetaine (CB) variants can be grafted spontaneously onto $Ti_3C_2T_x$ MXenes [135]. The method is comparable to the spontaneous grafting of diazonium salt modified zwitterions to gold nano-shell modified molecules via the consumption of surface plasmons (free electron cloud) inside the Au nano-shells [136], followed by the immobilization with a thiol labelled aptamer [137]. Han et al. established an interesting strategy by covalently coupling Polyethylene glycol (PEG) to the MXene surface for biosensing [138]. They employed (3-aminopropyl) triethoxysilane (APTES) as a linker between PEG and MXene. It was assumed that on one end, the APTES is able to form bonds with —OH groups, while on the other end, MXene can effectively create bonds with amino groups [139].

In another method by Wang and co-workers [140], polyacrylic acid was used to wrap Ti_3C_2 MXene to increase its dispersion and stability by providing functional groups, which in turn employed to covalently link the bioreceptor (a dual signal-tagged chimeric DNA probe (dcDNA)). The authors studied the fluorescence quenching efficiency of Ti_3C_2 MXene NSs for ultrasensitive detection of MCF-7 cells. At nanomolar concentration ranges, a dcDNA-functionalized Ti_3C_2 probe (dcDNA-Ti_3C_2) was used for in-vitro, real-time and multilayer simultaneous fluorescence imaging of cytoplasmic microRNA-21 and plasma membrane glycoprotein MUC1 [140]. To further enhance the MXene functionality, the 2D surface can be functionalized through physical adsorption and non-covalent interactions [141,142]. For example, Zheng et al. [143] demonstrated in-situ DNA adsorption on the surface of MXene via aromatic hydrophobic bases, which was then tailored by PtNPs and PdNPs to synthesize a Pd/Pt/Ti_3C_2/DNA hybrid to recognize dopamine. Initially, dsDNA was denatured to produce ssDNA, which was then immobilized on the MXene surface via π–π stacking between MXene structure and the aromatic nucleobases of DNA. After $PdCl_2$ was combined with ssDNA/MXene composites, Pd cations (Pd^{2+}) were electrostatically deposited on the phosphate backbone of negatively charged ssDNA oligonucleotide and acted as nucleation sites for

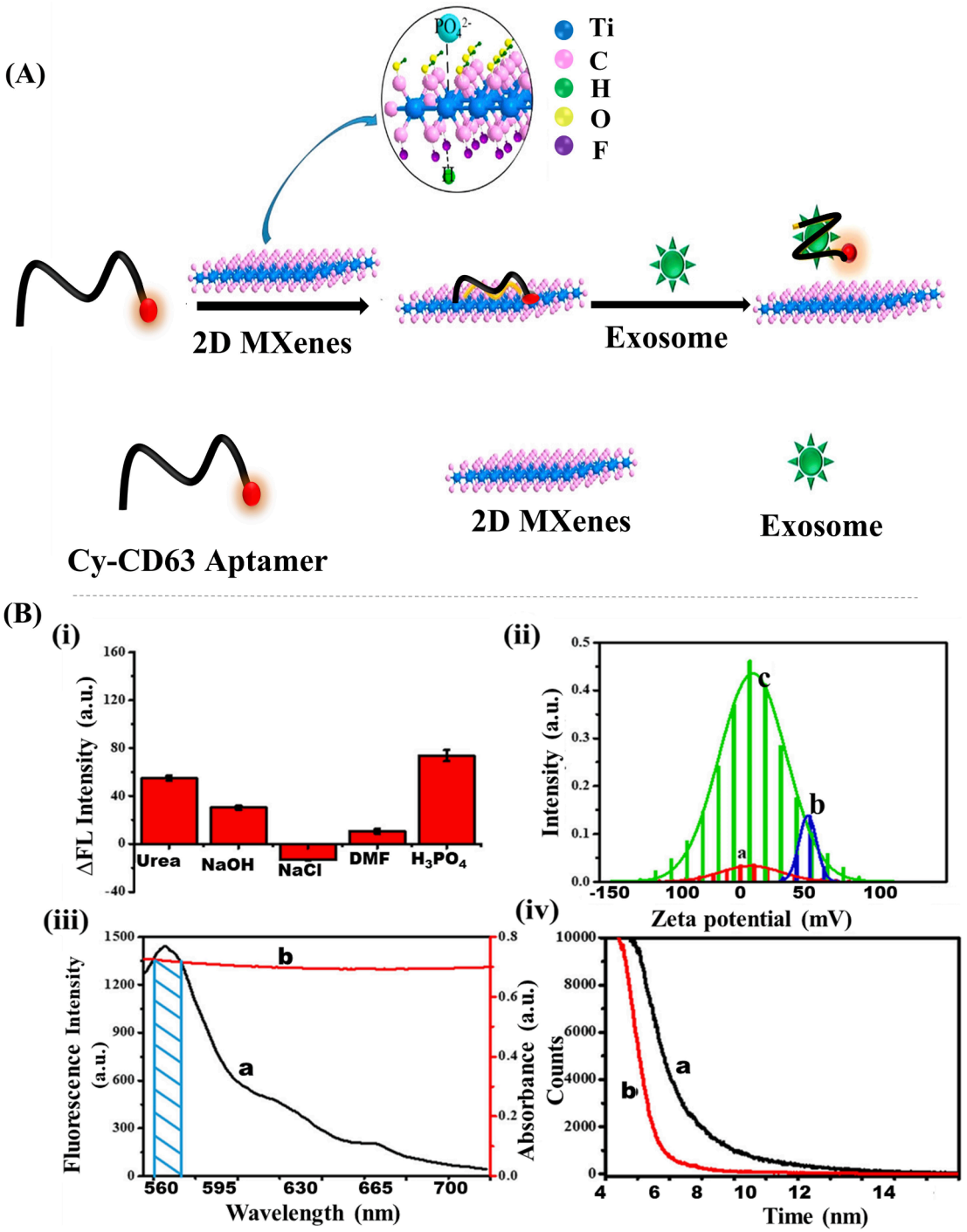

Fig. 4. (A). Fluorescent aptamer-Cy3-CD63 solution added into MXene solution. Exosomes were then added into it as target. The aptamer fluorescence was significantly quenched upon mixing it to MXenes in the first step. The fluorescence quickly recovered upon the addition of target exosomes. **(B)**-(i) ΔFL fluorescence intensities of reporter signal probe in varying environments such as H_3PO_4, urea, NaCl, NaOH, and DMF. (ii) Zeta potential measurements of (a) MXene NSs (b) aptamer and (c) aptamer + MXene. (iii) Fluorescence intensity of (a) aptamer Cy3-CD63 and the (b) UV–vis of MXene. (iv) the lifetime of fluorescence of (a) aptamer Cy3-CD63 and (b) MXene + aptamer Cy3-CD63. Reproduced with permission from [128] @ ACS 2018.

the formation of PdNPs. To improve the catalytic behavior, PtNPs were also grown [143]. Apart from physical adsorption, another technique for coupling aptamers to transducer surfaces is via electrostatic adsorption. In neutral buffers with a low osmolality (less than 100 mM), the negatively charged aptamers are adsorbed electrostatically on the surface of positively charged transducers [31]. Mn^{2+} has been shown to facilitate DNA adsorption onto unaltered Ti_2C MXene NSs, and its non-quenching feature makes it an exceptional candidate for biosensor applications. This demonstrates that Mn^{2+} facilitates DNA adsorption through the phosphate backbone, producing an electrostatic contact between Mn^{2+} and DNA, resulting in DNA adsorption on the MXene NSs [144]. Electrostatic interactions allow the immobilization of an HB5 aptamer on MXene layers with a remarkable selectivity against HER-2 positive cells in bio-sensing [145]. Moreover, an electrostatic interaction-based nanopore DNA sequencing method has been developed using MXene membranes [146]. Metal chelation and hydrogen bonding interactions enabled ssDNA to be adsorbed easily on an ultrathin Ti_3C_2 NSs surface [147]. Thus, MXene-based aptasensors have shown the ability to rapidly detect a wide range of targets. Herein, we give a comprehensive overview of the recent advances in the design, fabrication, and biomedical sensing applications of MXene-based aptasensors within the last three and a half year (since the introduction of the first MXene aptasensor in October 2018 to March 2022) for the detection of various cancer biomarkers/cells, mycotoxins, and other targets of biological importance.

4.1. Aptasensors for cancer diagnostics

Exosomes are nanosized (diameter 30–100 nm) extracellular vesicles released by mammalian cells that can be used for disease diagnostics and molecular monitoring and have recently become a research focus [148–150]. Exosomes were shown to be involved in the anticancer immune response and could be useful in the diagnosis of cancer-related public health problems. Notably, exosomes provide a multitude of molecular information received from microRNA, originating cells, proteins, and information relating to intercellular communication [151–153]. As a result, employing exosomes as markers has the potential to address present technological challenges in cancer diagnostics, including the cost of invasive screening, limited selectivity, and difficulty in early cancer diagnosis [154,155]. As per the literature, exosomes contain a unique protein called CD63 that is involved in membrane fusion, invasion, and membrane transport, which makes exosome detection convenient and simple [156]. The structure, functions, and sequence of CD63 aptamer have all been extensively investigated in the last decade, thanks to its ability to identify exosomes with high specificity. For this reason, the development of appropriate CD63 sensors is advantageous to address the inherent problems in simple and fast molecular analysis [128]. Zhang et al. tested the effectiveness of aptamer immobilization on MXene to develop a fluorescence ratiometric sensing system for exosome detection [128]. Cy3-CD63 aptamer probe was adsorbed onto MXene NSs, quenching Cy3′s intrinsic fluorescence. When exosomes containing the CD63 surface protein are present, the aptamer Cy3-CD63 preferably binds to the exosomes, allowing the fluorescence of Cy3 to be retrieved (Fig. 4A). The large surface area of MXenes is considered to facilitate aptamer adsorption via noncovalent interactions, while remarkable electronic features and a broad absorption spectrum play a role in quenching the fluorescence. Further experiments were conducted to explore the binding mode of MXene NSs with the Cy3-CD63 aptamer. Multiple desorption substances were introduced to examine the interaction mechanism between them, including a high dose of urea, which is considered to disrupt the hydrogen bond (confirming the existence of a hydrogen bond). The fluorescence restoration was marginally enhanced upon adding urea **(**Fig. 4**B-i)**, implying the presence of hydrogen bonding between them. The NaOH addition resulted in the desorption of aptamer from the MXene surface due to the increase in pH of the system. The NaCl addition resulted in high electrostatic adsorption, indicated by a slight decrease in the fluorescence. Interestingly, there was no substantial desorption of aptamers on the addition of an organic solvent, dimethyl formamide (DMF), showing the existence of some hydrophobic behavior. The nucleobases, phosphate, and functional groups of DNA are necessary for adsorption by hydrogen bonds (Fig. 4B-i).

Zeta potential results were used to investigate the fluorescence quenching mechanism (Fig. 4B-ii), and that the quenching process was not induced by electrostatic interactions. Overlapping the aptamer Cy3-CD63 fluorescence with the UV–vis of MXene, quenching was possibly caused by FRET (Fig. 4B-iii). When MXene NSs were added to the Cy3-CD63 aptamer to make the fluorescence probe, the fluorescence lifespan went down **(**Fig. 4**B-iv)** [128].

Using the *in-situ* produced aptamer-MXene-AuNPs nanocomposite for ultrasensitive recognition of exosomes, Zhang et al. [157] constructed an ECL aptasensor based on the CD63 aptamer-modified SA-PAM (sodium alginate (SA), and poly(acrylamide) (PAM)) electrode interface. The AuNPs were prepared *in-situ* on single layer Ti_3C_2 MXenes with the aptamer modification (AuNPs-MXene-Apt) where MXenes performed as both the stabilizer and the reductant (without necessitating extra stabilizer or reductant). MXene also provided conductive support to load more AuNPs and an abundance of active sites for recognition function. The AuNPs-MXenes-Apt nanohybrid made it possible to detect exosomes very well because it gave the catalytic surface the remarkable electro-catalytic properties of AuNPs, which made the luminol signal much better. The aptasensor was highly selective for exosomes, and proteins on their surface generated from several different cancerous cell lines (such as HepG2, OVCAR and HeLa, etc.). For exosome physiological function investigations and clinic diagnostics, it proved to be an extremely useful tool [157]. A high efficiency MXene-BPQDs (Black phosphorus quantum dots) nanoprobe was designed by Fang et al. [158] to determine the presence of exosomes using a photothermal and ECL dual-mode aptasensor. The peculiar structure of the SiO_2 Nano-urchin (SiO_2 NUs) was used as a sensing platform, thus offering aptamer with several immobilization sites. Exosomes could be captured using the aptamer's ability to recognize the EpCAM protein. As a result of the exosomes being altered on the electrode, they could recognize a signal probe labelled with Ab_{CD63}, allowing for the detection of exosomes using photo-thermal and ECL signal readouts simultaneously. This experiment effectively combined photo-thermal and ECL platforms together for the detection of exosomes, resulting in more promising outcomes [158].

Zhang et al. [159] designed an ECL sandwich aptasensor for exosome detection employing aptamer immobilized MXene NSs as an ECL nanoprobe. The ECL performance of luminol (100 μM luminol) were investigated using a (i) bare GCE electrode in comparison to

(ii) GCE electrode modified with MXene (GCE/MXene electrode). A comparison of the ECL performance on the GCE/MXenes electrode (curve b) and the bare GCE electrode (curve a) shows that MXenes significantly augment the ECL of luminol **(**Fig. 5**A)**. Nitrogen saturation suddenly reduced the ECL signal of the GCE/MXene electrode (curve c). Superoxide dismutase (SOD) introduction significantly lowered the ECL signal (curve d). According to these findings, the ECL performance of luminol was considered to be dependent on oxygen. The electro catalytic features of MXenes were thought to be responsible for the ECL behavior of luminol because they can accelerate O_2 reduction in a solution that contains trace oxygen. Light was subsequently emitted after the reactive oxygen species, including $O_2\bullet$, oxidized luminol to create 3-aminophthalate. These findings show that luminol on a GCE/MXenes electrode can behave in a way that makes it possible to make high-sensitivity ECL biosensors. To further ensure that an ECL aptasensor was more sensitive in the presence of MXene, a set of control experiments were carried out for ECL performance measurements. As depicted in the Fig. 5**B,** [159] the ECL emission spectra of the bare GCE electrode (curve a), GCE/AuNPs (curve b), and GCE/AuNPs-PNIPAM (Poly N-isopropylacrylamide) (curve c) without the incubation of Apt1 and exosomes exhibited slight emission. Additionally, the GCE/AuNPs-PNIPAM/Apt1 (curve d) and GCE/AuNPs-PNIPAM/Apt/exosomes (curve e) without Apt2-MXene nanoprobe adsorption

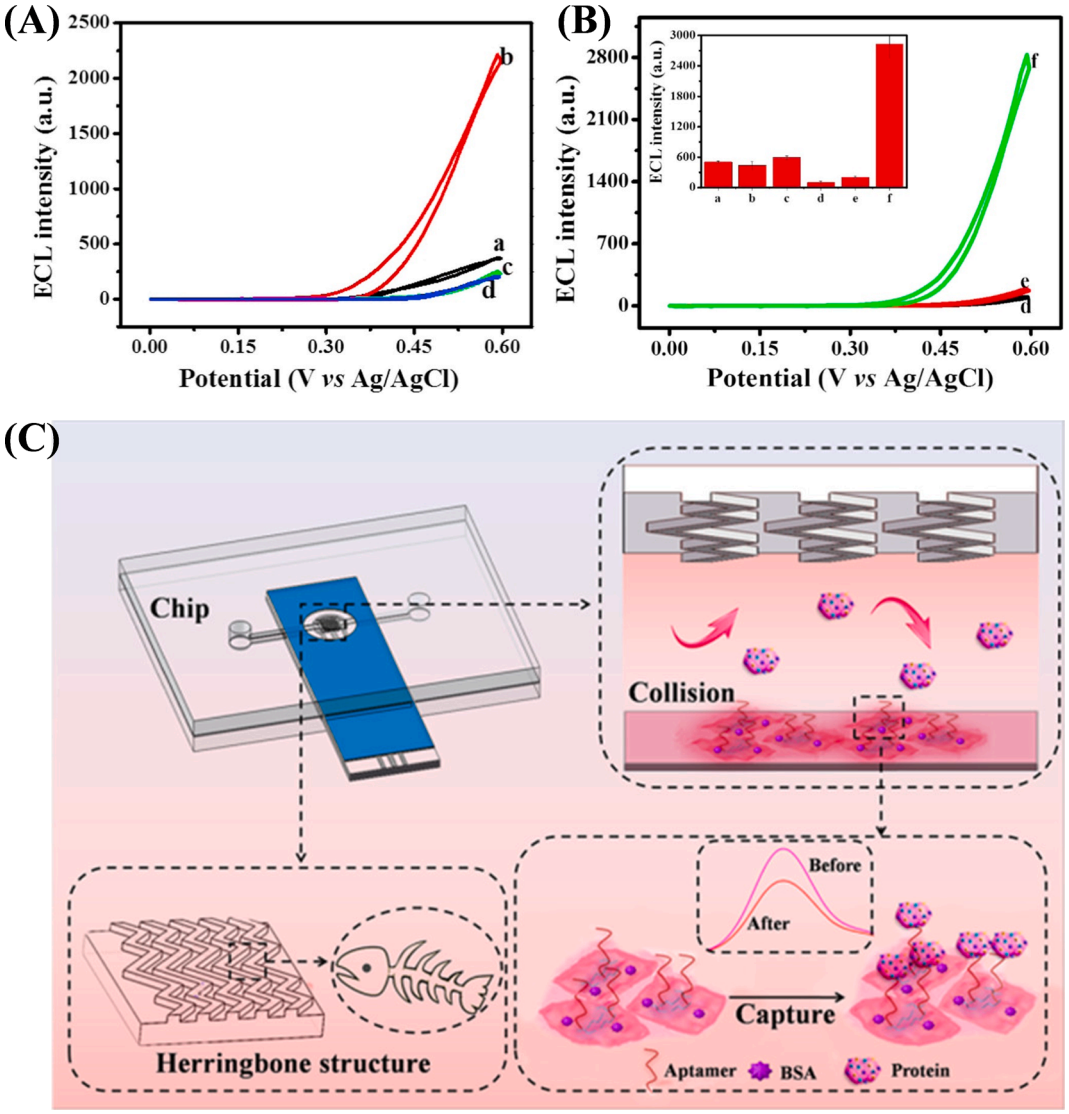

Fig. 5. (A) The ECL performance of a bare GCE electrode (curve a), GCE electrode modified with MXene (curve b) in 100 μM luminol. Curve c depicts the ECL intensity upon saturation with nitrogen, and finally the addition of SOD without de-aeration (curve d) (experiment was conducted in 100 μM luminol). **(B)** ECL performance of electrodes in 100 μM luminol (a) a bare GCE electrode, (b) GCE/AuNPs, (c) GCE/AuNPs-PNIPAM, (d) GCE/AuNPs-PNIPAM/Apt1, (e) GCE/AuNPs-PNIPAM/Apt/exosomes, (f) and GCE/AuNPs-PNIPAM/Apt1/exosomes/Apt2-MXene. The scan rate and photomultiplier tube (PMT) voltage was 100 mV s^{-1} and 600 V, respectively. The potential was 0–0.6 V (vs Ag/AgCl). The exosomes concentration was 1×10^5 particles μL^{-1} [159] @ Elsevier 2019. **(C)** Schematic view of the microfluidic electrochemical aptasensor and its use for the detection, capture and enrichment of carcinoembryonic antigen (CEA). Reproduced with permission from [164] @ ACS 2021.

demonstrated decreased ECL signals, attributable to the exosomes and Apt1 inhibiting electron transfer at the electrode interface. In comparison, a biosensor that was assembled with all the above-mentioned components demonstrated a remarkably high ECL signal (curve f). These findings suggest that Apt2 exhibits a great affinity for exosomes, and the increase in the ECL performance might be attributed to the Apt2-MXene nanoprobe's outstanding electron transport and electro catalytic abilities. Due to the large surface area of the Ti_3C_2 NSs, these were used as a nanocarrier to load a greater proportion of aptamers, enabling exosome identification with high sensitivity. The electrode surface was modified with an EpCAM protein binding aptamer (Apt1) to efficiently collect exosomes expressing EpCAM protein on their surface. To create a PEI/MXene hybrid, polyethylenimine (PEI) was electrostatically interacted with MXene. Using an amine-coupling approach, the positively charged hybrid was covalently linked to an aptamer (Apt2) specific for CD63 protein found on the exosomes surface. The catalytic features and high conductivity of Ti_3C_2 NSs can enhance electron flow across the electrode interface (MXenes-Apt2/exosomes/Apt1/PNIPAM-AuNPs/GCE), hence amplifying the ECL signals of the luminol. Subsequently, even in the absence of co-reactors, for example, H_2O_2, the ECL signal of luminol can be greatly enhanced. For the detection of exosomes in the serum samples, the ECL aptasensor worked effectively. This method provides a reliable, sensitive, and practicable means of detecting exosomes in clinical diagnostics [159].

The glycoprotein carcinoembryonic antigen (CEA) is a diverse tumor marker linked to colon, breast, and lung cancers [160,161]. CEA levels in the bloodstream of cancer patients are substantially greater than in healthy people [162]. As a result, reliable CEA detection in the blood is critical for clinical cancer detection and early diagnosis [163]. An integrated microfluidic-electrochemical aptasensor for the quantification of CEA was proposed by Zhao et al. [164]. The biosensing interface was constructed using a screen-printed carbon electrode (SPCE) customized with a unique nanocomposite called hemin-coated carboxylic carbon nanotube-decorated Ti_3C_2 NSs (He@CCNT/Ti_3C_2). Next, a microfluidic chip equipped with a herringbone construction was attached to the biosensing interface to create vertical fluid flow, which might increase the unique association between aptamer and CEA ligand. Following CEA capture, the development of an insulating protein layer reduces the efficiency of electron transport and thus the current signal. An electrochemical sensor chip for CEA determination was designed in accordance with the signal variations observed in the presence or absence of CEA, showing a promising future in the field of disease diagnostics (Fig. 5**C**). The advantages of this approach are as follows: (i) by combining the microfluidic system with electrochemical sensing, the mobility of the sensing device has been

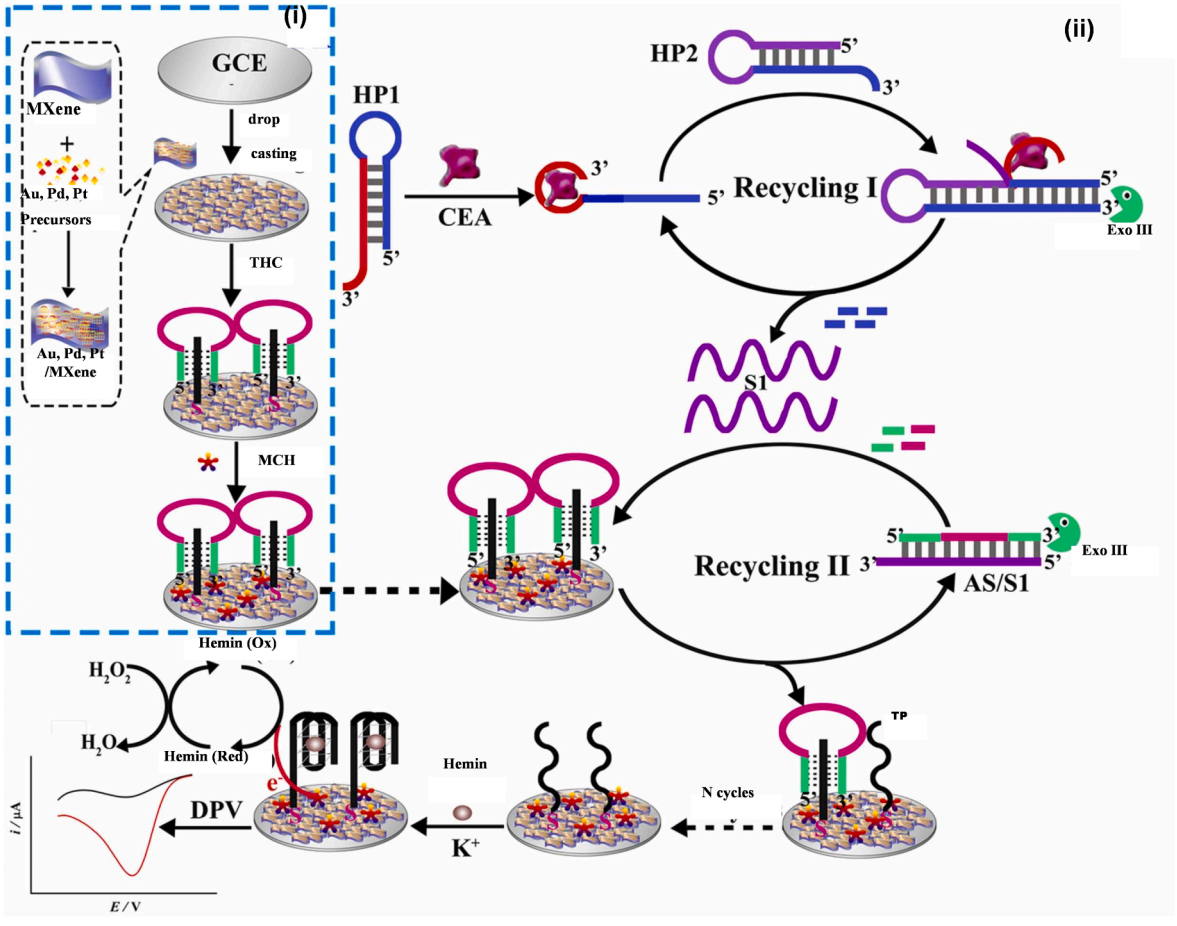

Fig. 6. **(i)** The Au-Pd-Pt/$Ti_3C_2T_x$ nanocomposite synthesis route and the sensing interface fabrication. **(ii)** The dual recycling amplifications assisted by Exo III for catalytic detection of carcinoembryonic antigen (CEA). Reproduced with permission from [165] @ Elsevier 2022.

significantly increased; (ii) the process of sample injection, enrichment, capture, and sensing has been done on a single integrated chip, which makes it easier to use; and (iii) the effect of drag force on target-aptamer interplay has been thoroughly discussed [164].

Song et al. [165] established a label-free sensor for the detection of CEA that combines a trimetallic nanocomposite Au-Pd-Pt/$Ti_3C_2T_x$ with a dual amplification system aided by Exo III and a catalytic interface in the form of a modified electrode (Fig. 6). Conformational transformation of the HP1 aptamer sequence (shown as the red region) occurs when it binds to CEA to make a CEA-HP1 complex, with the subsequent conformational shift and exposure of HP1 toehold at the 5′ end (shown as the blue region). The complex then hybridizes HP2 to make CEA/HP1/HP2 via a 3′ blunt end (active platform for Exo III). Exo III initiates recycling I by breaking the mononucleotides free from the CEA/HP1/HP2 complex's blunt 3′ end. This releases the HP1/CEA complex and the single-stranded DNA sequence (S1) to make a lot of S1. Additionally, the AS sequence in the triple-helix complex probes (THC) framework combines with S1 to construct the S1/AS duplex structure with a blunt 3′ part on one end that can be metabolized by Exo III to generate S1 and initiate cyclic separation of AS, resulting in the production of numerous free G-quadruplex-carrying thiolated probes (TP) (Recycling II) (Fig. 6). After the G-rich region of TP is stabilized with K^+, it can be folded into a G-quadruplex, which can subsequently bound to hemin to form hemin-G-quadruplex assemblies. These assemblies can activate enzymes that reduce H_2O_2 over Au-Pd-Pt/$Ti_3C_2T_x$/GCE to produce significantly better current responses for monitoring CEA at early stages with high sensitivity [165].

Mucin1 (MUC1), a transmembrane glycoprotein with a large molecular weight, has been identified as a biomarker towards early diagnosis of breast cancer attributed to its aberrant expression in cancer tissues [152,153,166]. For that reason, developing a highly

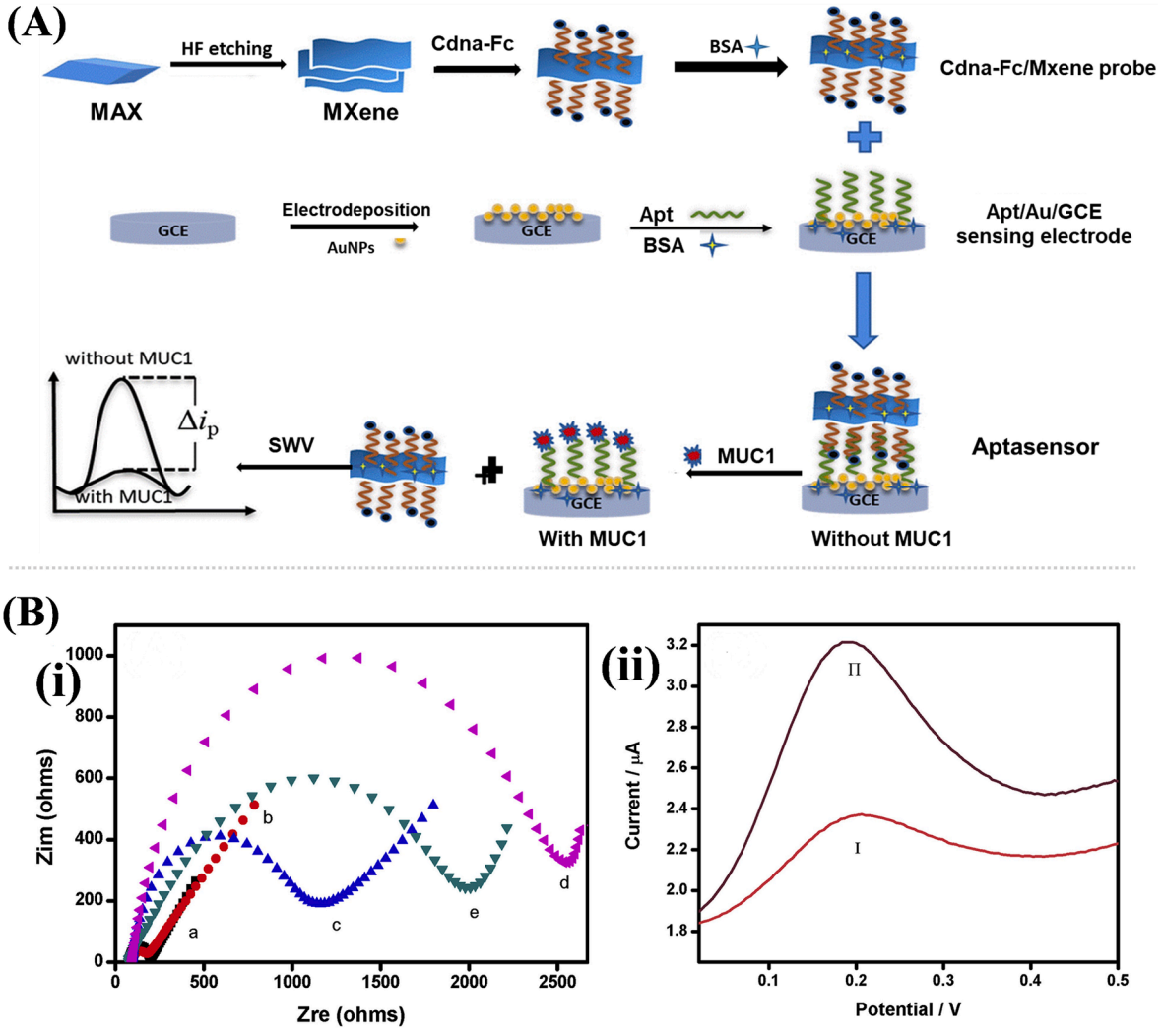

Fig. 7. **(A)** Schematic drawing of the construction method for a highly competitive EC aptasensor. cDNA-Fc probe binding on MXene nanosheet surface, the immobilization of aptamer on the sensing electrode decorated with AuNPs, and the coupling of aptamer containing electrode with MXene probe in the absence of MUC1. **(B)-(i)** EIS spectra (in 5 mM $K_3[Fe(CN)_6]/K_4[Fe(CN)_6]$ solution containing 0.1 M KCl) representing electrode surface modification: (a) GCE, (b) GCE/Au, (c) GCE/Au/Apt, (d) cDNA-Fc/MXene/ GCE/Au/Apt and (e) GCE/Au/Apt-MUC1. **(B)-(ii)** Comparison to show the SWV signal of electrodes in the presence or absence of MXene (in 0.1 M, pH PBS buffer at pH = 7.5): **(I)** GCE/Au/Apt/cDNA-Fc **(II)** GCE/Au/Apt/MXene/cDNA-Fc. Reproduced with permission from [167] @ Elsevier 2020.

Table 1
Sensing performance summary of various MXene based aptasensors.

MXene-Aptamer probe	Analytes	Detection methods	Detection limits	Linear range	Applications in	Ref
Cy3-CD63-Apt/Ti_3C_2	Exosomes	FRET	1.4×10^3 particles mL^{-1}	10^4 to 10^9 particles mL^{-1}	Cancer	[128]
$Ti_3C_2T_x$/Au/SiO_2/Apt	STX	EC	0.03 nM	1.0 nM to 200 nM	Food safety	[134]
Fe_2O_4@Ag-HB5 Apt/BSA/ Ti_3C_2/GE	HER2-positive CTCs	EC	47 cells mL^{-1}	10^2 to 10^6 cells mL^{-1}	Cancer	[145]
AuNPs-Ti_3C_2-CD63Apt/GCE/ SA-PAM	Exosomes	ECL	30 particles μL^{-1}	10^2 particles μL^{-1} to 10^5 particles μL^{-1}	Cancer	[157]
MCH/Apt/ILs/SiO_2NUs/GCE.	Exosomes	ECL and Photo-thermal	1.1×10^2 particleμL^{-1} exosomes	———————	Cancer	[158]
Apt2/Apt1/PNIPAM-AuNPs/ GCE/ Ti_3C_2	Exosomes (on MCF-7 cells)	ECL	125 particles μL^{-1}	———————	Cancer	[159]
Apt/He@CCNT/Ti_3C_2/SPCE	CEA	M-EC	2.88 pg mL^{-1}	10 to 1×10^6 pg mL^{-1}	Cancer	[164]
Au-Pd-Pt/$Ti_3C_2T_x$/HP1/ HP2	CEA	EC	0.32 fg mL^{-1}	———————	Cancer	[165]
cDNA-Fc/MXene/Apt/Au/GCE	MUC1	EC	0.33 pM	1.0 pM to 10 μM	Cancer	[167]
PPy@$Ti_3C_2T_x$/PMo_{12}/Apt	OPN	EC	0.98 fg mL^{-1}	0.05 pg mL^{-1} to 10.0 ng mL^{-1}	Cancer	[170]
Ti_3C_2/PAMAM-Au NPs/CD63-Apt/GCE	Exosomes	EC	229 particles μL^{-1}	5×10^2 particles μL^{-1} to 5×10^5 particles μL^{-1}	Cancer	[171]
$Ti_3C_2T_x$@FePcQDs hybrid/Apt	miRNA-155	EC	0.0043fM	0.01 to 1.0×10^4fM	Cancer	[175]
$Ti_3C_2T_x$MXene carbon dots or CoCu-ZIF@CDs/Apt	B16-F10 cells	EC	33 cells mL^{-1}	1×10^2 to 1×10^5 cells mL^{-1}	Cancer	[176]
AuNP dimers/ $Ti_3C_2T_x$ NSs/Apt	AFB1	SERS	0.6 pg mL^{-1}	0.001 to 100 ng. mL^{-1}	Food safety	[185]
GCE/P4VP/Apt/ $Ti_3C_2T_x$/GO-COOH/BSA	AFB1	EC	3 pg mL^{-1}	0.01 to 50 ng mL^{-1}	Food safety	[186]
Au − Ag Janus NPs/MXene NSs/ Apt	OTA	SERS	1.28 pM	———————————	Food safety	[187]
Ti_3C_2/Apt/Al	DON	EC	1 fg mL^{-1}	1 fg mL^{-1} to 1 ng mL^{-1}	Food safety	[189]
Ti_3C_2NSs-TDNs/GCE/Apt	Gliotoxin	EC	5 pM	5 pM to 10 nM	Food safety	[192]
Ti_3C_2/HD22Apt/HD1Apt/ NU172Apt@FAM	TB	FRET	5.27 pM	———————	Cardiovascular disease	[193]
MoS_2@$Ti_3C_2T_x$MXene NH/ SPCE/GNs/Apt	T4	EC	0.39 pg mL^{-1}	7.8×10^{-1} to 7.8×10^6 pg mL^{-1}	Thyroid disorders	[194]
Ti_3C_2 NSs@Apt/OPD/H_2O_2	TB	COL	1.0×10^{-11} M	1.0×10^{-11} to 1.0×10^{-8} M	Blood thrombin levels	[200]
POSS/PQDs/Ti_3C_2/Apt	*V.P*	FRET	30 cfu mL^{-1}	10^2 to 10^6 cfu mL^{-1}	Water borne pathogens	[208]
PBA-Fc@Pt@Ti_3C_2/Apt	*V.P*	ECL-COL	5 CFU mL^{-1} and 30 CFU mL^{-1}	———————	Food-borne pathogens	[209]
$Ti_3C_2T_x$/ZIF-8/GCE/Apt	HIV Protein	ECL	0.3 fM	1 fM to 1 nM	HIV/ AIDS	[212]
TDNA@Au/Ti_3C_2-MXene/Apt-H1/Apt-H2	cTnI	ECL	0.04 fM or 0.1 fM	0.1 fM^{-1}pM or 0.1 fM to 500 fM	MI/Heart Attack	[216]
Apt/MXene	TNF-α IFN-γ	EC	0.25 pg mL^{-1} 0.26 pg mL^{-1}	1 pg mL^{-1} to 10 ng mL^{-1}	Cytokine storm	[220]
CRISPR-Cas12a/gRNA-treated Ru(dcbpy)3 2+/ AuNPs@Ti_3C_2/GCE/Apt	Siglec-5	ECL	20.22 fM	———————	AML	[225]
CRISPR-Cas12a/crRNA/MXene/ FAM-Apt	LPS in Gram-negative Bacteria	FLR	11 pg mL^{-1} (LPS) & 23 CFU mL^{-1}	———————	Food safety	[229]
ZnO/N-Ti_3C_2/GCE/Apt	CAP	ECL	0.019 ng mL^{-1}	0.1 to 100 ng mL^{-1}	Food safety	[230]
Ti_3C_2–AgBrNCs/GCE/Apt	ENR	ECL	5.97×10^{-13} mol L^{-1}	1.0×10^{-12} to 1.0×10^{-6} mol L^{-1}	Food safety	[231]
PMXF-5/HP2/ssDNA/ AuNR/ HP1	TB	EC	0.67 pM	2 pM to 10 nM	Blood thrombin levels	[243]
PMXF5/HP2/ssDNA/ HCuPtA/HP1			16.67 pM	50 pM to 50 nM		
GOPS- Ti_3C_2-GCE/Apt	PD-L1 Protein	EC	0.01–100 ng mL^{-1}	7.8 pg mL^{-1}	Cancer	[244]
MXene-Au/PEI-UPNPs/Cas12a-crRNA/Apt	DON	LRET	0.64 ng/mL	1 to 500 ng/mL	Food safety	[245]
Au@$Nb_4C_3T_x$/GCE/Thiol-Apt	Pb^{2+}	EC	4 nM	10 nM to 5 μM	Environmental monitoring	[246]
Apt/MXene-AuNPs/GCE	CAP	EC	0.03 pM	0.0001 to 10 nM	Food safety	[247]
Nb_2C-SH QDs/N-58Apt	Nucleocapsid of SARS-CoV-2	SPR	4.9 pg mL^{-1}	0.05 to 100 ng mL^{-1}	COVID-19 diagnosis	[242]

EC = Electrochemical, PEC = Photoelectrochemical, FRET = Förster or fluorescence resonance energy transfer, FLR = Fluorescence, ECL = Electrogenerated chemiluminescence, COL = Colorimetric, Acute myelogenous leukemia = AML, OTA = Ochratoxin A, *Vibrio Parahaemolyticus* = (*V.P*),

Thrombin = TB, Thyroxine = T4, Streptomycin = STR, Cardiac-specific Troponin I = cTnI, Lipopolysaccharide = LPS, Saxitoxin = STX, Deoxynivalenol = DON, Severe acute respiratory syndrome coronavirus 2 = SARS-CoV-2, Osteopontin = OPN, Mucin1 = MUC1, Chloramphenicol = CAP, LRET = Luminescence resonance energy transfer, ENR = Enrofloxacin, Programmed death-ligand 1 = PD-L1, M-EC = Microfluidic Electrochemical, CEA = Carcinoembryonic antigen, TNF-α = Tumor necrosis factor α, IFN-γ = interferon gamma.

selective and sensitive approach for the recognition of MUC1 seems to be crucial for breast cancer early diagnosis. Wang et al. [167] used MXene to modify the electrode surface for the construction of a MUC1 detection aptasensor where MXene was firstly modified with ferrocene-labeled complementary DNA (cDNA-Fc) sensor to augment the sensing signals (as cDNA-Fc/MXene) against MUC1 detection. cDNA-Fc/MXene probe was immobilized with MUC1 aptamer via Au-S bond over glassy carbon electrode to fabricate cDNA-Fc/MXene/Apt/Au/GCE aptasensor. A competitive procedure causes cDNA-Fc/MXene to unhitch from the electrode surface. This causes a drop in electrical current signals, which can be compared to the peak of the current signals before the competition to correlate the amount of MUC1 that can bound to the electrode. The competitive recognition approach to bind MUC1 aptamer with either the cDNA-Fc probe or MUC1 biomarker enhanced the selectivity as shown in Fig. 7**A**. The detection of MUC1 in human blood serum demonstrated that the constructed aptasensor possesses the feasibility and potential for identifying the MUC1 biomarker in real clinical samples [167]. The suggested electrochemical aptasensor is competitive in nature as it displays a low limit of detection (LOD) and broad linear range **(**Table 1**)**. Since the Electrochemical impedance spectroscopy (EIS) is a valuable tool for determining the electron transfer characteristics of the electrodes. EIS curves demonstrated the properties of the electrode surface in the absence and then presence of MXene as a signal transducer. The curve d in the Fig. 7**B-i** shows the largest diameter of the EIS semicircle when the electrode surface was modified with MXene. When the electrode was incubated with the target (MUC1), the diameter of the semicircle was significantly reduced (curve e). This could be because the aptamer bound to MUC1 and released the MXene/cDNA-Fc probe. The ability of MXenes to behave like a signal amplifier was further validated via a Square Wave Voltammetry (SWV) experiment that was conducted in PBS buffer (0.1 M, pH 7.5). The MXene was utilized as the substrate for anchoring the probe (cDNA-Fc/MXene/Apt/Au/GCE), which produced a markedly elevated electrical signal **(**Fig. 7**B-ii-I)** as compared to the probe without MXene **(**Fig. 7**B-ii-II)**. This clearly depicts that the huge surface area of MXene allows it to hold a great proportion of Fc-cDNA signaling molecules, which increases the percentage of bound probe [167].

Osteopontin (OPN), a non-collagenous, chemokine-like protein, is essential for identifying the carcinogenic potential of different malignancies. By upregulating multiple signaling pathways, osteopontin plays a vital role in tumor metastasis, growth, invasion, and angiogenesis [168]. Consequently, cost-effective, simple, and early detection of OPN is a prerequisite [169]. A phosphomolybdic acid (PMo_{12}) and $Ti_3C_2T_x$ MXene nanohybrid incorporated into polypyrrole were synthesized and exploited by Zhou et al. [170] as a powerful system for strongly immobilizing the OPN to an RNA based-aptamer (via hydrogen bond, electrostatic interactions, and π-π stacking) in order to develop an ultrasensitive EC aptasensor for OPN detection **(**steps can be seen in Fig. 8**A)**. Not only did the $PPy@Ti_3C_2T_x/PMo_{12}$ composite exhibit a uniform surface morphology, a considerably high degree of crystallinity, and a multitude of chemical functionality, but it also exhibited excellent electrochemical properties. These characteristics provided the MXene composite with a high degree of stability and increased binding capability to the OPN aptamer. The sensor demonstrated high regeneration, adequate reproducibility, and selectivity in serum samples [170].

Vajhadin et al. constructed an EC sensor for extremely sensitive detection of cancer cells by employing an Au electrode modified with Ti_3C_2 NSs (1.5 m lateral size and 2 nm thickness) [145]. Electrostatic interactions were being used to immobilize an HB5 aptamer onto MXene layers to act as a sensing surface for the high selectivity recognition of HER-2 positive cells. To avoid electrode contamination by blood matrix, HER-2 positive circulating tumor cells (CTCs) were magnetically separated by $CoFe_2O_4$@Ag magnetic nanohybrids attached to HB5. A sandwich-like structure formed between functionalized MXene electrodes and magnetically trapped cells that efficiently protected the electron transport of a redox probe, allowing quantifiable cell detection via current signal changes **(**Fig. 8**B)** [145]. The proposed apta-cytosensor revealed the tremendous potential to detect tumor growth at a low cost by monitoring circulating tumor cells in blood samples. The total time required for analysis of the blood samples was estimated to be 75 min. While the efficiency of cytosensor was evaluated using the blood samples of cancer patients within 75 min, considerable efforts are required to verify the recent system using clinical samples from patients with multiple stages of cancer. Not only can this technology be utilized to detect different tumor cells by substituting another specific aptamer, but it may also be useful in targeted drug delivery.

Zhang et al. [171] developed an electrochemical aptasensor for sensitive measurement of exosomes and their surface proteins by using in situ synthesis of Fe_4 $[Fe(CN)_6]_3$ (Prussian Blue) on the surface of Ti_3C_2 MXene as a nanohybrid probe (PB-MXene). A CD63 functionalized poly(amidoamine) (PAMAM)-AuNPs electrode interface that can selectively interact with CD63 protein on exosomes originating from OVCAR cells was constructed. Moreover, the CD63-modified Ti_3C_2 MXene was employed as a nanocarrier for loading a larger amount of aptamer and was adsorbed on exosomes **(**Fig. 9**A)**. The Ti_3C_2 MXene may be used to generate PB in situ and efficiently load it, as well as magnify the electrochemical response at low concentration, minimizing interference from various electrochemically active species. Due to this double amplification process, exosomes can be detected electrochemically in a highly sensitive and selective manner [171].

An important function in the post-transcriptional control of gene expression is played by the large family of microRNAs (miRNAs) [172]. Cardiovascular disease, immunological dysfunction, kidney disease, neurological illness, diabetes, liver disease, arthritis, and cancer all seem to have miRNA overexpression as a biomarker [173]. MiRNAs are also useful for early cancer detection and prognosis. Importantly, human breast tumors have elevated levels of miRNA-155 [174]. As a result, accurate miRNA-155 diagnosis is essential for cancer detection at earlier stages. Duan et al. [175] presented a unique 0D/2D $Ti_3C_2T_x$@FePcQDs nanostructure that was synthesized by embedding phthalocyanine quantum dots (FePcQDs) into a $Ti_3C_2T_x$ NSs as matrix. The constructed nanopalatform was modified by anchoring aptamer and its complimentary DNA strands on the nanocomposite surface, thus using them to recognize the required

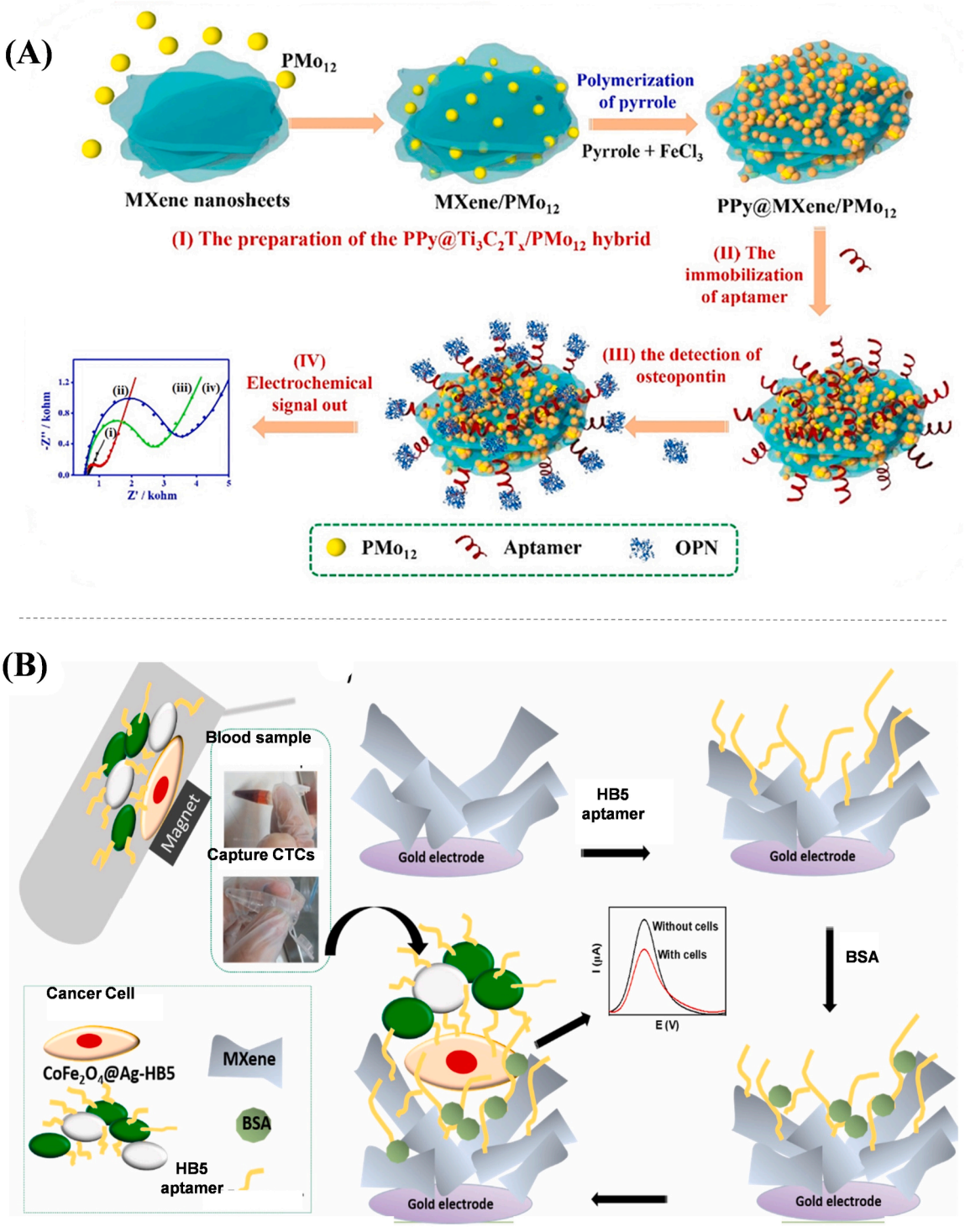

Fig. 8. (A) Schematic illustration of the steps involved aptasensor construction for osteopontin recognition, including (I) $PPy@Ti_3C_2T_x/PMo_{12}$ MXene nanocomposite synthesis, (II) the aptamer attachment to the MXene nanocomposite, (III) the osteopontin recognition, and (IV) the electrochemical signal detection. Reproduced with permission from [170] @ Elsevier 2019; **(B)** Schematic diagram of the aptasensor based on MXene for the identification of HER2-posetive cancer cells in blood samples: Magnetic isolation of the target cells from the blood using $CoFe_2O_4$@Ag-HB5, and electrochemical detection of cancer cells on an activated MXene surface. Reproduced with permission from [145] @ Elsevier 2022.

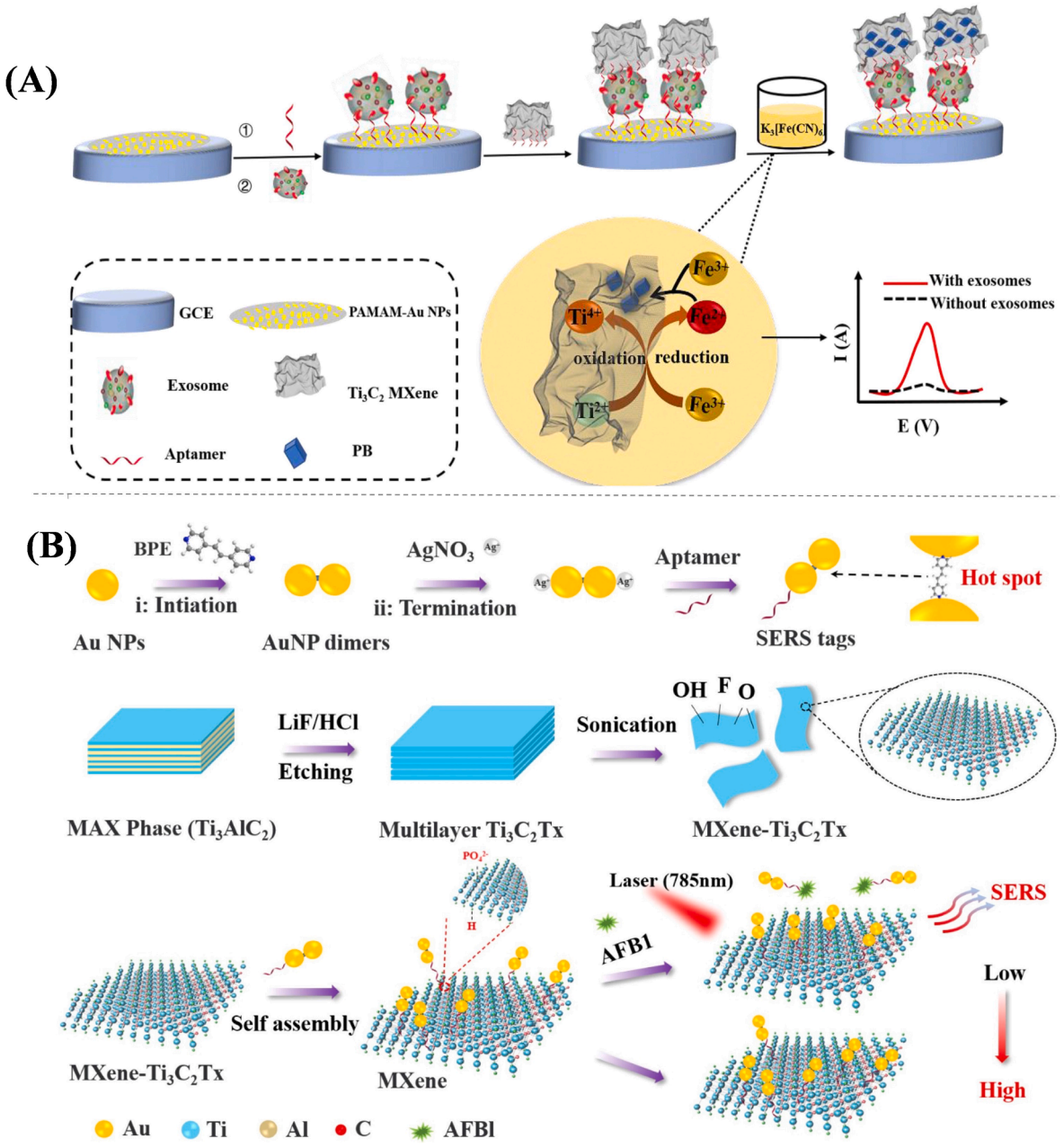

Fig. 9. **(A)** An EC aptasensor founded on PB-MXene-Apt probe to attain signal amplification at low potential, to detect exosomes. Reproduced with permission from [171] @ Elsevier 2021; **(B)** Schematic diagram of SERS aptasensor built on MXenes assemblies/AuNP dimers for AFB1 recognition. Reproduced with permission from [185] @ Elsevier 2021.

miRNA-155 expression via miRNA-155/cDNA hybridization [175]. When it comes to stability, conjugated structure, biocompatibility, and electrochemical activity, the $Ti_3C_2T_x$@FePcQDs-based aptasensor surpassed the individual components used in aptasensor manufacturing. Certain advantages were shown by aptasensor, including efficient hybridization of the miRNA-155/ cDNA, easy fabrication of the sensing device without using any electrochemical indicators and labelled probe, efficient cDNA coupling and promising potential for extending aptasensor applications for various targets by substituting aptamer probe. Thus, early stage cancer biomarker detection could benefit greatly using the current approach.

MXene-derived carbon dots (CDs) integrated with bimetallic CoCu-zeolite imidazole framework (ZIF) NSs (designated as CoCu-ZIF@CDs) were prepared by Liu et al. [176] as unique 0D and 2D heterogeneous nano-constructs, respectively. The nano-composites were used to immobilize B16-F10 cell targeting aptamer (via Vander Waal forces, electrostatic attractions, and π-π stacking) for B16-F10 living cells detection. The resulting CoCu-ZIF@CDs nanocomposite displayed advantages including outstanding

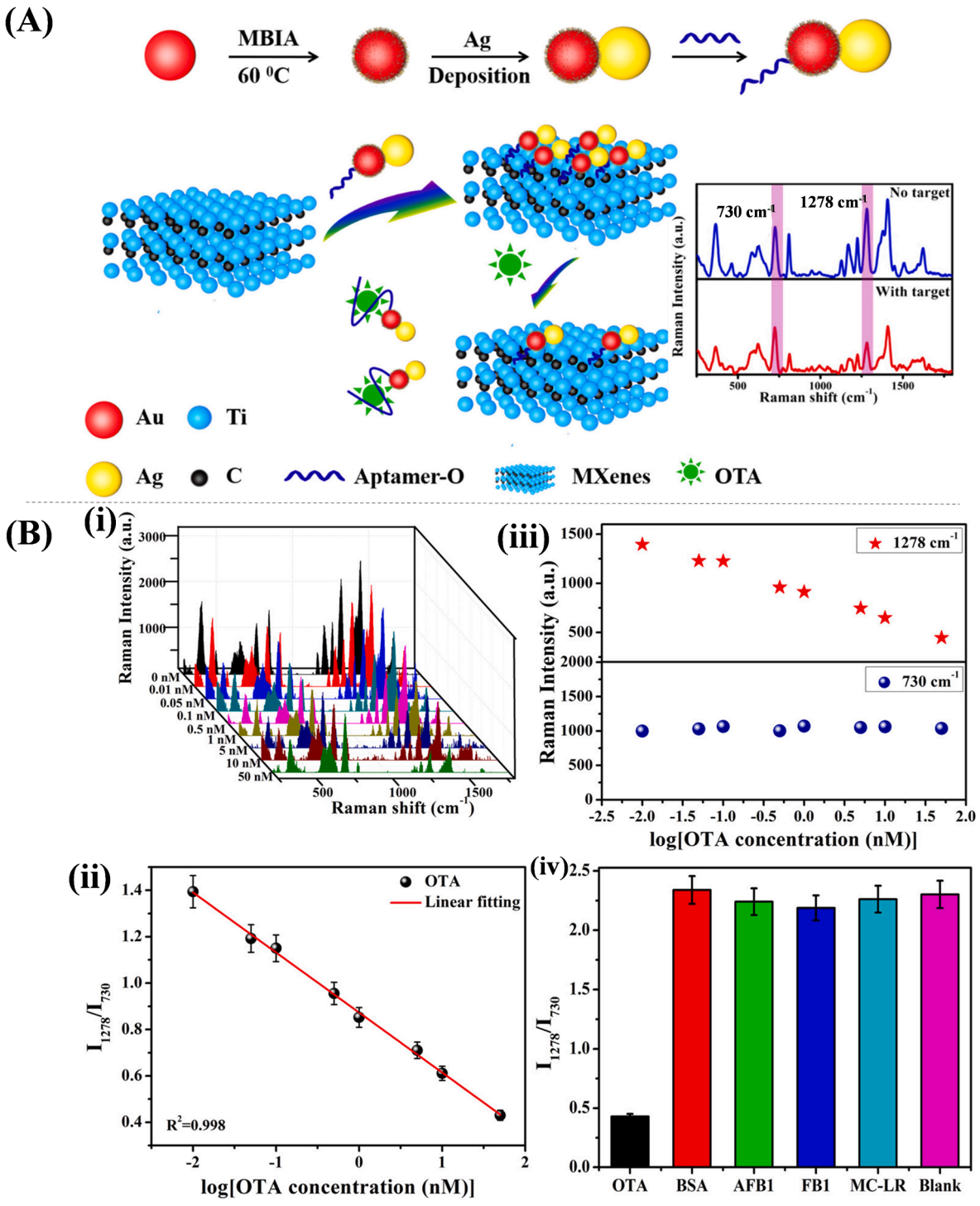

Fig. 10. **(A)** Schematic diagram to show the assembly of a SERS aptasensor involving MXene-Ag–Au Janus composite for the quantification of ochratoxin A (OTA). **(B)-(i)** Raman spectra of a SERS-based aptasensor for the detection of ochratoxin A at varying concentrations, **(ii)** corresponding plot of ratiometric signals (I_{1278}/I_{730}) vs OTA logarithmic concentrations, **(iii)** Plots of Ag–Au Janus NPs showing SERS intensities (red points) at 1278 cm^{-1} and at 730 cm^{-1} of MXenes NSs (blue points) vs OTA logarithmic concentrations, and **(iv)** Ratiometric intensities of I_{1278}/I_{730} in the presence of 5 nM MC-LR, OTA, AFB1, BSA, and FB1. The blank specified the sample without any chemical. Reproduced with permission from [187] @ ACS 2019. (For interpretation of the references to color in this figure legend, the reader is referred to the web version of this article.)

biocompatibility, mixed metal valence states of coordinated centers, superior electrochemical features, and high fluorescence efficiency. With the substantial quantity of CDs embedded in the porous NSs composite, the built cytosensor exhibited strong fluorescence efficiency and exceptional electrochemical properties. Furthermore, the porous nanostructure revealed active sites that can cause strong aptamer strand attachment via stacking interaction, electrostatic attraction between nitrogen-related molecules and aptamer strands, and Vander Waal forces. The combination of these characteristics results in enhanced sensing properties for the identification of living tumor cells via cell imaging and electrochemical methods. Not only does this work demonstrate the promising implications of MOF-related compounds in sensing areas, but it also demonstrates a viable method for the early detection of cancer biomarkers [176].

Aptasensors may offer various advantages over conventional cancer detection approaches, including versatility and enhanced test speed. Real-time fast detection can offer healthcare professionals with instantaneous interactive information that can be used to plan patient treatment. Additionally, aptasensors may enable lower testing costs, automated testing, and multi-target assessment. Biosensor related diagnostic tests may increase cancer diagnostic accuracy, resulting in improved prognosis. This technology has the potential to significantly improve the healthcare system in underserved populations and community settings [177].

4.2. MXene based aptasensors for the detection of mycotoxins

Mycotoxin, derived from the Greek term mukos, which means “fungus,” and the Latin term toxicum, which means “poison,” is considered a secondary metabolite released by fungi which invade crops during either storage or harvest [178]. This may result in animal and human diseases such as “mycotoxicosis” [179]. There are various forms of mycotoxins, including those that are mutagenic, teratogenic, nephrotoxic, carcinogenic, and immunosuppressive. They are extremely resistant to degradation, and thus persist in the food supply chain [180]. Mycotoxins damage a wide variety of agricultural stuffs, comprising cocoa, dried fruits, cereal-based foods, cereals, milk, wine, coffee beans, meat products and bakery, etc. which have been the backbone of several developing nations’ economies [181]. Because of their extremely toxic effects, mycotoxins infestation in foodstuffs has caused significant health concerns in both animals and humans [180]. To protect public health from such hazardous effects of the foodstuffs, global maximum permissible levels for the most toxic and abundant mycotoxins in certain foods have been determined [182,183]. As a result, reliable and sensitive analytical techniques are essential for monitoring mycotoxins content such as aflatoxin B1, ochratoxin A, Fusarium, gliotoxins, and marine toxins, etc, and establishing compliance with food safety requirements [184].

Mycotoxins are not only detrimental to animals and crops, but they also pose a major health danger to humans. Some mycotoxins such as aflatoxin B1 (AFB1) and ochratoxin A (OTA) are considered as highly poisonous carcinogens for humans [184]. Wu et al. [185] developed a ratiometric Surface-enhanced Raman Spectroscopy (SERS) aptasensor using MXene NSs doped with AuNP dimers containing nanogaps for AFB1. Chelation and hydrogen bonding interactions between MXene NSs and AuNP dimers modified with thiolated-aptamer created the MXene@AuNP dimer assemblies with the strongest Raman signals. Due to the aptamer’s preference to bind AFB1, this could stimulate the release of AuNP dimers from MXene NSs, allowing for the recognition and quantification of AFB1 target at even lower concentrations. The great specificity and sensitivity of the devised aptsensor in peanut samples were made possible by the enhanced affinity of aptamer for AFB1 and AuNP dimers’ dense SERS “hot spots” **(**Fig. 9**B)** [185]. Current findings show that this method can reliably and sensitively detect other small molecules and AFB1 in various foodstuffs, and it might be extended for other SERS tests as well. AFB1 was also detected using an electrochemical biosensor based on a $Ti_3C_2T_x$@GO-COOH-P4VP composite fabricated by Guo et al. [186]. The protonation and deprotonation dependent electrochemical aptasensor’s current signal switch (ON-OFF) was adjusted using pH-sensitive poly 4-vinyl pyridine (P4VP) as a smart material. The authors employed a modified $Ti_3C_2T_x$ MXene as a material to enhance the current signals while the additional carboxyl groups to GO-COOH made the fixation framework for the aptamers more stable. The synergistic effect of MXene together with aptamer offered a practical and effective way to detect AFB1 in acidic conditions with low LOD and wide linear working range.

For the quantitative and sensitive recognition of OTA, Zheng et al. [187] established a SERS aptasensor. The sequential development of silver islands on gold cores was employed to construct Ag-Au Janus nanoparticles (NPs). Using 2-mercaptobenzoimidazole-5-carboxylic acid (MBIA) as a Raman reporter and Ag-AuNPs to dramatically magnify the SERS signal, researchers were able to get impressive results. Ag-Au Janus NPs were synthesized with MXene NSs via chelation interactions and hydrogen bonding between OTA aptamer and MXene NSs. Due to the development of the OTA/aptamer complex in the presence of an OTA target, Ag-Au Janus NPs get desorbed from MXene NSs **(**Fig. 10**A)**, resulting in the decrease of the Raman signals of Ag-Au Janus NPs, whereas the signal of MXene NSs remains unchanged. To demonstrate the ratiometric design benefits, an internal standard-aptasensor was employed to detect OTA in the aqueous phase. The Raman spectra of Au–Ag Janus NPs **(**Fig. 10**B-i)** at 1278 cm^{-1} dropped as the OTA concentration (0.01–50 nM) was increased, exhibiting a concentration-dependent response, whereas the Raman spectra at 730 cm^{-1} attributable to MXene NSs, remained constant. Thus, the ratiometric peak intensity of I_{1278}/I_{730} dropped, enabling the detection of OTA through ratiometric SERS. Trends in the Raman spectra as a function of OTA concentration were quantified as presented in Fig. 10**B-ii**. Conversely, a high degree of linearity ($R^2 = 0.998$) was seen in the logarithmic concentration of the ratiometric Raman signals and OTA, suggesting that the use of an internal standard might increase quantification accuracy **(**Fig. 10**B-iii)**. Additionally, the created sensor showed a high degree of selectivity. A range of Raman signal outputs were recorded following incubation with nonspecific compounds at a concentration of 5 nM, including MC-LR, OTA, BSA, FB1, AFB1 and the blank (without any target). As can be seen from the data, none of those other interfering proteins or mycotoxins significantly altered the ratiometric peak signals unlike OTA **(**Fig. 10**B-iv)**. The Raman signals produced by MXene NSs were steady and distinctive, making it a perfect internal standard method for quantitative study. This sensor can detect OTA with good repeatability and high sensitivity by combining the inherent benefits of SERS with a ratiometric approach. This sensor has a number of useful applications for various biomolecule detections [187].

Certain Fusarium species produce a mycotoxin known as deoxynivalenol (DON), which is a widespread food and feed related

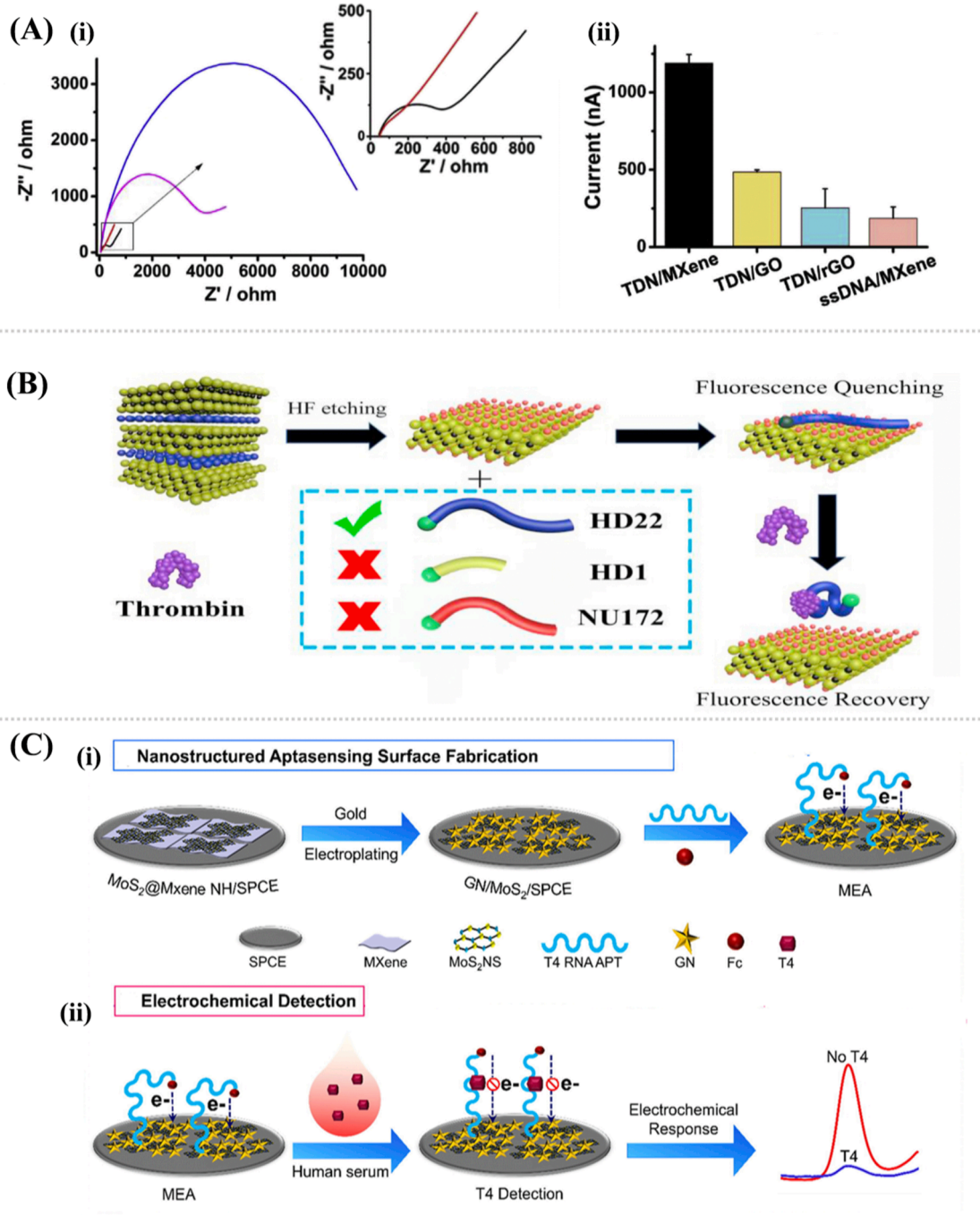

Fig. 11. **(A)-(i)** Nyquist plots of bare GCE electrode (black curve), GCE-MXene (red curve), GCE-TDN (blue curve), and GCE/MXene/TDN (pink curve) in 5 mM $K_3[Fe(CN)_6]/K_4[Fe(CN)_6]$ (1:1) containing 0.5 M KCl. **(ii)** Comparison of MXene/TDN biosensor with various control biosensors including GO/TDN, rGO/TDN and MXene/ssDNA biosensors. Reproduced with permission from [192] Elsevier 2019; **(B)** Schematic depiction of Ti_3C_2 based FRET sensor. MXene binding to a FAM-labelled aptamer effectively quenches the fluorescence due to FRET between MXene and FAM. Contrarily, aptamer detaches from MXene in the presence of thrombin, and therefore enables the fluorescence recovery. Reproduced with permission from [193] @ Elsevier 2021: **(C)-(i)** construction of the aptasensor based on $MoS_2@Ti_3C_2T_x$ nanocomposite and **(ii)** electrochemical detection mechanism for the quantification of thyroxine in human serum. Reproduced with permission from [194] @ Elsevier 2021. (For interpretation of the references to color in this figure legend, the reader is referred to the web version of this article.)

hazard. A highly sensitive and rapid approach to easily recognize and quantify DON is necessary because of the risks that could result from the inadvertent or intentional contamination of foodstuffs with DON [188]. Sangu et al. [189] designed an electrochemical aptasensor for the ultrasensitive detection of DON mycotoxin by immobilizing DON Aptamer as bio-receptor on Ti_3AlC_2 as sensing surface. This approach showed potential to detect mycotoxin in food and feed due to its cost effective, highly selective, stable and sensitive nature [189].

Gliotoxins are among the most poisonous metabolites released by *Aspergillus fumigatus* during its growth that can promote invasive aspergillosis by lowering immune response, Aspergillus propagation, direct body damage, and infections [190,191]. Based on tetrahedral DNA nanostructures (TDNs) and MXene NSs, a simple electrochemical aptasensor for gliotoxin aptasensing was developed by Wang et al. [192]. MXene was used as a high-conductivity and flexibility superstructure for immobilizing a high proportion of DNA nanostructures (DNs) onto the surface of the electrode. Since there are no complicated modifications required by this method, it lowers the complexity and cost of the assay dramatically. DNs were used as a hard scaffold to allow bio-receptors to bind to their targets. The large surface area of MXene NSs allows the excellent conductivity and immobilization of a substantial percentage of DNA probes, which enables the transport of electrons between the supporting electrode surface and electrochemical species. A competitive binding of the gliotoxin with its aptamer occurs by breaking the aptamer-complimentary strand hybrid (i.e., signal probe) where TDNs probes easily capture them. Using a streptavidin-specific aptamer, streptavidin-labeled horseradish peroxidase (HRP) is attracted to the surface of the electrode, which generates a strong catalytic signal. Fig. 11**A-i** depicts EIS plots of various modified electrodes. In comparison to the unmodified GCE (black curve), the MXene NSs modified electrode resulted in a decreased resistance (R_{ct}, red curve). This is due to the strong metallic conductivity and huge surface area of MXene. To understand how important MXene is, the authors constructed control EC biosensors with graphene oxide (GO) and reduced graphene oxide (rGO) rather than just MXene. When confronted with a 10 nM target, the GO-based biosensor produced a small current signal (at 485 nA), as shown in the Fig. 11**A-ii,** which could be attributed to the lower electron conduction ability of GO as compared to MXene.

Though rGO has strong conductivity, it was challenging to create a homogenous rGO solution, so TDN loading remains low (approximately 28.4%), resulting in poor signal production (~253 nA). Additionally, they developed an MXene-ssDNA complex customized electrode to determine the effectiveness of the TDN probe. The detection performance of the ssDNA probe was quite low on MXene NSs (without a 3D nanostructure). The electrochemical output (~186 nA) was considerably lower than its TDN/MXene-based analogue. These findings indicated that TDN/MXene-based biosensors performed better in terms of molecular recognition. The suggested sensor could detect gliotoxins with 5 pM LOD in real samples and outperformed conventional biosensors [192]. Overall, this technique established a new channel for mycotoxin detection in clinical settings via DNs and MXenes.

Marine toxins, which are mostly released by microalgae, cause severe damage to global environmental safety and human health. A wide range of marine toxins, including saxitoxin (STX), are thought to play a role in certain ion channel ailments, including neurodegenerative and cardiovascular diseases. STX is particularly hazardous to the entire ecological system, although it is produced by marine dinoflagellates. Through water and food intake, humans passively absorb these chemicals, resulting in serious health consequences [195]. STX is a water-soluble, extremely poisonous, thermostable, and acid-resistant compound. As a result, STX in saltwater can be bio-accumulated via marine organisms. It is critical to correctly quantify trace STX levels in seafood and seawater to assure their safety for ingestion [196]. Ullah et al. devised an electrolyte insulator-semiconductor biosensor using aptamer-modified $Ti_3C_2T_x$ MXene for the measurement of STX [134]. The abundant functional groups on MXene coupled with and high surface area enabled the aptamer modification that interacts specifically with STX and cause changes in the electrical signals. Constant capacitance and capacitance-voltage analysis confirmed that the sensor has a high selectivity, specificity, sensitivity, two-week stability and could be used to detect STX in real extracted muscle tissue samples. The approach (with LOD 0.03 nM) enabled cheap, fast and label-free identification of marine toxins, implying potential applications in the food industry and water quality monitoring [134].

4.3. MXene-based aptasensors for other analytes

This section deals with the determination of some valuable molecules via aptamer modified MXenes. For example, Thrombin (TB) is a naturally occurring protease that plays a role in the coagulation cascade. It turns fibrinogen into insoluble fibrin, which produces the fibrin gel in both pathological thrombosis and physiological conditions [197]. Thrombin also exhibits hormone-like features and is essential in the activation of platelets and thrombosis. Hence, thrombin is implicated in a variety of cardiovascular disorders [198], and it is believed to regulate a variety of processes involved in tissue repair and inflammation at the blood vessel wall. Since high thrombin concentrations in the blood are intricately linked with diseases, it is essential to be able to detect this protein at a trace level with great sensitivity [199]. Li et al., fabricated a label-free colorimetric aptasensor for TB detection by the peroxidase-mimicking enzymatic features of Ti_3C_2 NSs in combination with an ssDNA aptamer (Ti_3C_2@ssDNA nanocomplex) [200]. Negatively charged aptamer immobilization not only enhances the enzymatic function of MXene NSs but also recognizes the target in the presence of positively charged substrate o-phenylenediamine (OPD) oxidation by H_2O_2. The aptamer detaches from the surface of Ti_3C_2 NSs in the presence of TB to make a TB-aptamer complex that results in lowering the catalytic activity of the sensor. Enzymatic activity decreases further as the concentration of TB increases. By immobilizing the alternate aptamer sequences, this catalysis-based approach can be extended to quantify numerous other biological targets [200].

Cui et al. [193] employed aptamers labelled with fluorescein amidite (FAM) to construct a MXene-based aptasensor. Ti_3C_2 MXene was coupled to aptamers via chelation interactions and hydrogen bonds between Ti ions and phosphate groups, which resulted in a Förster or fluorescence resonance energy transfer (FRET) response between MXene and aptamers. Thrombin-binding aptamer (TBA) was labelled using FAM. Ti_3C_2 MXene effectively quenches the fluorescence signal via FRET between Ti_3C_2 and FAM. Due to the increased affinity of thrombin molecules for the TBA aptamer on the Ti_3C_2 surface, it interacts with TBA to create a quadruplex. The

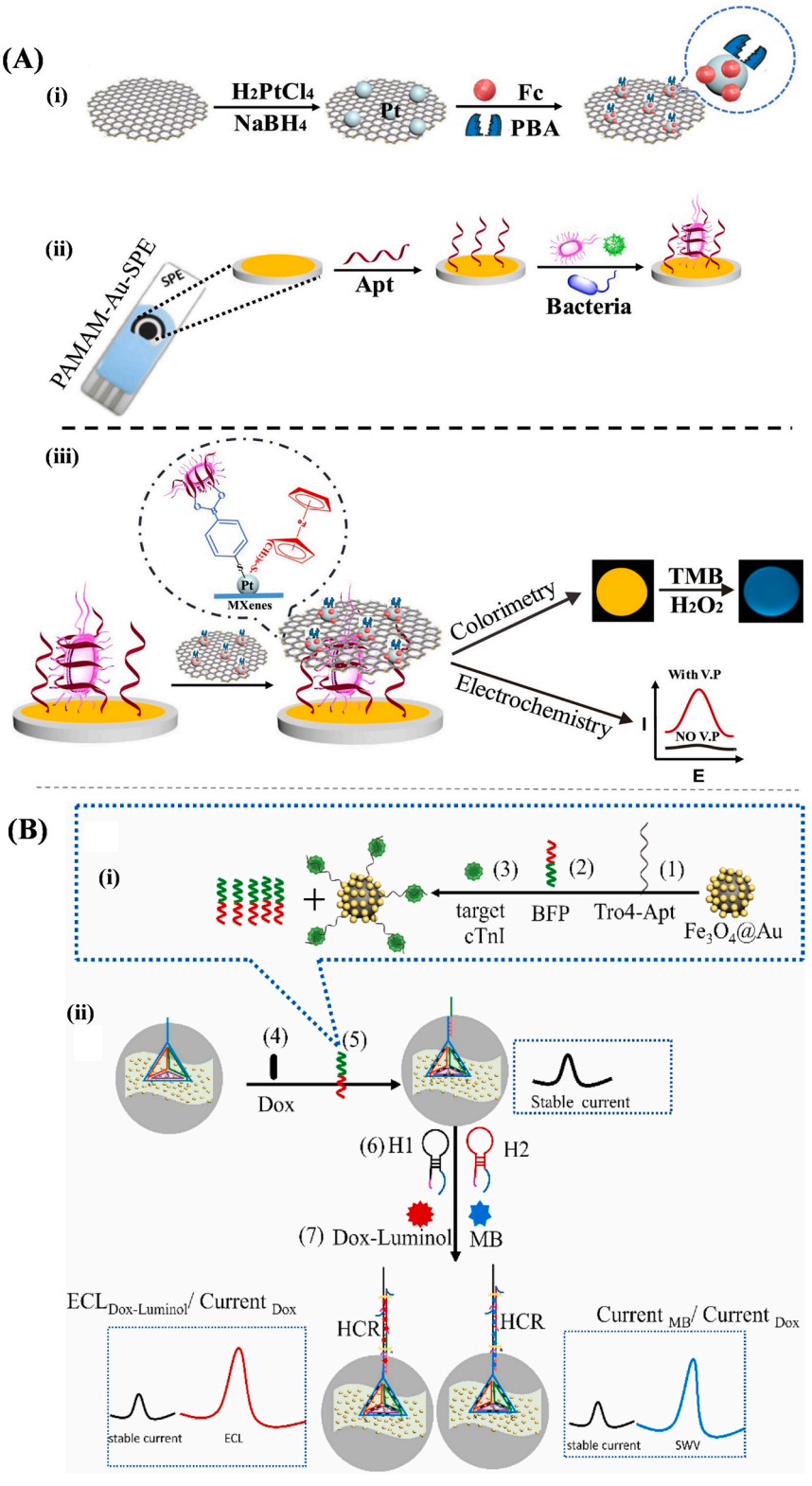

(caption on next page)

Fig. 12. (A) Schematic design showing the steps involved in the fabrication of **(i)** MXene based signal probe, and **(ii)** aptamer based bacterial capture sensor**, (iii)** the dual-mode EC and colorimetric aptasensors' working principle by the combination of signal probe and sensor capture to detect *V.P.* Reproduced with permission from [209] @ Elsevier 2021; **(B)** The depiction of **(i)** bifunctional probe release, and the high selectivity target identification approach and **(ii)** ratiometric aptasensor's working mechanism for cardiac troponin-I detection. Reproduced with permission from [216] @ Elsevier 2021.

quadruplex containing FAM was desorbed from the Ti_3C_2 surface, reducing FRET efficiency and regenerating fluorescence. Thus, the observed variations in the fluorescence spectrum of FAM were proportional to the thrombin concentration in a sample (Fig. 11**B**). Notably, this work establishes that 2D MXenes are an ideal substrate for selective, sensitive, and rapid biomolecule detection.

Thyroid dysfunction is the second most prevalent endocrine disorder [201]. Thyroxine (3,5,3′,5′-tetraiodothyronine) also known as T4, is the most commonly tested thyroid hormone used to check thyroid function [202]. In other words, serum T4 levels might be a more accurate indicator of thyroid normal function [203]. An electrochemical aptasensor based on MoS_2@$Ti_3C_2T_x$ MXene hybrid (MoS_2; molybdenum sulfide) was constructed by Kashefi-Kheyrabadi for rapid and sensitive detection of Thyroxine in human blood serum [194]. The nanohybrid was coated on the surface of a carbon electrode, which was then modified with gold nanostructures based on electroplating (Fig. 11**C-i**). The combination of MoS_2NSs with MXene improves the physicochemical features of the electrode to accommodate a 3D gold nanostructure based building block. It helps immobilize a greater proportion of T4 specific aptamers to bind to T4 and subsequently amplify the electrochemical signals (Fig. 11**C-ii**). MXene hybrid based electrochemical aptasensor (MEA) exploits electrochemical detection, the aptamer's specificity as a bio receptor, and nano-engineered sensor surface simultaneously to display fast (10 min), accurate, and superior analytical performance. The aptasensor results were comparable to those obtained using the standard ELISA method. With the possibilities of miniaturization, the MEA is considered as a feasible alternative to time consuming methods for the diagnosis of T4 in clinical specimens.

Vibrio parahaemolyticus (*V.P*), a Gram-negative halophilic bacteria that is frequently found in marine and estuarine environments, is a major foodborne pathogen which has the potential to cause disastrous outbreaks worldwide [204,205]. Consumption of contaminated food leads to severe gastroenteritis in humans [206]. As a result, it is critical to limit *V.P*-related food contamination in order to prevent food poisoning and guarantee the safety of seafood intake [207 208]. Hong et al. [208] developed a turn-on–type FRET nanobiosensor based on polyhedral oligomeric silsesquioxane-perovskite quantum dots (POS-PQDs-Apt/MXenes) nanocomposite for selective and sensitive *V.P* monitoring in water. Owing to the remarkable water-resistance and optical features of the POSS-PQDs-Apt and the excellent quenching behavior of MXenes, this platform is suitable for on-site monitoring of *V.P*. Additionally, the platform can be utilized to identify additional vibrio types by substituting a different aptamer in POSS-PQDs-Apt. Nevertheless, the assay had certain limitations. For example, the target was incubated with MXenes for up to 50 min, which might be avoided by grafting certain quenching groups onto the MXene surface [208]. To detect *V.P*., Wang et al. invented a dual-mode aptasensor based on colorimetric and electrochemical approaches (owing to the peroxidase-like and electrochemical features of the system) [209]. On the MXene surface, the platinum NPs, ferrocene, and mercapto-phenylboronic acid (PBA) were loaded to synthesize a PBA-Fc@Pt@MXenes nanocomposite. To adequately capture *V.P*, a screen-printed electrode with an aptamer-functionalized interface was developed. The interface with captured pathogenic bacteria was then coupled to PBA-Fc@Pt@MXenes nanocomposite to produce a sandwich like configuration which enabled the induction of TMB-H_2O_2 chromogenic activity, allowing the emission of visible signals. On the other hand, electrochemical behavior of the Fc on nanocomposite was further used to quantify the pathogen (Fig. 12**A**). Additionally, the screen-printed electrode was also customized with salmonella's aptamer in conjunction with the nanocomposite probe for in situ detection of salmonella [209].

Two lentiviruses, human immunodeficiency virus type 1 and 2 (HIV-1 and HIV-2), are considered responsible for acquired immunodeficiency syndrome (AIDS) in humans [210]. The HIV-1 epidemic is a severe public health problem that necessitates specialized diagnosis. To create point-of-care (POC) diagnostics with high sensitivity for monitoring HIV-1 viral load, extensive research studies have focused on using nano- and micro-scale technologies [211]. Wang et al. fabricated an electrochemical luminescence aptasensor by employing $Ti_3C_2T_x$ functionalized ZIF-8 as a luminescence emitter to identify HIV-1 protein [212]. Although the aptamer/$Ti_3C_2T_x$/ZIF-8/GCE composite material had a large specific surface area due to the combination of PAA with ZIF-8, allowing ZIF-8 to be inserted in a layered construction and resulting in quick electron transfer. The linear range of the sensor was large, with a limit of detection as low as 0.3 fM. After analyzing the data, researchers concluded that the sensor had potential for future use in the diagnosis and treatment of AIDS [212].

Heart attacks, or myocardial infarction (MI), are a leading cause of mortality and morbidity around the world. According to the World Health Organization (WHO), MI accounts for 30% of global deaths each year and is anticipated to reach more than 23 million by 2030 [213]. Cardiac troponin I (cTnI) is typically synthesized exclusively in the myocardium [214], and it is regarded as the 'gold standard' biomarker to identify heart failure, cardiac damage or MI owing to its excellent sensitivity and specificity [213,215]. Mi et al. [216] devised a ratiometric sensing strategy based on bifunctional probe (BFP) EC/EC (signal of methylene blue or MB) and ECL/EC (ECL probe with signal of doxorubicin or Dox-luminol) dual signal transduction and amplification for the detection of cTnI. The high affinity/specificity aptamer-Tro4 captures cTnI, liberating equivalent proportions of BFP (Fig. 12**B-i**). Part of the BFP stuck to tetrahedral DNA on the Ti_3C_2 MXene-Au sensing matrix, and another part started a hybrid chain reaction (HCR) with two hairpin structures, like H1 and H2. This caused EC and ECL signal currents with MB and Dox-Luminol, respectively (Fig. 12**B-ii**). The dual-signal ratio of ECL Dox-Luminol/Current Dox or Current MB/Current Dox was considered highly reproducible and accurate for the quantification of the cTnI. When combined with a transportable EC/ECL workstation, sensors are extremely likely to be used to screen for signs of cardiac injury in COVID-19 patients to reduce the mortality, particularly in mobile cabin hospitals [216].

Cytokines, as inflammatory modulators, are the essential components of our defensive system, protecting us from foreign pathogens. However, too much cytokine production destroys normal cells, triggering an unchecked inflammatory response through the immune system [217]. This is referred to as a "cytokine storm," which can kill even healthy people through an unknown pathophysiology. It has been linked in particular to the production of IFN-γ and TNF-α [218], both of which have been recently reported to induce mortality and cell death in SARS-CoV-2 [219]. Noh et al. describe the synthesis of an efficient, dual-target electrochemical aptasensor made of MXene (Ti_3C_2)/aptamer hybrid on an Au-based microgap electrode chip to detect IFN-γ and TNF-α cytokine storm indicators for the first time [220]. IFN-γ and TNF-α aptamers were used as bio-probes to capture cytokines and the concentration of cytokines were measured via the change in the electron transfer resistance (R_{ct}) by means of the EIS. This aptasensing technique seems to have several benefits, e.g., i) it is possible to detect both cytokine biomarkers in less than 10 min using alternating current electrothermal flow (ACEF); ii) by employing twelve Au microgap electrodes and two detection spots, the dual-target sensing system gives extremely reliable results using only 2 μL sample and is capable of differentiating between the two cytokines. However, a number of challenges need to be addressed, including: a) an interference analysis with other cytokines, for example, growth factor, colony stimulating factor, and interleukins at variable concentrations should be performed. b) Valid clinical sample evaluations with a variety

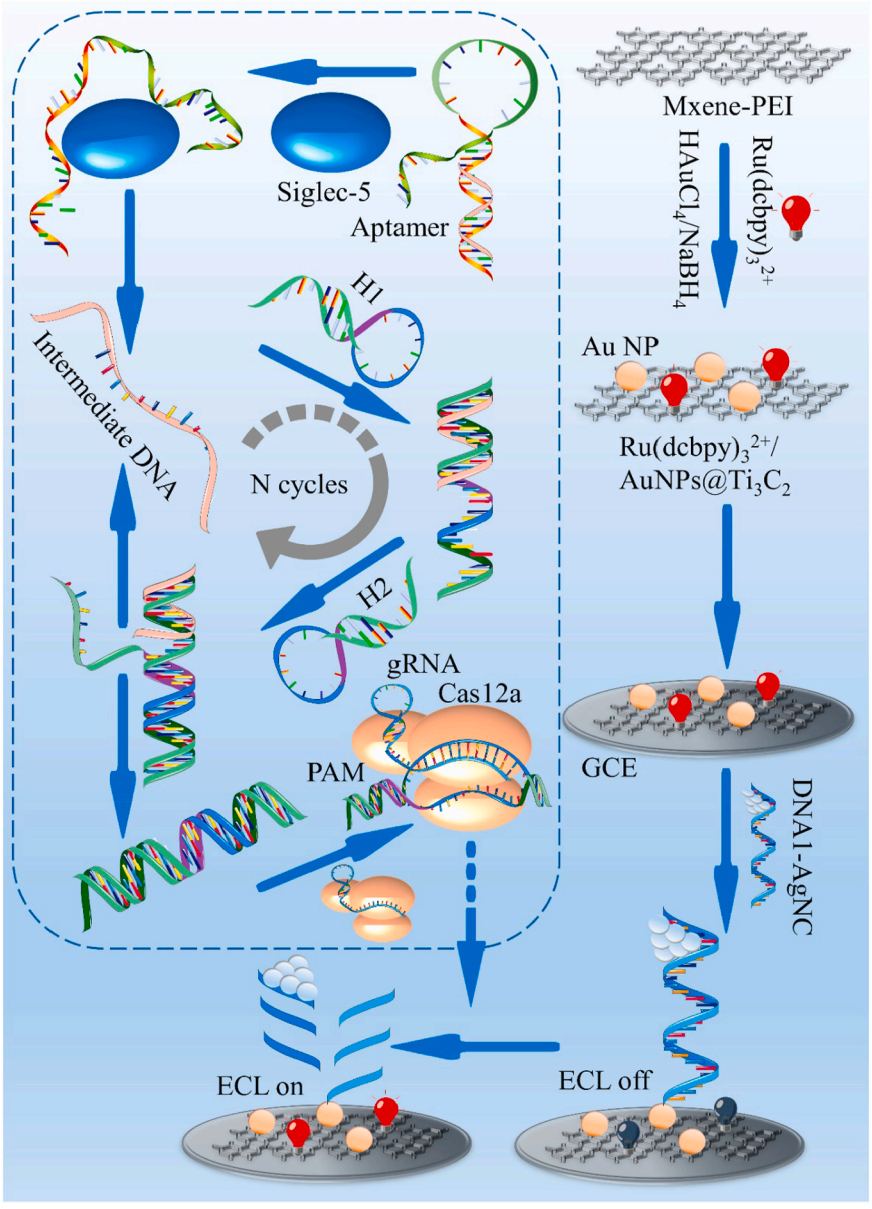

Fig. 13. Fabrication method and working principle of the suggested CRISPR-CHA based ECL aptasensor for the recognition of Siglec-5. Reproduced with permission from [225] @ Elsevier 2021.

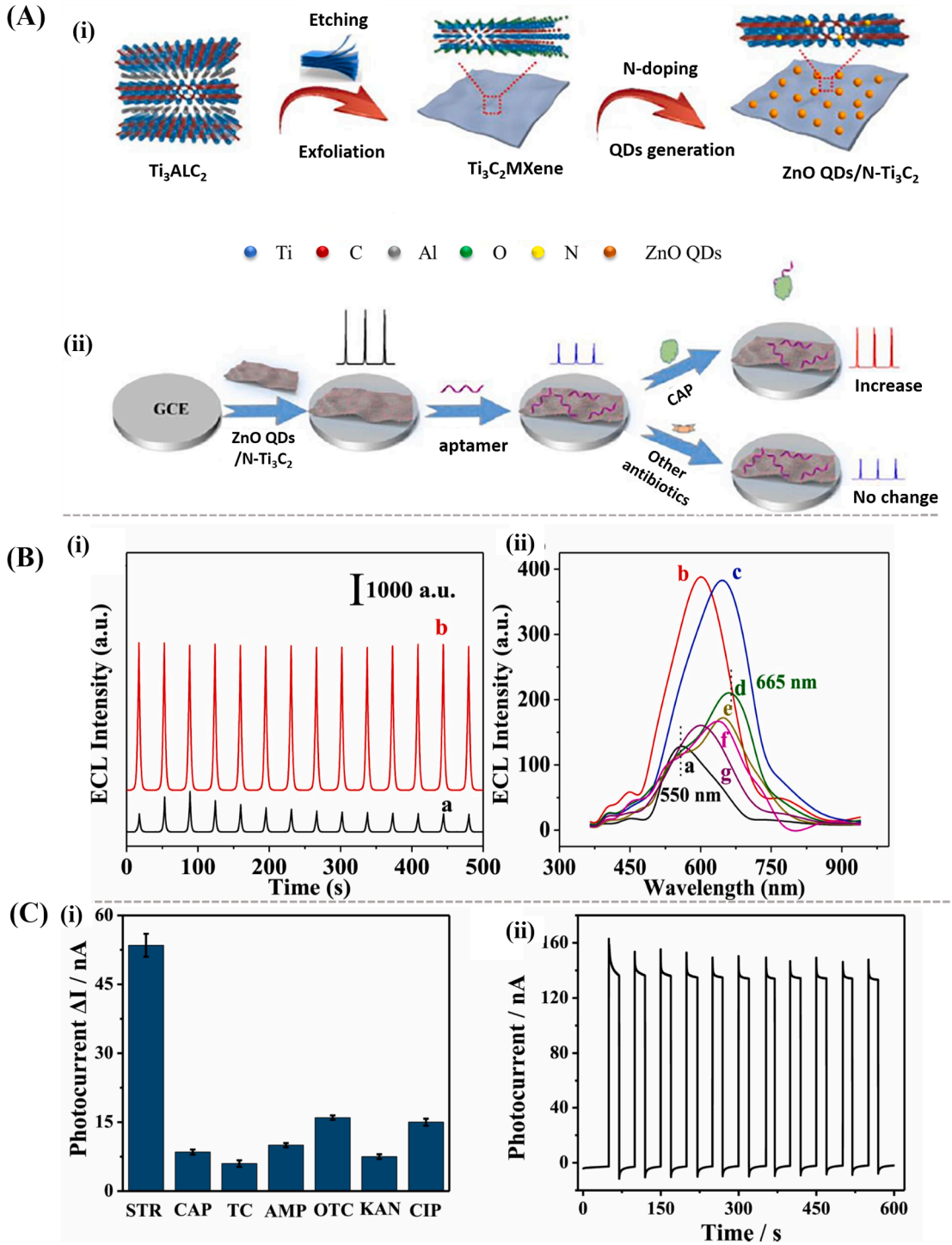

Fig. 14. **(A)-(i)** Schematic design involved in the synthesis of ZnO/N-Ti_3C_2 composite. (ii) The fabrication process of ZnO/N-Ti_3C_2 composite based ECL sensor and its application in CAP detection or quantification. Reproduced with permission from [230] @ Elsevier 2021; **(B)-(i)** ECL stability comparison in the presence and absence of MXene (a) intensity of pristine AgBr and (b) and 5% Ti_3C_2–AgBrNCs nanocomposites. **(ii)** ECL spectra of Ti_3C_2–AgBrNCs nanocomposite comprising different concentration of Ti_3C_2 MXene e.g., (a) 0%, (b) 3%, (c) 5%, (d) 10%, (e) 15%, (f) 25% and (g) 100% in PBS buffer. Reproduced with permission from [231] @ Elsevier 2022; **(C)-(i)** Selectivity and **(ii)** stability of the proposed photo electrochemical aptasensor founded on Bi_4VO_8Br/Ti_3C_2 composite for streptomycin detection. Reproduced with permission from [238] @ Elsevier 2021.

of patient groups are required. However, the proposed ultrafast electrochemical biosensor could be used in the future to detect different cytokines as immunological responses and cancer biomarkers at low concentrations and with small amount of samples [220].

The CRISPR-associated (Cas) proteins form an innate immune system that protects against invading genetic elements and several other phages [221]. CRISPR-Cas is a nuclease protein, while CRISPR RNA (crRNA, sometimes referred to as guide RNA or gRNA) is a small RNA fragment that can bind to the targeted nucleic acids [216]. Sialic acid-binding immunoglobulin (Ig)-like lectins (Siglecs) are type I transmembrane receptors found on the cell surface, comprising a transmembrane region, an intracellular and extracellular segment [222]. By identifying the glycan structure, it is able to regulate the malignancies, autoimmune disorders, and immunological balance in sepsis [223]. Siglec-9 and Siglec-5 are the most abundant lectins on the human cell surface. Siglec-5 may have a critical function in the body as an inhibitory receptor for leukocytes and is considered a promising marker for both acute myelogenous leukaemia (AML) and normal myelopoiesis [224]. As a result, developing novel siglec-5 tests can facilitate understanding of the pathogenesis of associated diseases and the development of new therapeutic agents. Zhang et al. developed a 2D ultra-thin $Ti_3C_2T_x$-based ECL aptasensor for the detection of Siglec-5 by combining a catalytic hairpin assembly (CHA) amplification strategy with the side-cutting feature of CRISPR-Cas12a [225]. The system can be used to detect new coronavirus-related proteins comprises four main parts; 1) a reporter system (a pre-assembled CRISPR-Cas12a effector with modified nucleic acid and gRNA ECL sensor); 2) an amplification system (isothermal amplification systems based on CHA); 3) a probe system (DNA activator for CRISPR-Cas12a and gRNA); and 4) a trigger system (termed K19) with a piece of intermediate DNA. CRISPR-Cas12a's binding to dsDNA is largely dependent on gRNA to recognize dsDNA. The authors created a CHA amplification scheme made of two DNA hairpins (H1 and H2). The dsDNA that results from the amplification is used to bind CRISPR-Cas12a. B H1 and H2 are composed of a single stem-loop DNA with a protruding 5′ terminus. The 5′ end of H1 comprises the intermediate DNA hybridization sequence, whereas the loop region carries the non-target strand (NTS) and the CRISPR-Cas12a's 5′-TTTA-3′ PAM. Moreover, the 5′ overhang of H2 has a sequence compatible with the intermediate DNA/H1 duplex. Following the production of the H1/H2 duplex, intermediate DNA is substituted by H2 and joins the next cycle that can result in the formation of further H1/H2 duplexes (**Fig. 13**). There are two innovative aspects to this approach: (i) the hybrid sequence of CRISPR-Cas12a supports the targeting approach to strengthen the indirect Siglec-5 amplification test by providing a pair of sites that are not in the dsDNA, (ii) dsDNA was also designed using CRISPR/Cas9 amplification to detect the output of intermediate DNA duplexes, which provided a common technique to detect biomarkers by converting analytes from proteins to intermediate DNA [225].

Lipopolysaccharide (LPS), a form of endotoxin, is the main component of Gram-negative bacteria's outer membrane [226]. It has the ability to modify a variety of humoral and cellular-mediated processes [227] including septic shock, a serious hazard to global health. Gram-negative pathogenic bacteria cause a wide variety of infectious diseases and the mortality of millions of people each year, accounting for a considerable proportion of the deaths worldwide [228]. Sheng et al. established a detection approach for Gram negative bacteria built on coupling CRISPR-Cas12a with MXene [229]. The aptamer's sequences were flexibly synthesized to activate CRISPR-Cas12a, while the target addition hindered CRISPR-Cas12a activation via its strong binding to the aptamer. At the same time, MXene enhances the binding of the target to the aptamer via its robust binding to the aptamer's complementary ssDNA, hence inhibiting CRISPR Cas12a activation. MXene NSs can bind FAM-labeled ssDNA and effectively quench the fluorescence attributable to its superiority in visible light absorption, which makes a significant contribution to the sensor's high sensitivity for Gram negative bacteria [229].

By employing a thermal annealing process to synthesize ZnO QDs coated on Ti_3C_2 MXene composite, Jiang et al. [230] employed a simple nitrogen source to regulate the nitrogen concentration of the composite (Fig. 14A-i) to construct an ECL aptasensor for chloramphenicol (CAP) detection. The Ti_3C_2 MXene matrix played a key role in the confinement of ZnO QDs growth and nucleation. Not only did the developed nanocomposites enhance electron transmission, but they also minimized the barrier to ZnO QDs reduction, leading to improved ECL efficiency. The ECL signals were drastically reduced after anchoring the CAP aptamer at the ZnO/N-Ti_3C_2 surface via π–π stacking interactions. This behavior may be explained by the steric hindrance effect and low conductivity of aptamer, which hampered the efficient electron transfer at the sensing surface. Afterwards, when an aptamer was used to bind CAP on the electrode surface, a considerable enhancement in the ECL signal was detected because of the creation of the aptamer-CAP complex, which was subsequently released from the sensing electrode and the ECL intensity was recovered (Fig. 14A-ii). As a result, CAP in the sample was quantified by measuring the change in ECL intensity. Aptasensor showed good stability and recovery rates, which suggests that it could be used in food analysis and environmental monitoring [230]. Another ECL, near-infrared (NIR) aptasensor built on a Ti_3C_2-AgBrNCs/$K_2S_2O_8$ composite was proposed by Jiang et al. [231] to monitor enrofloxacin (ENR) antibiotic for food safety applications. As the Ti_3C_2 proportion in the Ti_3C_2-AgBrNCs composite increased, the ECL emission wavelength spectra redshifted from 550 to 665 nm, which can be attributed to the surface-defect effect induced by the oxygen-containing functional groups in Ti_3C_2 NSs. In particular, the ECL emission spectra of Ti_3C_2–AgBrNCs at 665 nm not only exhibited a 3.5-fold enhanced ECL intensity but also highly stable ECL current signals in comparison to AgBrNCs only. A glassy carbon electrode was first modified with Ti_3C_2–AgBrNCs/$K_2S_2O_8$ composite followed by the immobilization of ENR specific aptamer to efficiently recognize, capture, and quantify ENR based on ECL signal changes. This study found that inorganic nanocomposites stabilized by MXene could be efficiently used as NIR ECL based luminophores [231]. ECL signal intensity significantly increases (nearly 3.5 folds) in the presence of MXene in the MXene-AgBr composite as compared to the pure AgBr, which is possible for two reasons. (i) Ti_3C_2 MXenes help to stabilize AgBr nanoclusters by preventing aggregation and increasing AgBr luminophore loading capacity, and (ii) by reducing AgBr passivation and increasing electron transfer on the electrode surface. It can be seen in Fig. 14B-i that the AgBr/GCE electrode showed a highly unstable ECL signal, whereas the addition of MXene (AgBrNCs-Ti_3C_2) significantly improved the stability issues. The authors make a comparison of their previous work for ECL emission at 400–500 nm of pure AgBr. They discovered that Ti_3C_2–AgBrNCs exhibited a clear red shift toward ~665 (in $K_2S_2O_8$ solution) (Fig. 14**B-ii)**, demonstrating that Ti_3C_2 can generate red-shifted NIR ECL [231].

Streptomycin (STR), a broad-spectrum antibiotic, is used to treat gram-negative pathogens in both animals and humans [232,233]. It can help relieve the symptoms of animal infections, including bee rot disease and many others [234]. Beekeepers employ STR in an inappropriate manner in order to maintain bee larvae health, and as a result, STR is found in several bee products [235]. Using STR uncontrollably or improperly can lead to the antibiotic's inclusion in the food chain and may have serious adverse implications for human health, including ototoxicity and nephrotoxicity. Streptomycin plasma level greater than 35 g/mL STR is potentially harmful [236]. Furthermore, STR metabolites in the aquatic system are challenging to entirely eliminate because of their great water solubility. Streptomycin sensing in a wide range of food and water samples is essential for human health safety and environmental monitoring [237]. You et al. [238] synthesized the Ti_3C_2/Bi_4VO_8Br composite via a one-pot solvothermal process and employed it as a photoactive material. It was customized on an ITO electrode and coupled to STR binding aptamer (as bio-receptor). Based on the aptamer's unique recognition of the target, an "on-off-on" photo-electrochemical (PEC) sensor was implemented to determine STR in honey samples, with good sensitivity and high repeatability.

The photocurrent behavior of commonly used interfering antibiotics (TC, CAP, AMP, CIP, OTC, and KAN) against STR was determined to ascertain the selectivity of the proposed setup. Increasing the concentration of interfering antibiotics by ten-fold than that of STR (500 nM versus 50 nM STR). No significant change in current signals was observed (Fig. 14C**-i)** which confirmed the high selectivity of the aptasensor. Additionally, the reproducibility and stability of the aptasensor were also investigated (Fig. 14C**-ii)** implying that the sensor's photocurrent intensity largely remained steady, and the performance was not significantly affected after storing the electrodes for two weeks at 4 °C. The constructed PEC sensor exhibited considerably high LOD and an optimal linear range with real samples, providing a more specific and reliable bio-sensing strategy for antibiotic identification in food quality monitoring [238].

The coronavirus (SARS-CoV-2 or 2019-nCoV) is rapidly spreading throughout the world, infecting humans, causing respiratory infections, and killing thousands of people every day. In comparison to SARS-CoV, SARS-CoV-2 is believed to transmit more readily through person-to-person touch, therefore contributed to the WHO's (World Health Organization) warning of a global pandemic on March 11, 2020 [239]. Widespread and rapid testing is critical in controlling the spread of COVID-19 throughout the world. Currently, immunoglobulin G/M (IgG and IgM) assays, computed tomography (CT) scans, real-time polymerase chain reaction (RT-PCR), and a variety of other tests have been utilized to diagnose COVID-19 [240]. They are, however, ineffective for early diagnosis and treatment. As a result, it is critical to develop novel methodologies for the detection of COVID-19 that are sensitive, specific, and rapid [241]. Chen et al., recently introduced the first and only SPR aptasensor by employing a sensitive layer of niobium carbide MXene QDs (Nb_2C-SH QDs) as a substrate to anchor N-gene-targeting aptamer probes to detect and quantify SARS-CoV-2 N-gene at early stages with high specificity [242]. The gold chip was decorated with Nb_2C-SH QDs, which were then coupled to the N58 aptamer via Au-S, hydrogen bond, π-π stacking, and electrostatic adsorption. The aptamer undergoes conformational switching on binding to the N-gene, thereby increasing the distance or contact area between the SPR chip and the aptamer with the subsequent changes in SPR signal flashed by the He-Ne laser (633 nm wavelength) to quantify the N-gene of SARS-CoV-2. The Nb_2C-SH QDs-based SPR sensor shows fast response, high sensitivity, and repeatability as compared to previously reported SPR sensors. Due to the highly conjugated framework, MXene phase, and thiol-functionalization, the synthesized Nb_2C-SH QDs demonstrated a strong binding connection with the gold chip by self-assembling forces produced by the Au-S bond, as well as robust bio-affinity for an amplified SPR effect and the aptamer strands. Besides exhibiting a low LOD throughout a broad linear range of N-gene concentrations, excellent repeatability, and great selectivity, this also favors the applicability of the proposed sensor system, which is capable of in situ analysis and is easy to manufacture. Unfortunately, the SPR sensor still has some flaws, including poor regenerability and repeatability when identifying N-genes [242].

5. Innovative trends of MXenes in optical aptasensors

Aptasensors may be a feasible choice for the fabrication of efficient biosensors because they are regarded to be selective for a particular analyte, committed to continuous detection, easy to use, rapid results, as well as possibly portable and inexpensive. Current MXene-based aptasensors have been classified electrochemically and optically based on the associated transducer type. While MXene-based EC aptasensors are gaining popularity, their optical aptasensors are also gaining traction. In this section, we will discuss about some of the new ideas in optical aptasensors that use MXene.

Due to their good reproducibility, quick analysis, outstanding selectivity, and high sensitivity, optical bio-sensing has gained considerable attention [250,251] in environmental, biomedical, and biochemical research in recent decades [249]. Optical analysis, which is dependent on the interaction between material and light, helps analyze samples by measuring changes in spectrum or intensity shift using a non-destructive method. With the advancement of nanotechnology and the emergence of novel nanomaterials, optical assessment has made tremendous advances. Among nanomaterials, MXene has gained increased attention in imaging and optical sensing for bio-analytes found in living cells or body fluids owing to its superior physicochemical features.

Regarding optical aptasensing platforms, two types of Ti_3C_2 MXenes are frequently used as developing nanomaterials: MXene NSs are commonly employed as cargo carriers, SERS components, and fluorescence quenchers, while MXene quantum dots (MQDs) are being utilized as signal tracers and luminescence species [252]. Additionally, MXenes NSs exhibit unique features that enable the construction of high-performance optical biosensors. To begin with, MXene NSs have several desirable features such as biocompatibility and strong hydrophilic nature, making them appropriate for a wide variety of sensing applications. The unique qualities of the MXene NSs, such as their mechanical properties, exceptional conductivity, and huge surface area, may promote their uses in sensor development as cargo carriers, SERS substrates, and fluorescence quenchers in imaging and biomedicine. Moreover, the evident benefits of MXene NSs, including favorable energy levels and a broader absorption spectrum, may end up making them have an intriguing potential for photo electrochemical, photo-thermal, and optical bio-sensing. MXenes have seen exceptional growth in the

optical sensing field as a result of the features outlined above [252]. On the other hand, MQDs might be more efficient fluorescent probes to provide luminescent responsiveness to target analytes than MXene NSs, due to their photo-luminescent nature, high photo-stability, solubility, and tunable size. MQDs have excellent emission characteristics due to their surface defects and quantum confinement [253]. Therefore, MQDs are being employed as fluorescence signals or tracers and extensively exploited in biological systems for optical sensing [253]. The classification of optical aptasensors is based on various identification strategies used, which include fluorescence, CL/ECL, colorimetric, SERS and SPR [254,255].

Fluorescence sensing is extremely effective in detecting biomolecules with high sensitivity [256,257]. MXenes offer significant advantages in terms of absorption of light between visible to near-infrared wavelengths [56]. MXenes have the ability to bind ssDNA aptamers and substantially extinguish the fluorescence from a fluorophore. As a result of its high affinity for ssDNA and its superiority in visible light absorption, MXene effectively quenches the fluorescence of fluorophore-labeled ssDNA, drastically reducing the background signal. Simultaneously, the high affinity of MXene for ssDNA could be used to improve the robustness of target-induced single-strand release, hence improving the specificity of the proposed technique [258]. Two main processes have been proposed for the fabrication of MXene-based fluorometric aptasensors. The first category involves the use of MXene NSs as powerful quenchers (acceptors) in FRET to induce "on/off" events in fluorophores or other luminous nanomaterials (donors), such as quantum dots, metal nanoclusters and organic dyes, etc. For example, the aptasensor proposed by Cui et al., [193] for thrombin detection and Hong et al., [208] for Vibrio detection (refer to Section 3 for details). The quenching system is influenced by the proximity separating donors from acceptors, which is altered when certain recognition processes occur. The other type of category incorporates luminescence MQDs in signal output constituents that may be quenched effectively and directly by adding analytes. As a result, multiple design schemes for fluorescence MXene based sensors with diverse properties can be devised [128].

Due to its low-cost, sensitive and simple properties, chemiluminescence (CL) based sensing is widely employed in a variety of fields [259]. It does not need an external source of light, unlike fluorescence, and it has a significantly longer life span than fluorescent species [260]. By combining the electrochemical characteristics with CL sensitivity, electro-generated chemiluminescence (ECL) is yet another excellent detection approach in aptasensing [261,262]. ECL has been broadly employed in analytical chemistry due to its good stability, sensitivity, easy controllability, low cost, and improved efficiency [263,264]. Thanks to the strong conductivity and huge surface area of MXene NSs, they can be exploited as ECL probes. For example, the MXene-based ECL aptasensor was designed to identify human breast cancer cells (MCF-7) exosomes [159]. Owing to a huge surface area, MXene NSs may accommodate a large number of aptamers, effectively increasing the sensitivity and lowering the detection limit of the various aptasensing devices. Aptamer transduction with various MXenes for ECL aptasensors has already been discussed in Section 4 ([159,157,158,212,216,225] (refer to the Table 1 for the literature cited). Thus, the use of MXenes in ECL aptasensors not only results in higher amplification and sensitivity of the ECL signal, but also leads to higher electrical transmission rate and improved stability, all of which have a number of advantages. More ECL aptasensors containing MXenes for various clinical indicators can be built using similar ideas. Similar approaches can be employed to fabricate more ECL aptasensors with MXenes for various other clinical biomarkers.

Colorimetric sensing is typically performed using specific types of visualizing reagents that undergoes color transformation in the presence of target biomolecules. The UV–vis spectrum can be used to accurately and easily measure the color change [265]. Intrinsic peroxidase activity has been found in Ti_3C_2 NSs. The negative charge of single-stranded DNA may easily be adsorbed onto Ti_3C_2 NSs, increasing their enzymatic catalytic activity. The surface of Ti_3C_2 NSs can be altered with ssDNA aptamers to generate a Ti_3C_2@ssDNA nanocomplex. The catalytic activity of this nanocomplex has been greatly increased. Once the analyte is added, the aptamers are desorbed from Ti_3C_2 NSs in order to bind to the target, causing a reduction in enzymatic activity [252]. The increased target concentration brings down the catalytic activity of Ti_3C_2 NSs towards substrate oxidation, allowing for direct determination of the target. ssDNA has a dual function of identifying biomolecules and enhancing enzymatic activity. This simple sensing concept can also be used to identify different analytes (small molecules, metal ions, and pathogens, etc.) [200]. The results indicate that in future, various MXene-based colorimetric aptasensors might be developed based on the enzyme-like catalytic activity of Ti_3C_2 NSs in combination with a particular target identification ability of aptamers.

MXene NSs provide an appropriate microenvironment for Raman tags, making them an attractive substrate for SERS. The potential SERS substrates can act as useful materials for supersensitive target identification [252]. Two SERS based aptasensors for OTA and AFB1 detection based on MXene-based nanocomposites have recently been reported by Zheng et al., [187] and Wu et al., [185] respectively **(**Table 1**)**. According to the findings, MXene-based materials have a wide range of applications in optical biosensing and aptasensing, and the principle can be applied to develop more relevant SERS aptasensors based on MXenes. Furthermore, because MXene has characteristics similar to graphene, various graphene-based SERS aptasensors, can be transformed to develop MXene based SERS aptasensors [262].

The Surface Plasmon Resonance (SPR) signal is considered a highly sensitive assay for detecting variations in the environment that has been widely used in sensing technology [266–268]. When collective electron oscillations are linked to electromagnetic waves, the surface plasmon wave propagates and exponentially decays along the metal-dielectric interface, resulting in SPR based on Kretschmann configuration phenomena. The SPR response is employed in biosensors to indicate the presence of a chemical reaction or biological event [25,269]. The SPR biosensor could be made as a chip involving layer-by-layer stacking of nanostructures on a substrate, with each monolayer of 2D material created via chemical vapor deposition [270]. MXenes have a strong attraction for biomolecules due to the characteristic abundance of hydroxyl and/or oxygen functional groups and full metal atomic layers, forming the SPR bio-interface [252]. Chen et al. recently devised the only SPR aptasensor with a few-layer Ti_3C_2 MXene coatings on the surface of metal thin films to improve sensitivity [242] (refer to Section 4.3 for details). $Ti_3C_2T_x$ MXene's band gap-adjustable performance was relative to the increased number of functional groups on its surface [271,272]. Despite these benefits, just one article was recently published on MXene-based SPR aptasensors [242], which might open new prospects for the advancement of other MXene-based SPR

aptasensors in the future.

6. Challenges and future perspectives

MXene-based aptasensors appear to be very useful since their detection sensitivity ranges from picomolar to femtomolar, which is much higher than that of traditional approaches like spectroscopy and chromatography. Despite these advancements, MXene-based aptasensors are still in their infancy in comparison to most of the other biosensing techniques. Nevertheless, aptasensors based on MXenes could be useful in the future for a wide range of applications once certain challenges are addressed.

I. Aptamer's shorter half-lives are a serious obstacle for the aptasensor industry. Further, the literature shows a lack of familiarity with aptamer surface immobilization approaches and a scarcity of aptamer varieties.
II. The MXene aptasensors exhibit high sensitivity in the range of nanomolar to femtomolar concentration with low LOD, however the signal transmission may vary due to quality of MXene and synthesis condition.
III. Practically, all MXene related aptasensors comprise molecular recognition components based on DNA aptamers. There seems to be only one report using RNA aptamers in combination with MXenes [170], perhaps owing to their intrinsic instability and expensive manufacture. RNA aptamers, on the other hand, have a stronger affinity for their targets in comparison to DNA aptamers. Additionally, they exhibit a greater structural switching ability upon binding to their appropriate targets, allowing for simpler and sensitive aptasensing techniques. More RNA aptamers might be used in the fabrication of MXene based aptasensors.
IV. The real-world applications of MXene-based aptasensors, i.e., the identification or quantification of the target molecules in complex environments and real samples, is significantly challenging such as drinking water, wastewater, serum, blood and food samples inevitably comprise a mixture of ions, particles and macromolecules that might generate nonspecific signals during the detection phase. As a result, research on aptasensors should investigate their detection limits in complex environments and undiluted real samples. Generally, the majority of published results were obtained under favorable laboratory settings.
V. Additional concerns involve the scalability of fabrication processes. The majority of aptasensor fabrication methods are optimized for fast laboratory scale production and cannot be scaled up for mass production. For aptasensors to be marketed on a large scale, fabrication techniques must be developed to construct massive supplies of aptasensors manufactured using inexpensive precursors and reliable specifications. This strategy is proposed for the commercialization of this kind of aptasensing approaches to be successful.
VI. The majority of MXene aptasensors are validated in the laboratory using buffers, whereas clinical detections imply complicated samples with variable environmental factors, including pH value, which might result in massive drift in result recording. For instance, the effect of pH on the breast cancer maker Mucin1 detection using a ferrocene-labeled complementary DNA/MXene aptasensor was calibrated prior to conducting real serum analysis [167]. Other variables, such as surface potential, environmental temperature and so on, have been reported infrequently. As with other electrochemical devices, the deviation of MXene aptasensors could be calibrated prior to practical target detection. Therefore, we predict that such MXene-based aptasensing devices would evolve into an effective regular analysis system capable of addressing a range of challenges.
VII. The use of MXenes in aptasensors is associated with various other challenges, e.g., MXene oxidation may affect the stability of biosensors in humid and hot environments; non-uniform surface terminations could affect its proper functioning, and the expensive MAX precursor may hinder the development of MXene aptasensors, etc. The described MXene-based aptasensors for genuine foodborne pathogens and mycotoxins detection in food safety still have significant limitations which need to be considered seriously.

Considering the challenges, we would like to provide several additional perspectives related to the future of MXene-based aptasensors in this section.

VIII. At the atomic or molecular level, the interactions between various MXenes and ssDNA aptamers must be thoroughly explored. Numerous investigations have demonstrated that the particular recognition of targets by aptamers coupled to MXenes released only a fraction of the aptamers, and as such, the predominant sensing mechanism was based on the conformational shift of aptamer molecules following target identification. Through molecular dynamics simulations, it is important to investigate the molecular level interactions and conformational transitions of ssDNA upon binding to MXenes.
IX. Portable MXene-based aptasensor devices with high sensitivity, low cost and rapid detection must be developed. Numerous MXene-based aptasensors described in this review could serve as inspiration for achieving this goal. Simultaneously, the portable electrochemical work station may also facilitate promising in situ analysis.
X. It is imperative to analyze the nanotoxicity and biocompatibility of MXene-based aptasensor devices, particularly for in vivo detection of target molecules in/on cells and biomedical sensing. Indeed, the choice of flexible MXene composites and engineerable surface terminations enables researchers to construct customizable MXenes with desired functionality. For example, considering fluorine's cytotoxicity, fluorine-free MXene $Ti_3C_2T_x$ (generally terminated by –O or –OH) is preferable to HF-etched MXene when it comes to MXene-based in vivo detection or cell biosensors development. Despite that metallic MXene $Ti_3C_2T_x$ is well-suited for use in traditional electrochemical bioassays, modifications to the precursors or etching method enable the production of MXenes with the appropriate band structures to meet the excitation condition requirements. Additionally, innovative MXene related nanocomposite aptasensors with intrinsic fluorescence emitting or quenching ability could also be established in this framework, resulting in the feasibility of label-free sensing probes.

XI. Developing novel, high affinity aptamers for diseases such as Alzheimer's, Parkinson's, diabetes, and many more may hold great potential in early diagnostic applications for clinical samples. In this context, versatile MXene based aptasensors may find commercial applications for the development of most desired point of care testing devices.

XII. The investigation of hetero-structures containing additional functional 2D NMs such as black phosphorus, transition metal sulphides, oxides, and graphene may provide additional prospects for improved selectivity and sensitivity. MXene-based nanohybrid composites with multifunctional properties are in high demand for optical bio-sensing recently.

XIII. Considerable attention is required to explore various emerging optical bio-sensing platforms such as ECL, SERS, colorimetric, SPR and certain coupling approaches based on MXene QDs and NSs. Because $Ti_3C_2T_x$ has garnered considerable attention, its stability needs to be improved, and it is suggested that various other MXenes must be investigated for the development of novel aptasensors. Due to the electromagnetic interference shielding characteristics of MXenes, magnetic-field stimulus/activated optical sensing platforms might also find significant applications in biological systems and biomedicine. Further research should be conducted to understand the correlation between the optical properties of MXene and their composition or structure, along with their edges. Computer-aided engineering of MXenes in relation to adjustable surface terminations, morphology, and appropriate size, could be another approach to enhance our understanding of how to promote MXene development for their sensing applications and optical features.

XIV. A more comprehensive understanding of aptamer immobilization strategies on various MXenes is required for multiplex sensing of biomolecules in a cost-effective and facile setting, particularly for point-of-care diagnostics.

XV. The exceptional electrical and mechanical features of $Ti_3C_2T_x$ MXene make it an excellent platform for wearable technology. Wearable MXene-based biosensors are playing substantial roles in the continuous and non-invasive tracking of a wearer's health and physiology in the human body, including disease diagnostics and therapy. Aptasensors based on wearable technology have also been commonly reported, e.g., wearable cortisol aptasensors [273]. Yet there is not even a single report describing the use of MXene-based aptasensors in wearable technology for an unknown reason. MXene based wearable biosensors may be efficiently converted into MXene-based aptasensors to broaden their potential application range.

XVI. Aptasensing with MXene is an emerging topic for which the majority of the research articles appeared in 2021 (22 reports). Some new combinations, e.g., MXene-based microfluidic or M-EC [164] and LRET [245] aptasensors, clearly indicate that this type of aptasensors are likely to become the most popular in the future.

XVII. Some MXenes other than $Ti_3C_2T_x$ or Ti_3C_2, e.g., Nb_2C [242] and $Nb_4C_3T_x$ [246], have been recently used to construct MXene-based aptasensors. It shows the growing interest of the scientific community towards exploring the benefits of a variety of MXenes in aptasensing in the upcoming years. Although the aptasensors reported for food/water safety might be extended for environmental monitoring, aptasensor with $Nb_4C_3T_x$ as a transducer [246] has recently started finding applications in environmental monitoring to detect the traces of heavy metals in the environmental samples as well (first MXene based aptasensors to detect Pb^{2+}). It may necessitate large-scale commercialization in the future owing to its broad-ranging application potential.

Commercialization necessitates innovations to ensure that these approaches can be used on a regular basis. Continued advancements in all these aptasensing strategies are conceivable by combining multiple approaches, hence overcoming the challenges of each method mutually. Moreover, future efforts should be directed towards the construction of less sophisticated technologies that can be easily utilized by non-professional individuals. The evaluation of representative MXene related aptasensors and future trends in this area are anticipated to further explore MXene's prospects for biomedical sensing advancements.

7. Conclusion

The current review summarized recent advances in the design and implementation of aptasensors based on MXene as a transducer. MXene, a newly emerged 2D material, has advanced at a rapid pace in recent years, serving as an important transducer for the fabrication of aptasensors. Since its discovery in 2011, MXene has captivated the interest of scientific community due to its unique features, which include catalytic features, ease of functionalization, superior metallic conductivity, and layered morphology. MXenes exhibit superior electrochemical properties than other 2-D NMs such as Mo_2S and graphene, etc. Some of its features, such as the existence of ample functional groups and good surface area are critical for developing improved biosensors integrating bio-receptors such as aptamers. Therefore, the fabrication of an aptasensor made by conjugation of aptamers with MXenes results in an increased sensitivity and selectivity. MXenes' non-covalent interactions with single stranded DNA aptamers are considered to play a key role in the development of high-performance MXene based aptasensors. It is obvious that single-stranded DNA aptamers have a higher affinity for MXenes than either the aptamer-target complex or double-stranded DNA, providing an insight into the sensing mechanisms of the majority of MXene-based aptasensors.

It was also found that $Ti_3C_2T_X$ is the dominant MXene involved in the field of aptasensing. Titanium carbide QDs and NSs exhibit remarkable optical and electrical characteristics that have been used in a variety of optical sensing devices. Additionally, by employing desired surface functionalization and engineering strategies, it is possible to synthesize MXenes with desired features, that might expand their optical uses beyond colorimetric, ECL, photo-thermal, fluorescence, PEC, SERS and SPR based aptasensing. The strategies described in this review encompass almost all the diverse approaches for fabricating MXene-based aptasensors, which may help readers comprehend new sensing methodologies and develop improved MXene-based aptasensors in healthcare testing applications. This review also summarizes the applications of various electrochemical aptasensors based on MXenes for the detection of numerous target anlytes. Although considerable efforts have focused on constructing and implementing optical aptasensing strategies based on MXenes, the investigations are comparatively scarce compared to electrochemical aptasensors. While a small number of reports

focused on MQDs and NSs as fluorescence technologies, alternative optical sensing methods such as SERS, colorimetric, PEC and SPR appear to be uncommon (each type has only one or two reports). The fundamental performance related parameters of the aptasensor, such as the LOD, linear working range, and reproducibility of results, are described adequately.

Current research demonstrating the use of innovative MXene nanomaterials in combination with aptamers tailored to identify a variety of targets of biological significance has opened up new opportunities in the food industry and healthcare. The situation has improved significantly over the current year, and recent breakthroughs in the field of MXene aptasensing well surpass the limitations outlined previously. While the majority of these aptasensors are still in the initial phase of development, attempts are being made to commercialize these devices in the future. Due to the increased interest and unwavering efforts from both the scientific and industrial communities, the existing constraints of MXene-based aptasensors are projected to be overcome shortly.

Declaration of Competing Interest

The authors declare that they have no known competing financial interests or personal relationships that could have appeared to influence the work reported in this paper.

Acknowledgement

This work was supported by “the Fundamental Research Funds for the Central Universities” YD2070002013, Higher Education Commission of Pakistan through NRPU grant No. 10699 and partially by KIST School Partnership Project 2022 (SPP-2022), Republic of Korea. This work is also supported by UREP28-063-1-008 project from QNRF, Qatar awarded to SAZ.

References

[1] Goldoni R, Farronato M, Connelly ST, Tartaglia GM, Yeo WH. Recent advances in graphene-based nanobiosensors for salivary biomarker detection. Biosens Bioelectron 2021;171(2020):112723. https://doi.org/10.1016/j.bios.2020.112723.
[2] Wang H, Yuan R, Chai Y, Niu H, Cao Y, Liu H. Bi-enzyme synergetic catalysis to in situ generate coreactant of peroxydisulfate solution for ultrasensitive electrochemiluminescence immunoassay. Biosens Bioelectron 2012;37(1):6–10. https://doi.org/10.1016/j.bios.2012.04.010.
[3] Tang H, Chen J, Nie L, Kuang Y, Yao S. A label-free electrochemical immunoassay for carcinoembryonic antigen (CEA) based on gold nanoparticles (AuNPs) and nonconductive polymer film. Biosens Bioelectron 2007;22(6):1061–7. https://doi.org/10.1016/j.bios.2006.04.027.
[4] Tanaka T, Matsunaga T. Fully automated chemiluminescence immunoassay of insulin using antibody - Protein A - Bacterial magnetic particle complexes. Anal Chem 2000;72(15):3518–22. https://doi.org/10.1021/ac9912505.
[5] Wu Ze, Fu Q, Yu S, Sheng L, Xu M, Yao C, et al. Pt@AuNPs integrated quantitative capillary-based biosensors for point-of-care testing application. Biosens Bioelectron 2016;85:657–63. https://doi.org/10.1016/j.bios.2016.05.074.
[6] Patel H, Rawtani D, Agrawal YK. A newly emerging trend of chitosan-based sensing platform for the organophosphate pesticide detection using Acetylcholinesterase- a review. Trends Food Sci Technol 2019;85(2018):78–91. https://doi.org/10.1016/j.tifs.2019.01.007.
[7] Yan X, Li H, Su X. Review of optical sensors for pesticides. TrAC - Trends Anal Chem 2018;103:1–20. https://doi.org/10.1016/j.trac.2018.03.004.
[8] Feng C, Dai S, Wang L. Optical aptasensors for quantitative detection of small biomolecules: A review. Biosens Bioelectron 2014;59(2014):64–74. https://doi.org/10.1016/j.bios.2014.03.014.
[9] Ellington AD, Szostak JW. In vitro selection of RNA molecules that bind specific ligands. Nature 1990;346(6287):818–22. https://doi.org/10.1038/346818a0.
[10] Tuerk C, Gold L. Systematic evolution of ligands by exponential enrichment: RNA ligands to bacteriophage T4 DNA polymerase. Science (80-) 1990;249(4968):505–10. https://doi.org/10.1126/science.2200121.
[11] Zahra QUA, Khan QA, Luo Z. Advances in optical aptasensors for early detection and diagnosis of various cancer types. Front Oncol 2021;11:632165. https://doi.org/10.3389/fonc.2021.632165.
[12] Citartan M, Ch'ng ES, Rozhdestvensky TS, Tang TH. Aptamers as the ‘capturing’ agents in aptamer-based capture assays. Microchem J 2016;128:187–97. https://doi.org/10.1016/j.microc.2016.04.019.
[13] Citartan M, Gopinath SCB, Tominaga J, Tan SC, Tang TH. Assays for aptamer-based platforms. Biosens Bioelectron 2012;34(1):1–11. https://doi.org/10.1016/j.bios.2012.01.002.
[14] Goud KY, Reddy KK, Satyanarayana M, Kummari S, Gobi KV. A review on recent developments in optical and electrochemical aptamer-based assays for mycotoxins using advanced nanomaterials. Microchim Acta 2020;187(1):1–32. https://doi.org/10.1007/s00604-019-4034-0.
[15] Kerman K, Tamiya E. Aptamer-functionalized Au nanoparticles for the electrochemical detection of thrombin. J Biomed Nanotechnol 2008;4(2):159–64. https://doi.org/10.1166/jbn.2008.013.
[16] Lu AH, Salabas EL, Schüth F. Magnetic nanoparticles: Synthesis, protection, functionalization, and application. Angew Chemie - Int Ed 2007;46(8):1222–44. https://doi.org/10.1002/anie.200602866.
[17] Wang H, Yang R, Yang L, Tan W. Nucleic acid conjugated nanomaterials for enhanced molecular recognition. ACS Nano 2009;3(9):2451–60. https://doi.org/10.1021/nn9006303.
[18] Wang G, Wang Y, Chen L, Choo J. Nanomaterial-assisted aptamers for optical sensing. Biosens Bioelectron 2010;25(8):1859–68. https://doi.org/10.1016/j.bios.2009.11.012.
[19] Yang W, Ratinac KR, Ringer SR, Thordarson P, Gooding JJ, Braet F. Carbon nanomaterials in biosensors: Should you use nanotubes or graphene. Angew Chemie - Int Ed 2010;49(12):2114–38. https://doi.org/10.1002/anie.200903463.
[20] Mahmoudpour M, Ding S, Lyu Z, Ebrahimi G, Du D, Ezzati Nazhad Dolatabadi J, et al. Aptamer functionalized nanomaterials for biomedical applications: Recent advances and new horizons. Nano Today 2021;39:101177. https://doi.org/10.1016/j.nantod.2021.101177.
[21] Hussain S, Abbas Zaidi S, Vikraman D, Kim HS, Jung J. Facile preparation of tungsten carbide nanoparticles for an efficient oxalic acid sensor via imprinting. Microchem J 2020;159:105404. https://doi.org/10.1016/j.microc.2020.105404.
[22] Shahzad F, Zaidi SA, Naqvi RA. 2D Transition metal carbides (MXene) for electrochemical sensing: A review. Crit Rev Anal Chem 2020:1–17. https://doi.org/10.1080/10408347.2020.1836470.
[23] Georgakilas V, et al. Functionalization of graphene: Covalent and non-covalent approach. Chem Rev 2012;112(11):6156–214. https://doi.org/10.1021/cr3000412.
[24] Koski KJ, Cui Y. The new skinny in two-dimensional nanomaterials. ACS Nano 2013;7(5):3739–43. https://doi.org/10.1021/nn4022422.
[25] Kuila T, Bose S, Khanra P, Mishra AK, Kim NH, Lee JH. Recent advances in graphene-based biosensors. Biosens Bioelectron 2011;26(12):4637–48. https://doi.org/10.1016/j.bios.2011.05.039.
[26] Liu Y, Dong X, Chen P. Biological and chemical sensors based on graphene materials. Chem Soc Rev 2012;41(6):2283–307. https://doi.org/10.1039/c1cs15270j.

[27] Justino CIL, Gomes AR, Freitas AC, Duarte AC, Rocha-Santos TAP. Graphene based sensors and biosensors. TrAC - Trends Anal Chem 2017;91:53–66. https://doi.org/10.1016/j.trac.2017.04.003.

[28] Chen D, Feng H, Li J. Graphene oxide: Preparation, functionalization, and electrochemical applications. Chem Rev 2012;112(11):6027–53. https://doi.org/10.1021/cr300115g.

[29] Mao HY, Laurent S, Chen W, Akhavan O, Imani M, Ashkarran AA, et al. Graphene: Promises, facts, opportunities, and challenges in nanomedicine. Chem Rev 2013;113(5):3407–24. https://doi.org/10.1021/cr300335p.

[30] Li Z, Li X, Jian M, Geleta GS, Wang Z. Two-dimensional layered nanomaterial-based electrochemical biosensors for detecting microbial toxins. Toxins (Basel) 2019;12:1–23. https://doi.org/10.3390/toxins12010020.

[31] Ping J, Zhou Y, Wu Y, Papper V, Boujday S, Marks RS, et al. Recent advances in aptasensors based on graphene and graphene-like nanomaterials. Biosens Bioelectron 2015;64:373–85. https://doi.org/10.1016/j.bios.2014.08.090.

[32] Cao J, Li J, Li D, Yuan Z, Zhang Y, Shulga V, et al. Strongly coupled 2D transition metal chalcogenide-MXene-carbonaceous nanoribbon heterostructures with ultrafast ion transport for boosting Sodium/Potassium Ions Storage. Nano-Micro Lett 2021;13(1). https://doi.org/10.1007/s40820-021-00623-5.

[33] Kshetri T, Tran DT, Le HT, Nguyen DC, Hoa HV, Kim NH, et al. Recent advances in MXene-based nanocomposites for electrochemical energy storage applications. Prog Mater Sci 2021;117:100733. https://doi.org/10.1016/j.pmatsci.2020.100733.

[34] Wang F, Yang CH, Duan M, Tang Y, Zhu JF. TiO_2 nanoparticle modified organ-like Ti_3C_2 MXene nanocomposite encapsulating hemoglobin for a mediator-free biosensor with excellent performances. Biosens Bioelectron 2015;74:1022–8. https://doi.org/10.1016/j.bios.2015.08.004.

[35] Wu L, Lu X, Dhanjai, Wu Z-S, Dong Y, Wang X, et al. 2D transition metal carbide MXene as a robust biosensing platform for enzyme immobilization and ultrasensitive detection of phenol. Biosens Bioelectron 2018;107:69–75. https://doi.org/10.1016/j.bios.2018.02.021.

[36] Deshmukh K, Kovářík T, Khadheer Pasha SK. State of the art recent progress in two dimensional MXenes based gas sensors and biosensors: A comprehensive review. Coord Chem Rev 2020;424:213514. https://doi.org/10.1016/j.ccr.2020.213514.

[37] Kalambate PK, Gadhari NS, Li X, Rao Z, Navale ST, Shen Y, et al. Recent advances in MXene–based electrochemical sensors and biosensors. TrAC - Trends Anal Chem 2019;120:115643. https://doi.org/10.1016/j.trac.2019.115643.

[38] Sinha A, Dhanjai, Zhao H, Huang Y, Lu X, Chen J, et al. MXene: An emerging material for sensing and biosensing. TrAC - Trends Anal Chem 2018;105:424–35. https://doi.org/10.1016/j.trac.2018.05.021.

[39] Kumar S, Lei Y, Alshareef NH, Quevedo-Lopez MA, Salama KN. Biofunctionalized two-dimensional Ti3C2 MXenes for ultrasensitive detection of cancer biomarker. Biosens Bioelectron 2018;121:243–9. https://doi.org/10.1016/j.bios.2018.08.076.

[40] Mathew M, Rout CS. Electrochemical biosensors based on $Ti_3C_2T_x$ MXene: future perspectives for on-site analysis. Curr Opin Electrochem 2021;30:100782. https://doi.org/10.1016/j.coelec.2021.100782.

[41] Hernandez FJ, Ozalp VC. Graphene and other nanomaterial-based electrochemical aptasensors. Biosensors 2012;2(1):1–14. https://doi.org/10.3390/bios2010001.

[42] Wang L, Wu A, Wei G. Graphene-based aptasensors: From molecule-interface interactions to sensor design and biomedical diagnostics. Analyst 2018;143(7):1526–43. https://doi.org/10.1039/c8an00081f.

[43] Farzin L, Shamsipur M, Sheibani S. A review: Aptamer-based analytical strategies using the nanomaterials for environmental and human monitoring of toxic heavy metals. Talanta 2017;174:619–27. https://doi.org/10.1016/j.talanta.2017.06.066.

[44] Meng W, Liu X, Song H, Xie Yu, Shi X, Dargusch M, et al. Advances and challenges in 2D MXenes: From structures to energy storage and conversions. Nano Today 2021;40:101273. https://doi.org/10.1016/j.nantod.2021.101273.

[45] Ho DH, Choi YY, Jo SB, Myoung J-M, Cho JH. Sensing with MXenes: Progress and Prospects. Adv Mater 2021;33(47):2005846. https://doi.org/10.1002/adma.202005846.

[46] Pu JH, Zhao X, Zha XJ, Bai Lu, Ke K, Bao RY, et al. Multilayer structured AgNW/WPU-MXene fiber strain sensors with ultrahigh sensitivity and a wide operating range for wearable monitoring and healthcare. J Mater Chem A 2019;7(26):15913–23. https://doi.org/10.1039/C9TA04352G.

[47] VahidMohammadi A, Rosen J, Gogotsi Y. The world of two-dimensional carbides and nitrides (MXenes). Science 2021;372(6547). https://doi.org/10.1126/science.abf1581.

[48] Anasori B, Gogotsi Y. 2D Metal Carbides and Nitrides (MXenes), Vol. 416. Berlin: Springer; 2019.

[49] Hu M, Zhang H, Hu T, Fan B, Wang X, Li Z. Emerging 2D MXenes for supercapacitors: Status, challenges and prospects. Chem Soc Rev 2020;49(18):6666–93. https://doi.org/10.1039/d0cs00175a.

[50] Nemani SK, Zhang B, Wyatt BC, Hood ZD, Manna S, Khaledialidusti R, et al. High-entropy 2D carbide MXenes: $TiVNbMoC_3$ and $TiVCrMoC_3$. ACS Nano 2021;15(8):12815–25. https://doi.org/10.1021/acsnano.1c02775.

[51] Shekhirev M, Shuck CE, Sarycheva A, Gogotsi Y. Characterization of MXenes at every step, from their precursors to single flakes and assembled films. Prog Mater Sci 2021;120(2020):100757. https://doi.org/10.1016/j.pmatsci.2020.100757.

[52] Gogotsi Y, Anasori B. The rise of MXenes. ACS Nano 2019;13(8):8491–4. https://doi.org/10.1021/acsnano.9b06394.

[53] Wu Y, Li X, Zhao H, Yao F, Cao J, Chen Z, et al. Recent advances in transition metal carbides and nitrides (MXenes): Characteristics, environmental remediation and challenges. Chem Eng J 2021;418:129296. https://doi.org/10.1016/j.cej.2021.129296.

[54] Yaqub A, Shafiq Q, Khan AR, Husnain SM, Shahzad F. Recent advances in the adsorptive remediation of wastewater using two-dimensional transition metal carbides (MXenes): A review. New J Chem 2021;45(22):9721–42. https://doi.org/10.1039/d1nj00772f.

[55] Anasori B, Xie Yu, Beidaghi M, Lu J, Hosler BC, Hultman L, et al. Two-dimensional, ordered, double transition metals carbides (MXenes). ACS Nano 2015;9(10):9507–16. https://doi.org/10.1021/acsnano.5b03591.

[56] Naguib M, Kurtoglu M, Presser V, Lu J, Niu J, Heon M, et al. Two-dimensional nanocrystals produced by exfoliation of Ti_3AlC_2. Adv Mater 2011;23(37):4248–53. https://doi.org/10.1002/adma.201102306.

[57] Cao J, Wang L, Li D, Yuan Z, Xu H, Li J, et al. $Ti_3C_2T_x$ MXene conductive layers supported bio-derived $Fe_{x-1}Se_x$/MXene/carbonaceous nanoribbons for high-performance half/full sodium-ion and potassium-ion batteries. Adv Mater 2021;33(34):2101535. https://doi.org/10.1002/adma.202101535.

[58] Cao J, Sun Z, Li J, Zhu Y, Yuan Z, Zhang Y, et al. Microbe-assisted assembly of $Ti_3C_2T_x$ MXene on fungi-derived nanoribbon heterostructures for ultrastable sodium and potassium ion storage. ACS Nano 2021;15(2):3423–33. https://doi.org/10.1021/acsnano.0c10491.

[59] Mashtalir O, Naguib M, Mochalin VN, Dall'Agnese Y, Heon M, Barsoum MW, et al. Intercalation and delamination of layered carbides and carbonitrides. Nat Commun 2013;4(1). https://doi.org/10.1038/ncomms2664.

[60] Alhabeb M, Maleski K, Anasori B, Lelyukh P, Clark L, Sin S, et al. Guidelines for synthesis and processing of two-dimensional titanium carbide ($Ti_3C_2T_x$ MXene). Chem Mater 2017;29(18):7633–44. https://doi.org/10.1021/acs.chemmater.7b02847.

[61] Lin H, Wang X, Yu L, Chen Y, Shi J. Two-Dimensional Ultrathin MXene Ceramic Nanosheets for Photothermal Conversion. Nano Lett 2017;17(1):384–91. https://doi.org/10.1021/acs.nanolett.6b04339.

[62] Nayak P, Jiang Q, Mohanraman R, Anjum D, Hedhili MN, Alshareef HN. Inherent electrochemistry and charge transfer properties of few-layered two-dimensional $Ti_3C_2T_x$ MXene. Nanoscale 2018;10(36):17030–7. https://doi.org/10.1039/c8nr01883a.

[63] Shahzad F, Alhabeb M, Hatter CB, Anasori B, Man Hong S, Koo CM, et al. Electromagnetic interference shielding with 2D transition metal carbides (MXenes). Science (80-) 2016;353(6304):1137–40. https://doi.org/10.1126/science.aag2421.

[64] Hart JL, Hantanasirisakul K, Lang AC, Anasori B, Pinto D, Pivak Y, et al. Control of MXenes' electronic properties through termination and intercalation. Nat Commun 2019;10(1). https://doi.org/10.1038/s41467-018-08169-8.

[65] Hantanasirisakul K, Alhabeb M, Lipatov A, Maleski K, Anasori B, Salles P, et al. Effects of synthesis and processing on optoelectronic properties of titanium carbonitride MXene. Chem Mater 2019;31(8):2941–51. https://doi.org/10.1021/acs.chemmater.9b00401.

[66] Li T, Yao L, Liu Q, Gu J, Luo R, Li J, et al. Fluorine-free synthesis of high-purity $Ti_3C_2T_x$ (T=OH, O) via alkali treatment. Angew Chemie - Int Ed 2018;57(21):6115–9. https://doi.org/10.1002/anie.201800887.

[67] Li M, Lu J, Luo K, Li Y, Chang K, Chen Ke, et al. Element replacement approach by reaction with lewis acidic molten salts to synthesize nanolaminated MAX phases and MXenes. J Am Chem Soc 2019;141(11):4730–7. https://doi.org/10.1021/jacs.9b00574.
[68] Urbankowski P, Anasori B, Makaryan T, Er D, Kota S, Walsh PL, et al. Synthesis of two-dimensional titanium nitride Ti_4N_3 (MXene). Nanoscale 2016;8(22):11385–91. https://doi.org/10.1039/C6NR02253G.
[69] Li Y, Shao H, Lin Z, Lu J, Liu L, Duployer B, et al. A general Lewis acidic etching route for preparing MXenes with enhanced electrochemical performance in non-aqueous electrolyte. Nat Mater 2020;19(8):894–9. https://doi.org/10.1038/s41563-021-00925-4.
[70] Kamysbayev V, Filatov AS, Hu H, Rui X, Lagunas F, Wang Di, et al. Covalent surface modifications and superconductivity of two-dimensional metal carbide MXenes. Science (80-) 2020;369(6506):979–83. https://doi.org/10.1126/science.aba8311.
[71] Sun W, Shah SA, Chen Y, Tan Z, Gao H, Habib T, et al. Electrochemical etching of Ti_2AlC to Ti_2CT_X (MXene) in low-concentration hydrochloric acid solution. J Mater Chem A 2017;5(41):21663–8. https://doi.org/10.1039/C7TA05574A.
[72] Li X, Li M, Yang Qi, Liang G, Huang Z, Ma L, et al. In situ electrochemical synthesis of MXenes without acid/alkali usage in/for an aqueous zinc ion battery. Adv Energy Mater 2020;10(36):2001791. https://doi.org/10.1002/aenm.202001791.
[73] Gogotsi Y. Chemical vapour deposition: Transition metal carbides go 2D. Nat Mater 2015;14(11):1079–80. https://doi.org/10.1038/nmat4386.
[74] Xu C, Wang L, Liu Z, Chen L, Guo J, Kang N, et al. Large-area high-quality 2D ultrathin Mo_2C superconducting crystals. Nat Mater 2015;14(11):1135–41. https://doi.org/10.1038/NMAT4374.
[75] Zhang Y, Wang S, Yu H, Zhang H, Chen Y, Mei L, et al. Atomic-layer molybdenum sulfide optical modulator for visible coherent light. Sci Rep 2015;5(1). https://doi.org/10.1038/srep11342.
[76] Geng D, Zhao X, Chen Z, Sun W, Fu W, Chen J, et al. Direct synthesis of large-area 2D Mo_2C on in situ grown graphene. Adv Mater 2017;29(35):1700072. https://doi.org/10.1002/adma.201700072.
[77] Shahzad F, Iqbal A, Kim H, Koo CM. 2D Transition metal carbides (MXenes): Applications as an electrically conducting material. Adv Mater 2020;32(51):1–23. https://doi.org/10.1002/adma.202002159.
[78] Lipatov A, Lu H, Alhabeb M, Anasori B, Gruverman A, Gogotsi Y, et al. Elastic properties of 2D $Ti_3C_2T_x$ MXene monolayers and bilayers. Sci Adv 2018;4(6). https://doi.org/10.1126/sciadv.aat0491.
[79] Pomerantseva E, Gogotsi Y. Two-dimensional heterostructures for energy storage. Nat Energy 2017;2(7):1–6. https://doi.org/10.1038/nenergy.2017.89.
[80] Bonaccorso F, Colombo L, Yu G, Stoller M, Tozzini V, Ferrari AC, et al. Graphene, related two-dimensional crystals, and hybrid systems for energy conversion and storage. Science 2015;347(6217):1246501. https://doi.org/10.1126/science.1246501.
[81] Wyatt BC, Rosenkranz A, Anasori B. 2D MXenes: Tunable mechanical and tribological properties. Adv Mater 2021;33(17):2007973. https://doi.org/10.1002/adma.202007973.
[82] Tang Q, Zhou Z, Shen P. Are MXenes promising anode materials for Li ion batteries? Computational studies on electronic properties and Li storage capability of Ti_3C_2 and $Ti_3C_2X_2$ (X = F, OH) monolayer. J Am Chem Soc 2012;134(40):16909–16. https://doi.org/10.1021/ja308463r.
[83] Razmi N, Baradaran B, Hejazi M, Hasanzadeh M, Mosafer J, Mokhtarzadeh A, et al. Recent advances on aptamer-based biosensors to detection of platelet-derived growth factor. Biosens Bioelectron 2018;113:58–71. https://doi.org/10.1016/j.bios.2018.04.048.
[84] Khalilzadeh B, Shadjou N, Charoudeh HN, Rashidi MR. Recent advances in electrochemical and electrochemiluminescence based determination of the activity of caspase-3. Microchim Acta 2017;184(10):3651–62. https://doi.org/10.1007/s00604-017-2466-y.
[85] Liu Z, Qi W, Xu G. Recent advances in electrochemiluminescence. Chem Soc Rev 2015;44(10):3117–42. https://doi.org/10.1039/c5cs00086f.
[86] Zahra QUA, Luo Z, Ali R, Khan MI, Li F, Qiu B. Advances in gold nanoparticles-based colorimetric aptasensors for the detection of antibiotics: An overview of the past decade. Nanomaterials 2021;11(4):840. https://doi.org/10.3390/nano11040840.
[87] Robati RY, Arab A, Ramezani M, Langroodi FA, Abnous K, Taghdisi SM. Aptasensors for quantitative detection of kanamycin. Biosens Bioelectron 2016;82:162–72. https://doi.org/10.1016/j.bios.2016.04.011.
[88] Li X, Lu Y, Liu Q. Electrochemical and optical biosensors based on multifunctional MXene nanoplatforms: Progress and prospects. Talanta 2021;235:122726. https://doi.org/10.1016/j.talanta.2021.122726.
[89] Khedri M, Ramezani M, Rafatpanah H, Abnous K. Detection of food-born allergens with aptamer-based biosensors. TrAC - Trends Anal Chem 2018;103:126–36. https://doi.org/10.1016/j.trac.2018.04.001.
[90] Bayat P, Taghdisi SM, Rafatpanah H, Abnous K, Ramezani M. In vitro selection of CD70 binding aptamer and its application in a biosensor design for sensitive detection of SKOV-3 ovarian cells. Talanta 2019;194:399–405. https://doi.org/10.1016/j.talanta.2018.10.063.
[91] Robertson DL, Joyce GF. Selection in vitro of an RNA enzyme that specifically cleaves single-stranded DNA. Nature 1990;344(6265):467–8.
[92] Lee JF, Stovall GM, Ellington AD. Aptamer therapeutics advance. Curr Opin Chem Biol 2006;10(3):282–9. https://doi.org/10.1016/j.cbpa.2006.03.015.
[93] Darmostuk M, Rimpelova S, Gbelcova H, Ruml T. Current approaches in SELEX: An update to aptamer selection technology. Biotechnol Adv 2014;33(6):1141–61. https://doi.org/10.1016/j.biotechadv.2015.02.008.
[94] Nguyen VT, Bin Seo H, Kim BC, Kim SK, Song CS, Gu MB. Highly sensitive sandwich-type SPR based detection of whole H5Nx viruses using a pair of aptamers. Biosens Bioelectron 2016;86:293–300. https://doi.org/10.1016/j.bios.2016.06.064.
[95] Guo W, Zhang C, Ma T, Liu X, Chen Z, Li S, et al. Advances in aptamer screening and aptasensors' detection of heavy metal ions. J Nanobiotechnology 2021;19(1):1–19. https://doi.org/10.1186/s12951-021-00914-4.
[96] Qi S, Duan N, Khan IM, Dong X, Zhang Y, Wu S, et al. Strategies to manipulate the performance of aptamers in SELEX, post-SELEX and microenvironment. Biotechnol Adv 2022:107902. https://doi.org/10.1016/j.biotechadv.2021.107902.
[97] Drolet DW, Moon-McDermott L, Romig TS. An enzyme-linked oligonucleotide assay. Nat Biotechnol 1996;14(8):1021–5. https://doi.org/10.1038/nbt0896-1021.
[98] Davis KA, Abrams B, Lin Y, Jayasena SD. Use of a high affinity DNA ligand in flow cytometry. Nucleic Acids Res 1996;24(4):702–6. https://doi.org/10.1093/nar/24.4.702.
[99] Alkhamis O, Canoura J, Yu H, Liu Y, Xiao Y. Innovative engineering and sensing strategies for aptamer-based small-molecule detection. TrAC - Trends Anal Chem 2019;121:115699. https://doi.org/10.1016/j.trac.2019.115699.
[100] Zahra QUA, et al. Graphene Based Nanohybrid Aptasensors in Environmental Monitoring: Concepts, Design and Future Outlook. Crit Rev Anal Chem 2022:1–22. https://doi.org/10.1080/10408347.2022.2025758.
[101] Billet B, Chovelon B, Fiore E, Oukacine F, Petrillo MA, Faure P, et al. Aptamer switches regulated by post-transition/transition metal ions. Angew Chemie - Int Ed 2021;60(22):12346–50. https://doi.org/10.1002/anie.202102254.
[102] Lubin AA, Plaxco KW. Folding-based electrochemical biosensors: The case for responsive nucleic acid architectures. Acc Chem Res 2010;43(4):496–505. https://doi.org/10.1021/ar900165x.
[103] Zhao L, Qi X, Yan X, Huang Y, Liang X, Zhang L, et al. Engineering aptamer with enhanced affinity by Ttiple helix-based terminal fixation. J Am Chem Soc 2019;141(44):17493–7. https://doi.org/10.1021/jacs.9b09292.
[104] Li D, Song S, Fan C. Target-responsive structural switching for nucleic acid-based sensors. Acc Chem Res 2010;43(5):631–41. https://doi.org/10.1021/ar900245u.
[105] Vinkenborg JL, Karnowski N, Famulok M. Aptamers for allosteric regulation. Nat Chem Biol 2011;7(8):519–27. https://doi.org/10.1038/nchembio.609.
[106] Zhang X, Qi B, Li Y, Zhang S. Amplified electrochemical aptasensor for thrombin based on bio-barcode method. Biosens Bioelectron 2009;25(1):259–62. https://doi.org/10.1016/j.bios.2009.06.026.
[107] Wang X, Zhou J, Yun W, Xiao S, Chang Z, He P, et al. Detection of thrombin using electrogenerated chemiluminescence based on $Ru(bpy)_3^{2+}$-doped silica nanoparticle aptasensor *via* target protein-induced strand displacement. Anal Chim Acta 2007;598(2):242–8. https://doi.org/10.1016/j.aca.2007.07.050.
[108] Cella LN, Sanchez P, Zhong W, Myung NV, Chen W, Mulchandani A. Nano aptasensor for protective antigen toxin of anthrax. Anal Chem 2010;82(5):2042–7. https://doi.org/10.1021/ac902791q.

[109] Qi X, Yan X, Zhao Y, Li L, Wang S. Highly sensitive and specific detection of small molecules using advanced aptasensors based on split aptamers: A review. TrAC - Trends Anal Chem 2020;133:116069. https://doi.org/10.1016/j.trac.2020.116069.

[110] Mei Z, Chu H, Chen W, Xue F, Liu J, Xu H, et al. Ultrasensitive one-step rapid visual detection of bisphenol A in water samples by label-free aptasensor. Biosens Bioelectron 2013;39(1):26–30. https://doi.org/10.1016/j.bios.2012.06.027.

[111] Ravalli A, Voccia D, Palchetti I, Marrazza G. Electrochemical, electrochemiluminescence, and photoelectrochemical aptamer-based nanostructured sensors for biomarker analysis. Biosensors 2016;6(3):39. https://doi.org/10.3390/bios6030039.

[112] Zhao WW, Xu JJ, Chen HY. Photoelectrochemical aptasensing. TrAC - Trends Anal Chem 2016;82:307–15. https://doi.org/10.1016/j.trac.2016.06.020.

[113] Dhiman A, Kalra P, Bansal V, Bruno JG, Sharma TK. Aptamer-based point-of-care diagnostic platforms. Sensors Actuators, B Chem 2017;246:535–53. https://doi.org/10.1016/j.snb.2017.02.060.

[114] Kim YS, Raston NHA, Gu MB. Aptamer-based nanobiosensors. Biosens Bioelectron 2016;76:2–19. https://doi.org/10.1016/j.bios.2015.06.040.

[115] Bostan HB, Danesh NM, Karimi G, Ramezani M, Shaegh SAM, Youssefi K, et al. Ultrasensitive detection of ochratoxin A using aptasensors. Biosens Bioelectron 2017;98:168–79. https://doi.org/10.1016/j.bios.2017.06.055.

[116] Burda C, Chen X, Narayanan R, El-Sayed MA. Chemistry and properties of nanocrystals of different shapes. Chem Rev 2005;105(4):1025–102. https://doi.org/10.1021/cr030063a.

[117] Baron R, Willner B, Willner I. Biomolecule-nanoparticle hybrids as functional units for nanobiotechnology. Chem Commun 2007;4:323–32. https://doi.org/10.1039/b610721b.

[118] Lu Y, Liu J. Smart nanomaterials inspired by biology: Dynamic assembly of error-free nanomaterials in response to multiple chemical and biological stimuli. Acc Chem Res 2007;40(5):315–23. https://doi.org/10.1021/ar600053g.

[119] Stewart ME, Anderton CR, Thompson LB, Maria J, Gray SK, Rogers JA, et al. Nanostructured plasmonic sensors. Chem Rev 2008;108(2):494–521. https://doi.org/10.1021/cr068126n.

[120] Wongkaew N, Simsek M, Griesche C, Baeumner AJ. Functional nanomaterials and nanostructures enhancing electrochemical biosensors and lab-on-a-chip performances: recent progress, applications, and future perspective. Chem Rev 2019;119(1):120–94. https://doi.org/10.1021/acs.chemrev.8b00172.

[121] Zhang S, Geryak R, Geldmeier J, Kim S, Tsukruk VV. Synthesis, assembly, and applications of hybrid nanostructures for biosensing. Chem Rev 2017;117(20):12942–3038. https://doi.org/10.1021/acs.chemrev.7b00088.

[122] Li Z, Liu C, Sarpong V, Gu Z. Multisegment nanowire/nanoparticle hybrid arrays as electrochemical biosensors for simultaneous detection of antibiotics. Biosens Bioelectron 2019;126(2018):632–9. https://doi.org/10.1016/j.bios.2018.10.025.

[123] Ariga K, Leong DT, Mori T. Nanoarchitectonics for hybrid and related materials for bio-oriented applications. Adv Funct Mater 2018;28(27):1702905. https://doi.org/10.1002/adfm.201702905.

[124] Ping J, Fan Z, Sindoro M, Ying Y, Zhang H. Recent advances in sensing applications of two-dimensional transition metal dichalcogenide nanosheets and their composites. Adv Funct Mater 2017;27(19):1605817. https://doi.org/10.1002/adfm.201605817.

[125] Xu B, Zhu M, Zhang W, Zhen Xu, Pei Z, Xue Qi, et al. Ultrathin MXene-micropattern-based field-effect transistor for probing neural activity. Adv Mater 2016;28(17):3333–9. https://doi.org/10.1002/adma.201504657.

[126] Xu B, Zhi C, Shi P. Latest advances in MXene biosensors. J Phys Mater 2020;3:031001.

[127] Chen Xu, Sun X, Xu W, Pan G, Zhou D, Zhu J, et al. Ratiometric photoluminescence sensing based on Ti_3C_2 MXene quantum dots as an intracellular pH sensor. Nanoscale 2018;10(3):1111–8. https://doi.org/10.1039/C7NR06958H.

[128] Zhang Q, Wang F, Zhang H, Zhang Y, Liu M, Liu Y. Universal Ti_3C_2 MXenes based self-standard ratiometric fluorescence resonance energy transfer platform for highly sensitive detection of exosomes. Anal Chem 2018;90(21):12737–44. https://doi.org/10.1021/acs.analchem.8b03083.

[129] Wang X, Chu C, Shen L, Deng W, Yan M, Ge S, et al. An ultrasensitive electrochemical immunosensor based on the catalytical activity of MoS_2-Au composite using Ag nanospheres as labels. Sensors Actuators, B Chem 2015;206:30–6. https://doi.org/10.1016/j.snb.2014.09.028.

[130] Yin H, Zhou Y, Zhang H, Meng X, Ai S. Electrochemical determination of microRNA-21 based on graphene, LNA integrated molecular beacon, AuNPs and biotin multifunctional bio bar codes and enzymatic assay system. Biosens Bioelectron 2012;33(1):247–53. https://doi.org/10.1016/j.bios.2012.01.014.

[131] Ji J, Zhao L, Shen Y, Liu S, Zhang Y. Covalent stabilization and functionalization of MXene via silylation reactions with improved surface properties. FlatChem 2019;17:100128. https://doi.org/10.1016/j.flatc.2019.100128.

[132] Cao W-T, Feng W, Jiang Y-Y, Ma C, Zhou Z-F, Ma M-G, et al. Two-dimensional MXene-reinforced robust surface superhydrophobicity with self-cleaning and photothermal-actuating binary effects. Mater Horizons 2019;6(5):1057–65. https://doi.org/10.1039/C8MH01566J.

[133] Lim S, Park H, Yang J, Kwak C, Lee J. Stable colloidal dispersion of octylated Ti_3C_2-MXenes in a nonpolar solvent. Colloids Surfaces A Physicochem Eng Asp 2019;579:123648. https://doi.org/10.1016/j.colsurfa.2019.123648.

[134] Ullah N, Chen W, Noureen B, Tian Y, Du L, Wu C. An Electrochemical $Ti_3C_2T_x$ aptasensor for sensitive and label-free detection of marine biological toxins. Sensors 2021;21(14):4938. https://doi.org/10.3390/s21144938.

[135] Lorencova L, Gajdosova V, Hroncekova S, Bertok T, Jerigova M, Velic D, et al. Electrochemical investigation of interfacial properties of $Ti_3C_2T_x$ MXene modified by aryldiazonium betaine derivatives. Front Chem 2020:553. https://doi.org/10.3389/fchem.2020.00553.

[136] Bertok T, Lorencova L, Hroncekova S, Gajdosova V, Jane E, Hires M, et al. Advanced impedimetric biosensor configuration and assay protocol for glycoprofiling of a prostate oncomarker using Au nanoshells with a magnetic core. Biosens Bioelectron 2019;131:24–9. https://doi.org/10.1016/j.bios.2019.01.052.

[137] Zhao L-y, Sun Y-L, Mao Li, Lian H-Z, Sheng D. Universal gold nanoparticle modified hybrid monolithic substrate developed for facile in-column post-functionalization. Talanta 2021;225:121993. https://doi.org/10.1016/j.talanta.2020.121993.

[138] Han X, Jing X, Yang D, Lin H, Wang Z, Ran H, et al. Therapeutic mesopore construction on 2D Nb_2C MXenes for targeted and enhanced chemo-photothermal cancer therapy in NIR-II biowindow. Theranostics 2018;8(16):4491–508. https://doi.org/10.7150/thno.26291.

[139] Liu G, Zou J, Tang Q, Yang X, Zhang Y, Zhang Qi, et al. Surface modified Ti_3C_2 MXene nanosheets for tumor targeting photothermal/photodynamic/chemo synergistic therapy. ACS Appl Mater Interfaces 2017;9(46):40077–86. https://doi.org/10.1021/acsami.7b13421.

[140] Wang S, Wei S, Wang S, Zhu X, Lei C, Huang Y, et al. Chimeric DNA-functionalized titanium carbide MXenes for simultaneous mapping of dual cancer biomarkers in living cells. Anal Chem 2019;91(2):1651–8. https://doi.org/10.1021/acs.analchem.8b05343.

[141] Huang H, Jiang R, Feng Y, Ouyang H, Zhou N, Zhang X, et al. Recent development and prospects of surface modification and biomedical applications of MXenes. Nanoscale 2020;12(3):1325–38. https://doi.org/10.1039/C9NR07616F.

[142] Dai C, Chen Yu, Jing X, Xiang L, Yang D, Lin H, et al. Two-dimensional tantalum carbide (MXenes) composite nanosheets for multiple imaging-guided photothermal tumor ablation. ACS Nano 2017;11(12):12696–712. https://doi.org/10.1021/acsnano.7b07241.

[143] Zheng J, Wang B, Ding A, Weng B, Chen J. Synthesis of MXene/DNA/Pd/Pt nanocomposite for sensitive detection of dopamine. J Electroanal Chem 2018;816:189–94. https://doi.org/10.1016/j.jelechem.2018.03.056.

[144] Huang Z, Liu B, Liu J. Mn^{2+}-assisted DNA oligonucleotide adsorption on Ti_2C MXene nanosheets. Langmuir 2019;35(30):9858–66. https://doi.org/10.1021/acs.langmuir.9b01810.

[145] Vajhadin F, Mazloum-Ardakani M, Shahidi M, Moshtaghioun SM, Haghiralsadat F, Ebadi A, et al. MXene-based cytosensor for the detection of HER2-positive cancer cells using $CoFe_2O_4$@Ag magnetic nanohybrids conjugated to the HB5 aptamer. Biosens Bioelectron 2022;195:113626. https://doi.org/10.1016/j.bios.2021.113626.

[146] Mojtabavi M, Vahidmohammadi A, Liang W, Beidaghi M, Wanunu M. Single-molecule sensing using nanopores in two-dimensional transition metal carbide (MXene) membranes. ACS Nano 2019;13(3):3042–53. https://doi.org/10.1021/acsnano.8b08017.

[147] Lu L, Han X, Lin J, Zhang Y, Qiu M, Chen Y, et al. Ultrasensitive fluorometric biosensor based on Ti_3C_2 MXenes with Hg^{2+}-triggered exonuclease III-assisted recycling amplification. Analyst 2021;146(8):2664–9. https://doi.org/10.1039/D1AN00178G.

[148] Liu MX, Zhang H, Zhang XW, Chen S, Yu YL, Wang JH. Nanozyme sensor array plus solvent-mediated signal amplification strategy for ultrasensitive ratiometric fluorescence detection of exosomal proteins and cancer identification. Anal Chem 2021;93(25):9002–10. https://doi.org/10.1021/acs.analchem.1c02010.

[149] Liu C, Wei X, Hao S, Zong B, Chen X, Li Z, et al. Label-free, fast response, and simply operated silver ion detection with a $Ti_3C_2T_x$ MXene field-effect transistor. Anal Chem 2021;93(22):8010–8. https://doi.org/10.1021/acs.analchem.1c01094.

[150] Zhang J, Sheng A, Wang P, Yang J, Tang L, Chen F. Mxene coupled with crispr-cas12a for analysis of endotoxin and bacteria. Anal Chem 2021;93(10):4676–81. https://doi.org/10.1021/acs.analchem.1c00371.

[151] Jeong S, Park J, Pathania D, Castro CM, Weissleder R, Lee H. Integrated magneto-electrochemical sensor for exosome analysis. ACS Nano 2016;10(2):1802–9. https://doi.org/10.1021/acsnano.5b07584.

[152] Budnik V, Ruiz-Cañada C, Wendler F. Extracellular vesicles round off communication in the nervous system. Nat Rev Neurosci 2016;17(3):160–72. https://doi.org/10.1038/nrn.2015.29.

[153] Tkach M, Théry C. Communication by extracellular vesicles: where we are and where we need to go. Cell 2016;164(6):1226–32. https://doi.org/10.1016/j.cell.2016.01.043.

[154] Christianson HC, Svensson KJ, Van Kuppevelt TH, Li JP, Belting M. Cancer cell exosomes depend on cell-surface heparan sulfate proteoglycans for their internalization and functional activity. Proc Natl Acad Sci 2013;110(43):17380–5. https://doi.org/10.1073/pnas.1304266110.

[155] Wang Y-M, Liu J-W, Adkins GB, Shen W, Trinh MP, Duan L-Y, et al. Enhancement of the intrinsic peroxidase-like activity of graphitic carbon nitride nanosheets by ssDNAs and Its application for detection of exosomes. Anal Chem 2017;89(22):12327–33. https://doi.org/10.1021/acs.analchem.7b03335.

[156] Xia Y, Liu M, Wang L, Yan An, He W, Chen M, et al. A visible and colorimetric aptasensor based on DNA-capped single-walled carbon nanotubes for detection of exosomes. Biosens Bioelectron 2017;92:8–15. https://doi.org/10.1016/j.bios.2017.01.063.

[157] Zhang H, Wang Z, Wang F, Zhang Y, Wang H, Liu Y. In situ formation of gold nanoparticles decorated Ti_3C_2 MXenes nanoprobe for highly sensitive electrogenerated chemiluminescence detection of exosomes and their surface proteins. Anal Chem 2020;92(7):5546–53. https://doi.org/10.1021/acs.analchem.0c00469.

[158] Fang D, Zhao D, Zhang S, Huang Y, Dai H, Lin Y. Black phosphorus quantum dots functionalized MXenes as the enhanced dual-mode probe for exosomes sensing. Sensors Actuators, B Chem 2020;305:127544. https://doi.org/10.1016/j.snb.2019.127544.

[159] Zhang H, Wang Z, Zhang Q, Wang F, Liu Y. Ti_3C_2 MXenes nanosheets catalyzed highly efficient electrogenerated chemiluminescence biosensor for the detection of exosomes. Biosens Bioelectron 2019;124(2019):184–90. https://doi.org/10.1016/j.bios.2018.10.016.

[160] Li Y, Chen Y, Deng D, Luo L, He H, Wang Z. Water-dispersible graphene/amphiphilic pyrene derivative nanocomposite: High AuNPs loading capacity for CEA electrochemical immunosensing. Sensors Actuators, B Chem 2017;248:966–72. https://doi.org/10.1016/j.snb.2017.02.138.

[161] Lee SX, Lim HN, Ibrahim I, Jamil A, Pandikumar A, Huang NM. Horseradish peroxidase-labeled silver/reduced graphene oxide thin film-modified screen-printed electrode for detection of carcinoembryonic antigen. Biosens Bioelectron 2017;89:673–80. https://doi.org/10.1016/j.bios.2015.12.030.

[162] Hasanzadeh M, Shadjou N. Advanced nanomaterials for use in electrochemical and optical immunoassays of carcinoembryonic antigen. A review. Microchim Acta 2017;184(2):389–414. https://doi.org/10.1007/s00604-016-2066-2.

[163] Danesh NM, Yazdian-Robati R, Ramezani M, Alibolandi M, Abnous K, Taghdisi SM. A label-free aptasensor for carcinoembryonic antigen detection using three-way junction structure and ATMND as a fluorescent probe. Sensors Actuators, B Chem 2018;256:408–12. https://doi.org/10.1016/j.snb.2017.10.126.

[164] Zhao P, Zheng J, Liang Yi, Tian F, Peng L, Huo D, et al. Functionalized carbon nanotube-decorated MXene nanosheet-enabled microfluidic electrochemical aptasensor for Carcinoembryonic Antigen determination. ACS Sustain Chem Eng 2021;9(46):15386–93.

[165] Song X, Gao H, Yuan R, Xiang Y. Trimetallic nanoparticle-decorated MXene nanosheets for catalytic electrochemical detection of carcinoembryonic antigen via Exo III-aided dual recycling amplifications. Sensors Actuators B Chem 2022;359:131617. https://doi.org/10.1016/j.snb.2022.131617.

[166] Li C, Zhang M, Zhang Z, Tang J, Zhang B. Microcantilever aptasensor for detecting epithelial tumor marker Mucin 1 and diagnosing human breast carcinoma MCF-7 cells. Sensors Actuators, B Chem 2019;297:126759. https://doi.org/10.1016/j.snb.2019.126759.

[167] Wang H, Sun J, Lu L, Yang X, Xia J, Zhang F, et al. Competitive electrochemical aptasensor based on a cDNA-ferrocene/MXene probe for detection of breast cancer marker Mucin1. Anal Chim Acta 2020;1094:18–25. https://doi.org/10.1016/j.aca.2019.10.003.

[168] Gimba ERP, Brum MCM, De Moraes GN. Full-length osteopontin and its splice variants as modulators of chemoresistance and radioresistance (Review). Int J Oncol 2019;54(2):420–30. https://doi.org/10.3892/ijo.2018.4656.

[169] Rangaswami H, Bulbule A, Kundu GC. Osteopontin: Role in cell signaling and cancer progression. Trends Cell Biol 2006;16(2):79–87. https://doi.org/10.1016/j.tcb.2005.12.005.

[170] Zhou S, Gu C, Li Z, Yang L, He L, Wang M, et al. $Ti_3C_2T_x$ MXene and polyoxometalate nanohybrid embedded with polypyrrole: Ultra-sensitive platform for the detection of osteopontin. Appl Surf Sci 2019;498:143889. https://doi.org/10.1016/j.apsusc.2019.143889.

[171] Zhang H, Wang Z, Wang F, Zhang Y, Wang H, Liu Y. Ti_3C_2 MXene mediated Prussian blue in situ hybridization and electrochemical signal amplification for the detection of exosomes. Talanta 2021;224(2020):121879. https://doi.org/10.1016/j.talanta.2020.121879.

[172] Wang JY, Xiao L, Wang JY. Posttranscriptional regulation of intestinal epithelial integrity by noncoding RNAs: Noncoding RNAs in gut epithelial integrity. WIREs RNA 2017;8(2):e1399. https://doi.org/10.1002/wrna.1399.

[173] Wang J, Chen J, Sen S. MicroRNA as biomarkers and diagnostics. J Cell Physiol 2016;231(1):25–30. https://doi.org/10.1002/jcp.25056.

[174] Cardoso AR, Moreira FTC, Fernandes R, Sales MGF. Novel and simple electrochemical biosensor monitoring attomolar levels of miRNA-155 in breast cancer. Biosens Bioelectron 2016;80:621–30. https://doi.org/10.1016/j.bios.2016.02.035.

[175] Duan F, Guo C, Hu M, Song Y, Wang M, He L, et al. Construction of the 0D/2D heterojunction of $Ti_3C_2T_x$ MXene nanosheets and iron phthalocyanine quantum dots for the impedimetric aptasensing of microRNA-155. Sensors Actuators B Chem 2020;310:127844. https://doi.org/10.1016/j.snb.2020.127844.

[176] Liu Y, Huang S, Li J, Wang M, Wang C, Hu B, et al. 0D/2D heteronanostructure–integrated bimetallic CoCu-ZIF nanosheets and MXene-derived carbon dots for impedimetric cytosensing of melanoma B16-F10 cells. Microchim Acta 2021;188(3):1–12. https://doi.org/10.1007/s00604-021-04726-z.

[177] Wang L, Xiong Q, Xiao F, Duan H. 2D nanomaterials based electrochemical biosensors for cancer diagnosis. Biosens Bioelectron 2017;89:136–51. https://doi.org/10.1016/j.bios.2016.06.011.

[178] Chauhan R, Singh J, Sachdev T, Basu T, Malhotra BD. Recent advances in mycotoxins detection. Biosens Bioelectron 2016;81:532–45. https://doi.org/10.1016/j.bios.2016.03.004.

[179] Christensen CM, Nelson GH. Mycotoxins and mycotoxicoses. Mod Vet Pract 1976;57(5):367–71. https://doi.org/10.1002/047126363x.agr300.

[180] Henry SH, Bosch FX, Troxell TC, Bolger PM. Reducing liver cancer–global control of aflatoxin. Science 1999;286(5449):2453–4. https://doi.org/10.1126/science.286.5449.2453.

[181] Vidal JC, Bonel L, Ezquerra A, Hernández S, Bertolín JR, Cubel C, et al. Electrochemical affinity biosensors for detection of mycotoxins: A review. Biosens Bioelectron 2013;49:146–58. https://doi.org/10.1016/j.bios.2013.05.008.

[182] Anfossi L, Giovannoli C, Baggiani C. Mycotoxin detection. Curr Opin Biotechnol 2016;37:120–6. https://doi.org/10.1016/j.copbio.2015.11.005.

[183] Xue Z, Zhang Y, Yu W, Zhang J, Wang J, Wan F, et al. Recent advances in aflatoxin B1 detection based on nanotechnology and nanomaterials-A review. Anal Chim Acta 2019;1069:1–27. https://doi.org/10.1016/j.aca.2019.04.032.

[184] Zhou Q, Tang D. Recent advances in photoelectrochemical biosensors for analysis of mycotoxins in food. TrAC - Trends Anal Chem 2020;124:115814. https://doi.org/10.1016/j.trac.2020.115814.

[185] Wu Z, Sun DW, Pu H, Wei Q, Lin X. $Ti_3C_2T_x$ MXenes loaded with Au nanoparticle dimers as a surface-enhanced raman scattering aptasensor for AFB1 detection. Food Chem 2021;372:131293. https://doi.org/10.1016/j.foodchem.2021.131293.

[186] Guo W, Umar A, Algadi H, Albargi H, Ibrahim AA, Cui K, et al. Design of a unique "ON/OFF" switch electrochemical aptasensor driven by the pH for the detection of Aflatoxin B1 in acid solutions based on titanium carbide/ carboxylated graphene oxide- poly(4-vinyl pyridine)/Aptamer composite. Microchem J 2021;169:106548. https://doi.org/10.1016/j.microc.2021.106548.

[187] Zheng F, Ke W, Shi L, Liu H, Zhao Y. Plasmonic Au-Ag Janus nanoparticle engineered ratiometric surface-enhanced raman scattering aptasensor for ochratoxin A detection. Anal Chem 2019;91(18):11812–20. https://doi.org/10.1021/acs.analchem.9b02469.

[188] Ngundi MM, Qadri SA, Wallace EV, Moore MH, Lassman ME, Shriver-Lake LC, et al. Detection of deoxynivalenol in foods and indoor air using an array biosensor. Environ Sci Technol 2006;40(7):2352–6. https://doi.org/10.1021/es052396q.

[189] Sangu SS, Illias NM, Ong CC, Gopinath SCB, Saheed MSM. MXene-sased aptasensor: Characterization and high-performance voltammetry detection of deoxynivalenol. Bionanoscience 2021;11(2):314–23. https://doi.org/10.1007/s12668-021-00847-0.

[190] Dagenais TRT, Keller NP. Pathogenesis of Aspergillus fumigatus in invasive aspergillosis. Clin Microbiol Rev 2009;22(3):447–65. https://doi.org/10.1128/CMR.00055-08.

[191] Gao S, Zheng X, Tang Y, Cheng Y, Hu X, Wu J. Development of a fluorescently labeled aptamer structure-switching assay for sensitive and rapid detection of gliotoxin. Anal Chem 2019;91(2):1610–8. https://doi.org/10.1021/acs.analchem.8b05094.

[192] Wang H, Li H, Huang Y, Xiong M, Wang F, Li C. A label-free electrochemical biosensor for highly sensitive detection of gliotoxin based on DNA nanostructure/MXene nanocomplexes. Biosens Bioelectron 2019;142:111531. https://doi.org/10.1016/j.bios.2019.111531.

[193] Cui H, Fu X, Yang L, Xing S, Wang XF. 2D titanium carbide nanosheets based fluorescent aptasensor for sensitive detection of thrombin. Talanta 2021;228:122219. https://doi.org/10.1016/j.talanta.2021.122219.

[194] Kashefi-Kheyrabadi L, Koyappayil A, Kim T, Cheon YP, Lee MH. A MoS_2@$Ti_3C_2T_x$ MXene hybrid-based electrochemical aptasensor (MEA) for sensitive and rapid detection of Thyroxine. Bioelectrochemistry 2021;137:107674. https://doi.org/10.1016/j.bioelechem.2020.107674.

[195] Wang Q, Fang J, Cao D, Li H, Su K, Hu N, et al. An improved functional assay for rapid detection of marine toxins, saxitoxin and brevetoxin using a portable cardiomyocyte-based potential biosensor. Biosens Bioelectron 2015;72:10–7. https://doi.org/10.1016/j.bios.2015.04.028.

[196] Jin X, Chen J, Zeng X, Xu LJ, Wu Y, Fu FF. A signal-on magnetic electrochemical immunosensor for ultra-sensitive detection of saxitoxin using palladium-doped graphitic carbon nitride-based non-competitive strategy. Biosens Bioelectron 2019;128(2018):45–51. https://doi.org/10.1016/j.bios.2018.12.036.

[197] Holland CA, Henry AT, Whinna HC, Church FC. Effect of oligodeoxynucleotide thrombin aptamer on thrombin inhibition by heparin cofactor II and antithrombin. FEBS Lett 2000;484(2):87–91. https://doi.org/10.1016/S0014-5793(00)02131-1.

[198] Li LD, Zhao HT, Chen ZB, Mu XJ, Guo L. Aptamer biosensor for label-free impedance spectroscopy detection of thrombin based on gold nanoparticles. Sensors Actuators, B Chem 2011;157(1):189–94. https://doi.org/10.1016/j.snb.2011.03.048.

[199] Centi S, Tombelli S, Minunni M, Mascini M. Aptamer-based detection of plasma proteins by an electrochemical assay coupled to magnetic beads. Anal Chem 2007;79(4):1466–73. https://doi.org/10.1021/ac061879p.

[200] Li M, Peng X, Han Y, Fan L, Liu Z, Guo Y. Ti_3C_2 MXenes with intrinsic peroxidase-like activity for label-free and colorimetric sensing of proteins. Microchem J 2021;166:106238. https://doi.org/10.1016/j.microc.2021.106238.

[201] Liao N, Zhuo Y, Chai YQ, Xiang Y, Han J, Yuan R. Reagentless electrochemiluminescent detection of protein biomarker using graphene-based magnetic nanoprobes and poly-l-lysine as co-reactant. Biosens Bioelectron 2013;45(1):189–94. https://doi.org/10.1016/j.bios.2013.02.005.

[202] Islam KN, Ihara M, Dong J, Kasagi N, Mori T, Ueda H. Direct construction of an open-sandwich enzyme immunoassay for one-step noncompetitive detection of thyroid hormone T4. Anal Chem 2011;83(3):1008–14. https://doi.org/10.1021/ac102801r.

[203] Zhang Q, Chen X, Tu F, Yao C. Ultrasensitive enzyme-free electrochemical immunoassay for free thyroxine based on three dimensionally ordered macroporous chitosan-Au nanoparticles hybrid film. Biosens Bioelectron 2014;59:377–83. https://doi.org/10.1016/j.bios.2014.03.068.

[204] Butt AA, Aldridge KE, Sanders CV. Infections related to the ingestion of seafood. Part II: Parasitic infections and food safety. Lancet Infect Dis 2004;4(5):294–300. https://doi.org/10.1016/S1473-3099(04)01005-9.

[205] Kampeera J, Pasakon P, Karuwan C, Arunrut N, Sappat A, Sirithammajak S, et al. Point-of-care rapid detection of *Vibrio parahaemolyticus* in seafood using loop-mediated isothermal amplification and graphene-based screen-printed electrochemical sensor. Biosens Bioelectron 2019;132:271–8. https://doi.org/10.1016/j.bios.2019.02.060.

[206] Wu Y, Wen J, Ma Y, Ma X, Chen Y. Epidemiology of foodborne disease outbreaks caused by *Vibrio parahaemolyticus*, China, 2003–2008. Food Control 2014;46:197–202. https://doi.org/10.1016/j.foodcont.2014.05.023.

[207] Li X, Su Y, Chu H, Lyu S, Tian J, Xu W. Rapid strand replacement primer thermostat visual sensor based on Bst DNA polymerase and pyrophosphatase for detecting *Vibrio parahaemolyticus*. Food Chem 2020;310(2019):125955. https://doi.org/10.1016/j.foodchem.2019.125955.

[208] Hong J, Wang W, Wang J, Wang X, Xie H, Li T, et al. A turn-on–type fluorescence resonance energy transfer aptasensor for vibrio detection using aptamer-modified polyhedral oligomeric silsesquioxane-perovskite quantum dots/Ti_3C_2 MXenes composite probes. Microchim Acta 2021;188(2). https://doi.org/10.1007/s00604-020-04679-9.

[209] Wang W, Xiao S, Jia Z, Xie H, Li T, Wang Q, et al. A dual-mode aptasensor for foodborne pathogens detection using Pt, phenylboric acid and ferrocene modified Ti_3C_2 MXenes nanoprobe. Sens Actuators, B 2022;351:130839. https://doi.org/10.1016/j.snb.2021.130839.

[210] Sharp PM, Hahn BH. Origins of HIV and the AIDS pandemic. Cold Spring Harb Perspect Med 2011;1(1):1–22. https://doi.org/10.1101/cshperspect.a006841.

[211] Lifson MA, Ozen MO, Inci F, Wang ShuQi, Inan H, Baday M, et al. Advances in biosensing strategies for HIV-1 detection, diagnosis, and therapeutic monitoring. Adv Drug Deliv Rev 2016;103:90–104. https://doi.org/10.1016/j.addr.2016.05.018.

[212] Wang Y, Sun W, Li Y, Zhuang X, Tian C, Luan F, et al. Imidazole metal-organic frameworks embedded in layered $Ti_3C_2T_x$ Mxene as a high-performance electrochemiluminescence biosensor for sensitive detection of HIV-1 protein. Microchem J 2021;167:106332. https://doi.org/10.1016/j.microc.2021.106332.

[213] Han X, Li S, Peng Z, Othman AM, Leblanc R. Recent development of cardiac troponin I detection. ACS Sensors 2016;1(2):106–14. https://doi.org/10.1021/acssensors.5b00318.

[214] Panteghini M, Pagani F, Yeo K-T, Apple FS, Christenson RH, Dati F, et al. Evaluation of imprecision for cardiac troponin assays at low-range concentrations. Clin Chem 2004;50(2):327–32. https://doi.org/10.1373/clinchem.2003.026815.

[215] Fathil MFM, Md Arshad MK, Gopinath SCB, Hashim U, Adzhri R, Ayub RM, et al. Diagnostics on acute myocardial infarction: Cardiac troponin biomarkers. Biosens Bioelectron 2015;70:209–20. https://doi.org/10.1016/j.bios.2015.03.037.

[216] Mi X, Li H, Tan R, Feng B, Tu Y. The TDs / aptamer cTnI biosensors based on HCR and Au / Ti_3C_2 MXene amplification for screening serious patient in COVID-19 pandemic. Biosens Bioelectron 2021;192:113482. https://doi.org/10.1016/j.bios.2021.113482.

[217] Longo DL, Fajgenbaum DC, June CH. Cytokine Storm. N Engl J Med 2020;383(23):2255–73. https://doi.org/10.1056/NEJMra2026131.

[218] Ragab D, Salah Eldin H, Taeimah M, Khattab R, Salem R. The COVID-19 cytokine storm; What we know so far. Front Immunol 2020;11(June):1–4. https://doi.org/10.3389/fimmu.2020.01446.

[219] Karki R, Sharma BR, Tuladhar S, Williams EP, Zalduondo L, Samir P, et al. Synergism of TNF-α and IFN-γ triggers inflammatory cell death, tissue damage, and mortality in SARS-CoV-2 infection and cytokine shock syndromes. Cell 2021;184(1):149–68. https://doi.org/10.1016/j.cell.2020.11.025.

[220] Noh S, Lee H, Kim J, Jang H, An J, Park C, et al. Rapid electrochemical dual-target biosensor composed of an Aptamer/MXene hybrid on Au microgap electrodes for cytokines detection. Biosens Bioelectron 2022;207:114159. https://doi.org/10.1016/j.bios.2022.114159.

[221] Hille F, Richter H, Wong SP, Bratovič M, Ressel S, Charpentier E. The biology of CRISPR-Cas: Backward and forward. Cell 2018;172(6):1239–59. https://doi.org/10.1016/j.cell.2017.11.032.

[222] Schauer R. Sialic acids as regulators of molecular and cellular interactions. Curr Opin Struct Biol 2009;19(5):507–14. https://doi.org/10.1016/j.sbi.2009.06.003.

[223] MacAuley MS, Crocker PR, Paulson JC. Siglec-mediated regulation of immune cell function in disease. Nat Rev Immunol 2014;14(10):653–66. https://doi.org/10.1038/nri3737.

[224] Virgo P, Denning-Kendall PA, Erickson-Miller CL, Singha S, Evely R, Hows JM, et al. Identification of the CD33-related Siglec receptor, Siglec-5 (CD170), as a useful marker in both normal myelopoiesis and acute myeloid leukaemias. Br J Haematol 2003;123(3):420–30. https://doi.org/10.1046/j.1365-2141.2003.04625.x.

[225] Zhang K, Fan Z, Yao Bo, Ding Y, Zhao J, Xie M, et al. Exploring the trans-cleavage activity of CRISPR-Cas12a for the development of a Mxene based electrochemiluminescence biosensor for the detection of Siglec-5. Biosens Bioelectron 2021;178:113019. https://doi.org/10.1016/j.bios.2021.113019.

[226] Raetz CRH, Whitfield C. Lipopolysaccharide endotoxins. Annu Rev Biochem 2002;71:635–700. https://doi.org/10.1146/annurev.biochem.71.110601.135414.

[227] Liao VH, Chou W, Chio C, Ju Y, Liao C. A probabilistic approach to quantitatively assess the inhalation risk for airborne endotoxin in cotton textile workers. J Hazard Mater 2010;177(1–3):103–8. https://doi.org/10.1016/j.jhazmat.2009.11.151.

[228] Jones KE, Patel NG, Levy MA, Storeygard A, Balk D, Gittleman JL, et al. Global trends in emerging infectious diseases. Nature 2008;451(7181):990–3. https://doi.org/10.1038/nature06536.

[229] Sheng A, Wang P, Yang J, Tang L, Chen F, Zhang J. MXene coupled with CRISPR-Cas12a for analysis of endotoxin and bacteria. Anal Chem 2021;93:4676–81. https://doi.org/10.1021/acs.analchem.1c00371.

[230] Jiang D, Wei M, Du X, Qin M, Shan X, Chen Z. One-pot synthesis of ZnO quantum dots/N-doped Ti_3C_2 MXene: Tunable nitrogen-doping properties and efficient electrochemiluminescence sensing. Chem Eng J 2022;430:132771. https://doi.org/10.1016/j.cej.2021.132771.

[231] Jiang D, Wei M, Du X, Qin M, Shan X, Wang W, et al. Ultrasensitive near-infrared aptasensor for enrofloxacin detection based on wavelength tunable AgBr nanocrystals electrochemiluminescence emission triggered by O-terminated Ti_3C_2 MXene. Biosens Bioelectron 2022;200:113917. https://doi.org/10.1016/j.bios.2021.113917.

[232] Granja RHMM, Niño AMM, Zucchetti RAM, Niño REM, Patel R, Salerno AG. Determination of streptomycin residues in honey by liquid chromatography-tandem mass spectrometry. Anal Chim Acta 2009;637(1–2):64–7. https://doi.org/10.1016/j.aca.2009.01.006.

[233] Zhou N, Wang J, Zhang J, Li C, Tian Y, Wang J. Selection and identification of streptomycin-specific single-stranded DNA aptamers and the application in the detection of streptomycin in honey. Talanta 2013;108:109–16. https://doi.org/10.1016/j.talanta.2013.01.064.

[234] Farouk F, Azzazy HME, Niessen WMA. Challenges in the determination of aminoglycoside antibiotics, a review. Anal Chim Acta 2015;890:21–43. https://doi.org/10.1016/j.aca.2015.06.038.

[235] Liu D, Xu X, Shen X, Luo L, Li L, Yan X, et al. Construction of the direct Z-scheme CdTe/APTES-WO_3 heterostructure by interface engineering for cathodic 'signal-off' photoelectrochemical aptasensing of streptomycin at sub-nanomole level. Sensors Actuators, B Chem 2020;305:127210. https://doi.org/10.1016/j.snb.2019.127210.

[236] Danesh NM, Ramezani M, Emrani AS, Abnous K, Taghdisi SM. A novel electrochemical aptasensor based on arch-shape structure of aptamer-complimentary strand conjugate and exonuclease I for sensitive detection of streptomycin. Biosens Bioelectron 2016;75:123–8. https://doi.org/10.1016/j.bios.2015.08.017.

[237] Zhu Q, Liu L, Wang R, Zhou X. A split aptamer (SPA)-based sandwich-type biosensor for facile and rapid detection of streptomycin. J Hazard Mater 2020;403:2021. https://doi.org/10.1016/j.jhazmat.2020.123941.

[238] You F, Wei J, Cheng Y, Wen Z, Ding C, Hao N, et al. Selective and sensitive photoelectrochemical aptasensor for streptomycin detection based on Bi_4VO_8Br/Ti_3C_2 nanohybrids. J Hazard Mater 2021;414:125539. https://doi.org/10.1016/j.jhazmat.2021.125539.

[239] Song Y, Song J, Wei X, Huang M, Sun M, Zhu L, et al. Discovery of aptamers targeting the receptor-binding domain of the SARS-CoV-2 spike glycoprotein. Anal Chem 2020;92(14):9895–900. https://doi.org/10.1021/acs.analchem.0c01394.

[240] Cui F, Zhou HS. Diagnostic methods and potential portable biosensors for coronavirus disease 2019. Biosens Bioelectron 2020;165:112349. https://doi.org/10.1016/j.bios.2020.112349.

[241] Zhang L, Fang X, Liu X, Ou H, Zhang H, Wang J, et al. Discovery of sandwich type COVID-19 nucleocapsid protein DNA aptamers. Chem Commun 2020;56(70):10235–8. https://doi.org/10.1039/D0CC03993D.

[242] Chen R, Kan L, Duan F, He L, Wang M, Cui J, et al. Surface plasmon resonance aptasensor based on niobium carbide MXene quantum dots for nucleocapsid of SARS-CoV-2 detection. Microchim Acta 2021;188(10):1–10. https://doi.org/10.1007/s00604-021-04974-z.

[243] Yang P, Guo X, Zhang J, Chen C, Gan Y, Xie W, et al. Picomolar thrombin detection by orchestration of triple signal amplification strategy with hierarchically porous $Ti_3C_2T_x$ MXene electrode material-catalytic hairpin assembly reaction-metallic nanoprobes. Biosens Bioelectron 2022;208:114228. https://doi.org/10.1016/j.bios.2022.114228.

[244] Li B, Pu W, Weng L, Lyu P, Xu H, Zhang W, et al. Aptamer-functionalized Ti_3C_2-MXene nanosheets with one-step potentiometric detection of programmed death-ligand 1. Electroanalysis 2022;34(1):2–7. https://doi.org/10.1002/elan.202100438.

[245] Lin X, Li C, Meng X, Yu W, Duan N, Wang Z, et al. CRISPR-Cas12a-mediated luminescence resonance energy transfer aptasensing platform for deoxynivalenol using gold nanoparticle-decorated $Ti_3C_2T_x$ MXene as the enhanced quencher. J Hazard Mater 2022;433:128750. https://doi.org/10.1016/j.jhazmat.2022.128750.

[246] Rasheed PA, Pandey R, Jabbar K, Mahmoud K. $Nb_4C_3T_x$ (MXene)/Au/DNA aptasensor for the ultraselective electrochemical detection of lead in water samples. Electroanalysis 2022. https://doi.org/10.1002/elan.202100685.

[247] Yang J, Zhong W, Yu Qi, Zou J, Gao Y, Liu S, et al. MXene–AuNP-based electrochemical aptasensor for ultra-sensitive detection of chloramphenicol in honey. Molecules 2022;27(6):1871. https://doi.org/10.3390/molecules27061871.

[249] Wrobel TP, Bhargava R. Infrared spectroscopic imaging advances as an analytical technology for biomedical sciences. Anal Chem 2018;90(3):1444–63. https://doi.org/10.1021/acs.analchem.7b05330.

[250] Xu J, Zhao W, Song S. Functional nanoprobes for ultrasensitive detection of biomolecules : an update. Chem Soc Rev 2014;43(5):1601–11. https://doi.org/10.1039/c3cs60277j.

[251] Li Z, Askim JR, Suslick KS. The optoelectronic nose : Colorimetric and fluorometric sensor arrays. Chem Rev 2019;119(1):231–92. https://doi.org/10.1021/acs.chemrev.8b00226.

[252] Zhu X, Zhang Y, Liu M, Liu Y. 2D titanium carbide MXenes as emerging optical biosensing platforms. Biosens Bioelectron 2021;171:112730. https://doi.org/10.1016/j.bios.2020.112730.

[253] Rafieerad A, Yan W, Sequiera GL, Sareen N, Abu-El-Rub E, Moudgil M, et al. Application of Ti_3C_2 MXene quantum dots for immunomodulation and regenerative medicine. Adv Healthc Mater 2019;8(16):1900569. https://doi.org/10.1002/adhm.201900569.

[254] Koyun S, Akgönüllü S, Yavuz H, Erdem A, Denizli A. Surface plasmon resonance aptasensor for detection of human activated protein C. Talanta 2019;194(2018):528–33. https://doi.org/10.1016/j.talanta.2018.10.007.

[255] Lee SH, Park YE, Lee JE, Lee HJ. A surface plasmon resonance biosensor in conjunction with a DNA aptamer-antibody bioreceptor pair for heterogeneous nuclear ribonucleoprotein A1 concentrations in colorectal cancer plasma solutions. Biosens Bioelectron 2020;154(2019):112065. https://doi.org/10.1016/j.bios.2020.112065.

[256] Fang A, Wu Q, Lu Q, Chen H, Li H, Liu M, et al. Upconversion ratiometric fluorescence and colorimetric dual-readout assay for uric acid. Biosens Bioelectron 2016;86:664–70. https://doi.org/10.1016/j.bios.2016.07.055.

[257] Zhu X, Zhao T, Nie Z, Liu Y, Yao S. Non-redox modulated fluorescence strategy for sensitive and selective ascorbic acid detection with highly photoluminescent nitrogen-doped carbon nanoparticles via solid-state synthesis. Anal Chem 2015;87(16):8524–30. https://doi.org/10.1021/acs.analchem.5b02167.

[258] Manzanares-Palenzuela CL, Pourrahimi AM, Gonzalez-Julian J, Sofer Z, Pykal M, Otyepka M, et al. Interaction of single- and double-stranded DNA with multilayer MXene by fluorescence spectroscopy and molecular dynamics simulations. Chem Sci 2019;10(43):10010–7. https://doi.org/10.1039/C9SC03049B.

[259] Cho S, Park L, Chong R, Kim YT, Lee JH. Rapid and simple G-quadruplex DNA aptasensor with guanine chemiluminescence detection. Biosens Bioelectron 2014;52:310–6. https://doi.org/10.1016/j.bios.2013.09.017.

[260] Choi HK, Lee JH. Role of magnetic Fe_3O_4 graphene oxide in chemiluminescent aptasensors capable of sensing tumor markers in human serum. Anal Methods 2013;5(24):6964–8. https://doi.org/10.1039/c3ay41683f.

[261] Wang XY, Gao A, Lu CC, He XW, Yin XB. An electrochemiluminescence aptasensor for thrombin using graphene oxide to immobilize the aptamer and the intercalated $Ru(phen)_3^{2+}$ probe. Biosens Bioelectron 2013;48:120–5. https://doi.org/10.1016/j.bios.2013.04.003.

[262] Zhou H, Zhang YY, Liu J, Xu JJ, Chena HY. Efficient quenching of electrochemiluminescence from K-doped graphene–CdS: Eu NCs by G-quadruplex–hemin and target recycling-assisted amplification for ultrasensitive DNA biosensing. Chem Commun 2013;49(22):2246–8. https://doi.org/10.1039/c3cc38990a.

[263] Wang F, Lin J, Yu S, Cui X, Ali A, Wu T, et al. Anti-site defects-assisted enhancement of electrogenerated chemiluminescence from in situ Mn^{2+} doped supertetrahedral chalcogenide nanoclusters. ACS Appl Mater Interfaces 2018;10(44):38223–9. https://doi.org/10.1021/acsami.8b13635.

[264] Yan Z, Wang F, Deng P, Wang Yu, Cai K, Chen Y, et al. Sensitive electrogenerated chemiluminescence biosensors for protein kinase activity analysis based on bimetallic catalysis signal amplification and recognition of Au and Pt loaded metal-organic frameworks nanocomposites. Biosens Bioelectron 2018;109:132–8. https://doi.org/10.1016/j.bios.2018.03.004.
[265] Li Y, Kang Z, Kong L, Shi H, Zhang Y, Cui M. MXene-Ti_3C_2/CuS nanocomposites: Enhanced peroxidase-like activity and sensitive colorimetric cholesterol detection. Mater Sci Eng, C 2019;104:110000. https://doi.org/10.1016/j.msec.2019.110000.
[266] Zeng S, Hu S, Xia J, Anderson T, Dinh XQ, Meng XM, et al. Graphene–MoS_2 hybrid nanostructures enhanced surface plasmon resonance biosensors. Sensors Actuators B Chem 2015;207:801–10. https://doi.org/10.1016/j.snb.2014.10.124.
[267] Wu L, Guo J, Xu H, Dai X, Xiang Y. Ultrasensitive biosensors based on long-range surface plasmon polariton and dielectric waveguide modes. Photonics Res 2016;4(6):262–6. https://doi.org/10.1364/PRJ.4.000262.
[268] Esteban Ó, Naranjo FB, Díaz-herrera N, Valdueza-felip S, Navarrete M, González-cano A. High-sensitive SPR sensing with Indium Nitride as a dielectric overlay of optical fibers. Sensors Actuators B Chem 2011;158:372–6. https://doi.org/10.1016/j.snb.2011.06.038.
[269] Maharana PK, Jha R. Chalcogenide prism and graphene multilayer based surface plasmon resonance affinity biosensor for high performance. Sensors Actuators B Chem 2012;169:161–6. https://doi.org/10.1016/j.snb.2012.04.051.
[270] Duan X, Wang C, Shaw JC, Cheng R, Chen Yu, Li H, et al. Lateral epitaxial growth of two-dimensional layered semiconductor heterojunctions. Nat Nanotechnol 2014;9(12):1024–30. https://doi.org/10.1038/NNANO.2014.222.
[271] Madadrang CJ, Kim HY, Gao G, Wang N, Zhu J, Feng H, et al. Adsorption behavior of EDTA-graphene oxide for Pb (II) removal. ACS Appl Mater Interfaces 2012;4(3):1186–93. https://doi.org/10.1021/am201645g.
[272] Zhang Q, et al. Nanoscale water purification by unique sandwich-like MXene/magnetic iron oxide nanocomposites. Nanoscale 2016;8(17):7085–93. https://doi.org/10.1039/c5nr09303a.
[273] An JE, Kim KH, Park SJ, Seo SE, Kim J, Ha S, et al. Wearable cortisol aptasensor for simple and rapid real-time monitoring. ACS Sensors 2022;7(1):99–108. https://doi.org/10.1021/acssensors.1c01734.